

Chem Catalysis, Volume 1

Supplemental information

A well-defined diamine

from lignin depolymerization mixtures

for constructing bio-based polybenzoxazines

Xianyuan Wu, Maxim V. Galkin, and Katalin Barta

Supplemental Experimental Procedures

Table of Contents

1. General information	1
1.1 Preparation of Ni-PMO catalyst.....	3
1.2 Preparation of model compounds	3
1.3 Spectral data of the model compounds	5
1.4 General experimental procedure.....	31
2. Catalytic conversion of bisphenols to MBC over Raney nickel catalyst	32
2.1 Establishing the reaction conditions for bisphenols production	32
2.2 GC-MS traces of catalytic demethoxylation/hydrogenation of BGH to MBC over Raney nickel catalyst	33
2.3 Recycling test for catalytic demethoxylation and hydrogenation of BGH to MBC over Raney nickel catalyst	36
2.4 Catalytic demethoxylation and hydrogenation of lignin-derived bisphenols.	37
2.5 Catalytic demethoxylation and hydrogenation of lignin-derived dimers β-1 and β-β	37
2.6 GC FID traces toward the production of MBC diol based on lignin to vanillin process	43
3. Catalytic direct amination of MBC with ammonia to obtain MBCA over Raney nickel catalyst	44
3.1 Detailed analysis of the crude MBCA obtained from the amination of MBC	44
3.2 Recycling test for catalytic amination of MBC to MBCA over Raney nickel catalyst	47
4. Synthesis and characterizations of poly (S-MBCA), poly (PG-MBCA), poly (G-MBCA) and poly (E-MBCA)	48
4.1 DSC thermograms of S-MBCA , PG-MBCA , G-MBCA and E-MBCA	48
4.2 TGA plots of poly (S-MBCA), poly (PG-MBCA), poly (G-MBCA) and poly (E-MBCA)	48
4.3 DSC thermograms of poly (S-MBCA), poly (PG-MBCA), poly (G-MBCA) and poly (E-MBCA)	49
4.4 FTIR spectra of S-MBCA , PG-MBCA , G-MBCA and E-MBCA before and after polymerization	49
4.5 DMA curve of poly (S-MBCA).....	50
5. Notes	51
6. Spectral data of isolated compounds.	54
7. Supplemental references	57

1. General information

Column chromatography was performed using Merck silica gel type 9385 230–400 mesh and typically dichloromethane and methanol or EtOAc and pentane as eluent.

Thin layer chromatography (TLC): Merck silica gel 60, 0.25 mm. The components were visualized by UV or KMnO₄ staining.

Gas Chromatography (GC) was used for product identification as well as determination of conversion and selectivity values.

At the University of Groningen (RUG): Product identification was performed by GC-MS (Shimadzu QP2010 Ultra) equipped with an HP-1MS column, and helium as carrier gas.

GC-MS analysis method (RUG): The temperature program started at 50 °C for 5 min, heated by 10 °C·min⁻¹ to 320 °C and held for 5 min. Conversion and products selectivity were determined by GC-FID (Shimadzu GC-2014) equipped with an HP-5MS column using nitrogen as carrier gas.

GC-FID analysis method (RUG): The temperature program started at 50 °C for 5 min, heated by 10 °C·min⁻¹ to 320 °C and held for 5 min.

At the University of Graz (UniGraz): Product identification was performed by GC-MS (5975C MSD) equipped with an HP-5 MS column, and helium as carrier gas.

GC-MS method (UniGraz): The temperature program started at 50 °C for 5 min, heated by 10 °C·min⁻¹ to 325 °C and held for 5 min. Conversion and products selectivity were determined by GC-FID (Agilent 8890 GC) equipped with an HP-5MS column using nitrogen as carrier gas.

GC-FID analysis method (UniGraz): The temperature program started at 50 °C for 5 min, heated by 10 °C·min⁻¹ to 325 °C and held for 5 min.

Nuclear Magnetic Resonance (NMR) spectroscopy:

At the University of Groningen: ¹H, ¹³C NMR and 2D NMR spectra were recorded on a Varian Mercury Plus 400, Agilent MR 400 (400 and 101 MHz, respectively) and a Bruker Avance NEO 600 (600 and 151 MHz, respectively);

At the University of Graz: ¹H, and ¹³C NMR spectra were recorded on a Bruker Avance III 300 MHz (300 and 75 MHz, respectively) and 2D NMR spectra were recorded on a Bruker Avance III 700 MHz with Cryoplatfrom and a 5mm Triple-Resonance cryoprobe (700 and 175 MHz, respectively).

¹H, ¹³C NMR and 2D NMR spectra were recorded at RT. Chemical shift values are reported in ppm with the solvent resonance as the internal standard (CDCl₃: 7.26 for ¹H, 77.0 for ¹³C; CD₃OD: 3.31 for ¹H, 49.0 for ¹³C; DMSO-d₆: 2.50 for ¹H, 39.5 for ¹³C). Data are reported as follows: chemical shifts, multiplicity (s = singlet, d = doublet, t = triplet, q = quartet, br. = broad, m = multiplet), coupling constants (Hz), and integration.

Gel Permeation Chromatography (GPC) GPC was performed at the University of Graz on a SHIMADZU NEXERA equipped 2×SDV analytical Linear M (8×300 mm, 5µm) plus 1×precolumm SVD (8×50mm, 5µm). The columns were operated at 40 °C with a flow-rate of 1 mL·min⁻¹ of THF. Detection was accomplished at 40 °C using an SPD-M40 photoarray detector in series. The molecular weight estimations were performed using polystyrene standards of known molecular weight distribution.

Differential Scanning Calorimetry (DSC) was conducted at the University of Graz on a Perkin Elmer DSC 8500. In a typical procedure, the sample (5-10 mg) was weighed into a DSC pan and then capped

with a lid. The sample was sealed and heated from 25 to 250 °C with a heating rate of 10 °C·min⁻¹. Then, it was cooled to 25 °C with a heating rate of 10 °C·min⁻¹. Subsequently, a second heating scan to 250 °C with the same heating rate was performed. All of experiments were performed under N₂ flow with a flow rate of 20 mL·min⁻¹.

Thermogravimetric analysis (TGA) was performed at the University of Graz on a Netzsch Jupiter STA 449C thermogravimetric analyzer. Typically, the sample (1-3 mg) was weighed into a platinum pan. The sample was heated from 20 to 550 °C with a heating rate of 10 °C·min⁻¹ under N₂ flow with a flow rate of 20 mL·min⁻¹. The temperatures were recorded when 5% weight loss ($T_{5\%}$) and 90% weight loss rate ($T_{90\%}$) occurred.

Inductively coupled plasma mass spectrometry (ICP-MS) was performed at University of Graz on an Agilent 7900 ICP-MS. Typically, the samples were solubilized with 5 mL HNO₃ in the MLS ultraclave and then heated to 250 °C for 30 mins before analysis by ICP-MS.

Dynamic Mechanical Analysis (DMA) measurements were conducted on a NETZSCH DSC 204 F1 Instrument in the tension mode with an amplitude of 10 mm. The specimen with the dimension of 50 × 5 1.5 mm was tested with a heating rate of 3 °C min⁻¹ from 25 to 380 °C at a frequency of 1 Hz.

Abbreviations

1A: 4-((4-hydroxycyclohexyl)methyl)-2-methoxyphenol

2A: 4-((4-hydroxycyclohexyl)methyl)-2-methoxycyclohexanol

3A: 4,4'-methylenediphenol

4A: 4-((4-hydroxycyclohexyl)methyl)phenol

5A: 4-(cyclohexylmethyl)phenol

6A: dodecahydro-1H-fluorene

1B: 4-((4-aminocyclohexyl)methyl)cyclohexanol

2B: 4,4'-bis((4-aminocyclohexyl)methyl)dicyclohexylamine

BHH (5A): 4,4'-methylenediphenol

MBCA: 4,4'-methylenebiscyclohexanamine

BGH: 4-(4-hydroxybenzyl)-2-methoxyphenol

E: eugenol

BGG: 4,4'-methylenebis(2-methoxyphenol)

G: guaiacol

BSH: 4-(4-hydroxybenzyl)-2,6-dimethoxyphenol

PG: propyl guaiacol

BSG: 4-(4-hydroxy-3-methoxybenzyl)-2,6-dimethoxyphenol

S: sesamol

BSS: 4,4'-methylenebis(2,6-dimethoxyphenol)

β-1-diol: 4,4'-(ethane-1,2-diyl)dicyclohexanol

MBC: 4,4'-methylenebiscyclohexanol

β-β-diol: 4,4'-(butane-1,4-diyl)dicyclohexanol

β-1: 4,4'-(ethane-1,2-diyl) bis(2-methoxyphenol)

β-β: 4,4'-(butane-1,4-diyl) bis(2-methoxyphenol)

1.1 Preparation of Ni-PMO catalyst

The Ni-PMO catalyst was prepared according to our previously reported procedure [1]. In a typical procedure, a solution containing $\text{AlCl}_3 \cdot 6\text{H}_2\text{O}$ (12.07 g, 0.05 mol), $\text{Ni}(\text{NO}_3)_2 \cdot 6\text{H}_2\text{O}$ (8.72 g, 0.03 mol) and $\text{MgCl}_2 \cdot 6\text{H}_2\text{O}$ (24.4 g, 0.12 mol) in deionized water (200 mL) was dropwise added to a solution containing Na_2CO_3 (5.30 g, 0.05 mol) in water (300 mL) at 60 °C under vigorous stirring. The pH value was always kept between 9 and 10 by addition of small portions of a 1 M solution of NaOH. The mixture was vigorously stirred at 60 °C for 72 h. After cooling to RT, the light blue solid was filtered and resuspended in a 2 M solution of Na_2CO_3 (300 mL) and stirred overnight at 40 °C. The catalyst precursor was filtered and washed with deionized water until chloride free. After drying the solid for 6 h at 100 °C followed by the calcination at 460 °C for 24 h in air, Ni-PMO was obtained.

1.2 Preparation of model compounds

Preparation of methoxylated bisphenols: The methoxylated bisphenols were synthesized using substituted hydroxybenzyl alcohols and substituted phenols as starting materials by acid-catalyzed electrophilic aromatic substitution based on the reported procedure with slight modification [2]. Typically, a 100 mL three neck round-bottomed flask was charged with 1 mmol (154 mg) of vanillyl alcohol, 10 mmol (940 mg) of phenol, 30 wt.% Amberlyst 15 catalyst based on vanillyl alcohol, equipped with a magnetic stirring bar. The mixture was heated to 60 °C for 1 h. After completion of the reaction, the mixture was dissolved in 50 mL DCM and filtered to remove the catalyst. The obtained solution was combined and the solvent was removed under reduced pressure. Then the product was purified by column chromatography filled with a silica gel (*n*-hexane: EtOAc 200:30, 200: 40, 200:50). Finally, 0.908 mmol (209 mg) of a white solid **BGH** containing *p-p'*/*m-p'* isomers with GC ratio of 87: 13 was obtained in a yield of 90.8%. The other methoxylated bisphenols (**BHH**, **BSH**, **BGG**, **BSG**, **BSS**) were prepared using the same preparation method as described for **BGH**, typically yielding 30–90% of product.

Preparation of MBC diol: In a typical procedure, a 1L high pressure Parr autoclave was charged with 2 g Raney nickel catalyst, 5 g bisphenol **F**, 100 mL isopropanol, and equipped with mechanical stirring. The reactor was sealed, purged 3 times with H_2 and then pressurized with H_2 (40 bar). The reactor was heated to 150 °C for 4 h under stirring at 400 rpm. After completion of the reaction, the reactor was cooled to RT. Then 0.1 mL solution was collected through a syringe and injected to GC-MS or GC-FID after filtration through a PTFE filter (0.45 μm). The Raney nickel was separated from the solution by centrifugation and subsequent decantation and additionally washed with isopropanol (3×30 mL). Then the isopropanol soluble fractions were combined and the solvent was removed under reduced pressure. The product (4, 4'-methylenebiscyclohexanol) was obtained as a white solid (5.194 g, 24.5 mmol) in a 98% yield as a mixture of isomers (*cis-cis*: *cis-trans*: *trans*: *trans* with the ratio of 10: 43: 47).

Synthesis of guaiacyl 4,4'-(ethane-1,2-diyl) bis(2-methoxyphenol) β -1 was performed according to previously reported procedure with slight modifications [3]. In a typical procedure, 150 mg, 1 mmol of 2-methoxy-4-vinylphenol, 12.7 mg, 0.02 mmol of Hoveyda catalyst (2 mol %) and 3 mL of dimethyl carbonate was charged in a dry and Argon flushed Schlenk tube reactor, equipped with a magnetic stirrer. The reaction mixture was heated to 80 °C for 4 h under stirring at 400 rpm. After completion of

the reaction, the reactor was cooled to room temperature. Then the crude product was purified by column chromatography on silica gel, using ethyl acetate: pentane (1:1) as eluent. 0.158 g, 0.58 mmol of solid was obtained in a yield of 58.0 %. The obtained solid was immediately transferred to a 100 mL high-pressure Parr autoclave, equipped with an overhead stirrer. Then 20 mg Pd/C and 20 mL methanol was added. The reactor was sealed, purged 3 times with H₂ and then pressurized with H₂ (30 bar) under stirring overnight. After completion of the reaction, the solvent was removed under reduced vacuum and 0.151 g, 0.55 mmol of white solid 4,4'-(ethane-1,2-diyl) bis(2-methoxyphenol) **β-1** was obtained in a yield of 95 %.

Preparation of 4,4'-(butane-1,4-diyl) bis(2-methoxyphenol) β-β was performed according to previously reported procedure with slight modifications^[4]. In a typical procedure, 10 g, 60.9 mmol of eugenol, 205 mg of first-generation Grubbs catalyst (0.4 mol %) was charged in a dry and Argon flushed Schlenk tube reactor, equipped with a magnetic stirrer under vacuum for 48 h. After completion of the reaction, the resulting solid was dissolved in 500 mL, 1M of NaOH and was filtered through Celite Pad. Then, to a rapidly stirring solution, concentrated HCl was dropwise added until a pale gray solid was precipitated. The suspension was filtered and subjected to washing with deionized water three times (3×50 mL). After that, the solid mixture was dissolved in dichloromethane (200 mL) and washed with deionized water three times (3×50 mL), following by drying over anhydrous MgSO₄ and the solvent was evaporated under reduced pressure. Then the crude product was subjected to recrystallization using solvents ethyl acetate and hexane with ratio of 1:5 (vol/vol) to get rid of residual eugenol. The purified product was immediately transferred to a 100 mL high-pressure Parr autoclave, equipped with an overhead stirrer. Then 200 mg Pd/C and 40 mL methanol was added. The reactor was sealed, purged 3 times with H₂ and then pressurized with H₂ (40 bar) under stirring overnight. After completion of the reaction, the solvent was removed under reduced vacuum to provide 4.57 g, 8.78 mmol of guaiacyl bisphenol **β-β** in a yield of 52 % (based on eugenol)

Preparation of benzoxazine monomers PG-MBCA, G-MBCA and E-MBCA: The solventless microwave irradiation synthesis of **G-MDCA**, **PG-MBCA** and **E-MBCA** were performed according to the reported procedure^[5]. Typically, a Milestone microwave reactor tube equipped with a magnetic stirrer was charged with **MBCA** (10 mmol, 2.10 g), paraformaldehyde (40 mmol, 1.20 g) and guaiacol (20 mmol, 2.48 g). The microwave reactor output power was set to 200 W. The mixture was heated to 80 °C for 3 min and 100 °C for 11 min. After the reaction was completed, the mixture was purified by a silica gel column chromatography (*n*-hexane: EtOAc from 4:1 to 1:1). Finally, the yellow solid **G-MBCA** (2.6 g) was obtained in a yield of 51.4%.

Preparation of benzoxazine monomer S-MBCA: The conventional solvent synthesis of **S-MBCA** was performed according to a reported procedure^[6]. Typically, a 250 mL single neck round-bottomed flask equipped with a magnetic stirrer was charged with **MBCA** (10 mmol, 2.10 g), paraformaldehyde (40 mmol, 1.20 g) and sesamol (20 mmol, 2.76 g) in 100 mL absolute ethanol. The mixture was heated and refluxed at 70 °C overnight under N₂. After the reaction was completed, the product was precipitated at the bottom of the flask as white solid and separated by simple filtration and washed three times with 50 mL anhydrous ethanol. Finally, the white solid (5.24 g) was obtained in an excellent, 98% yield.

1.3 Spectral data of the model compounds

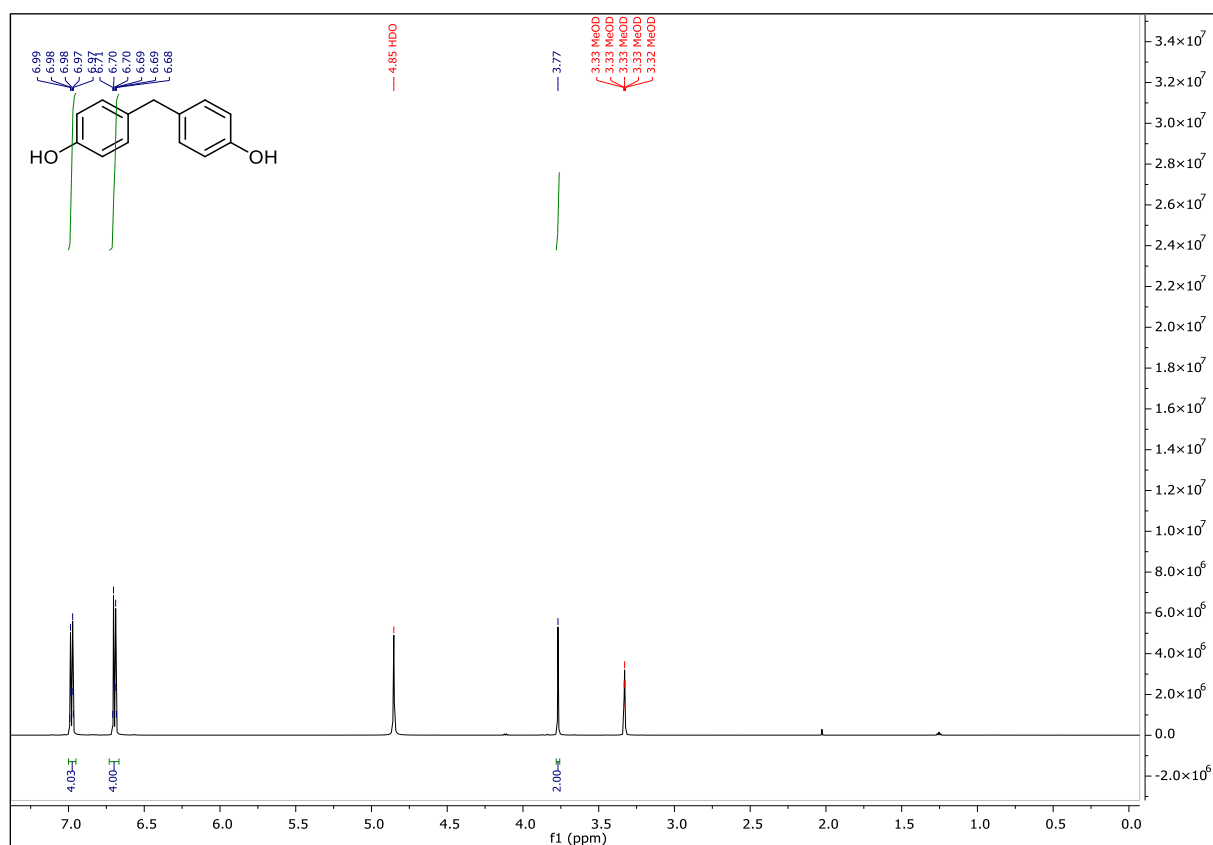


Figure S1. ¹H NMR spectrum of *p, p'*-BHH

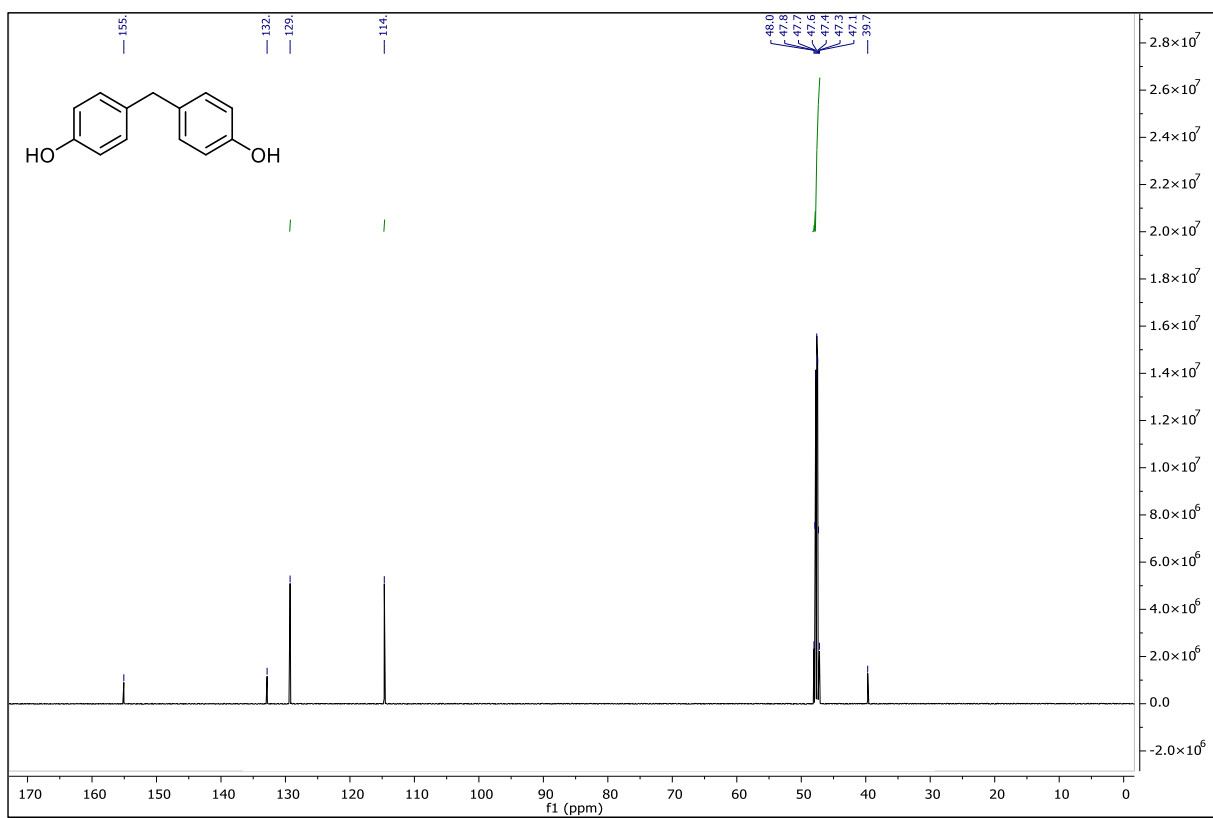


Figure S2. ¹³C NMR spectrum of *p, p'*-BHH

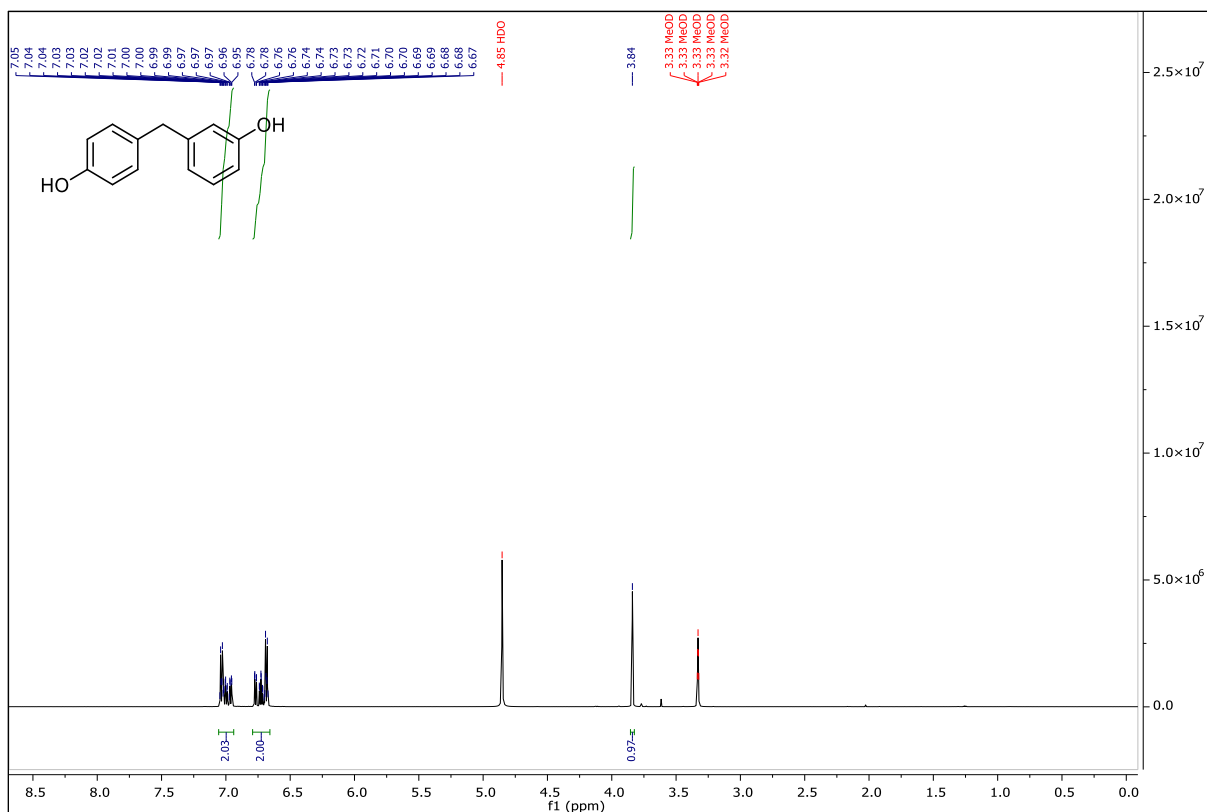


Figure S3. ¹H NMR spectrum of *m, p'*-BHH

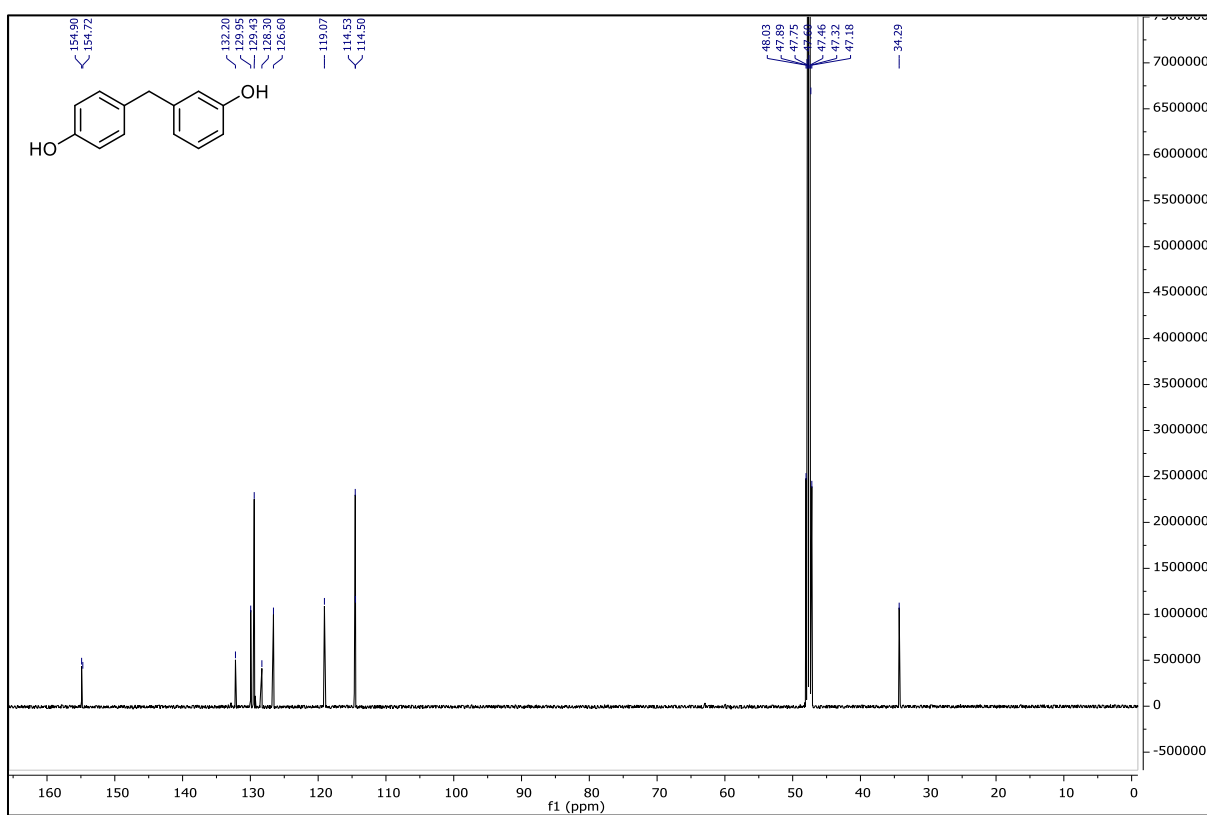


Figure S4. ¹³C NMR spectrum of *m, p'*-BHH

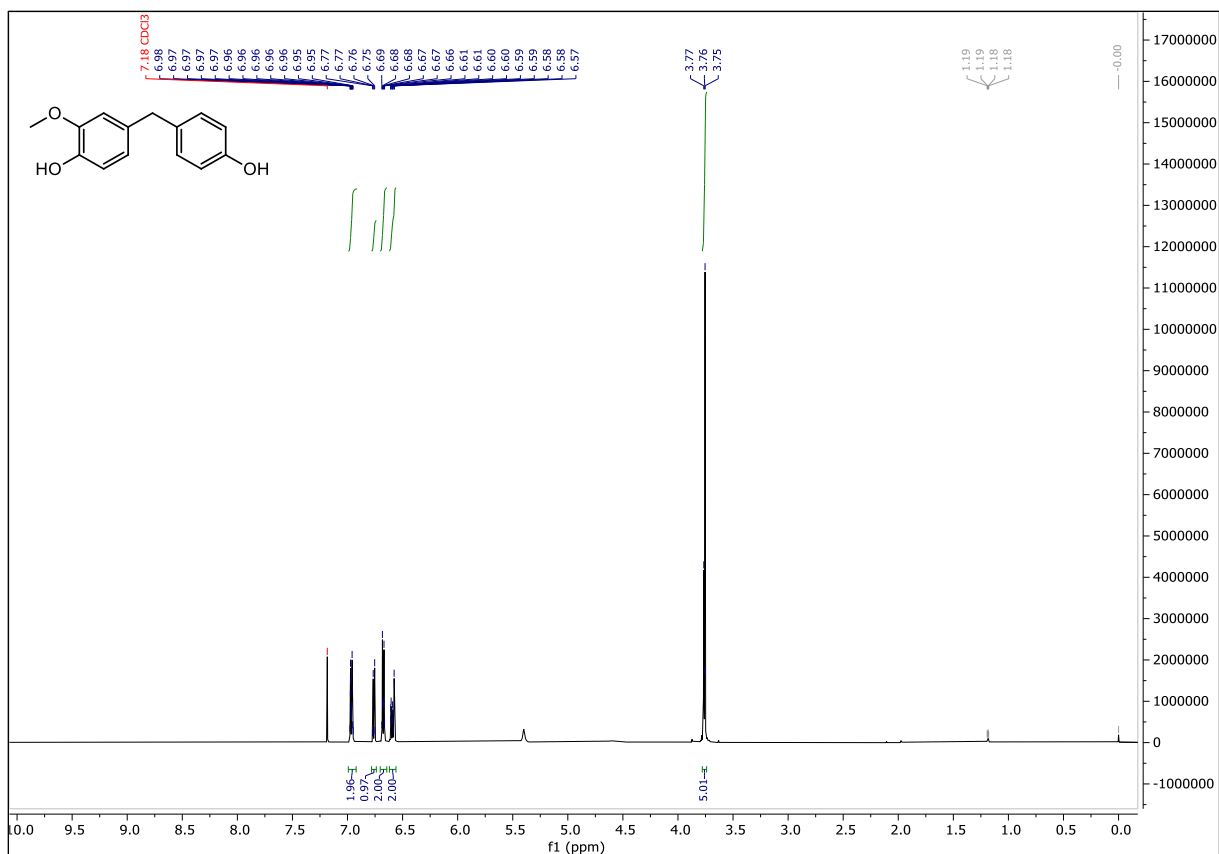


Figure S5. ¹H NMR spectrum of *p, p'*-BGH

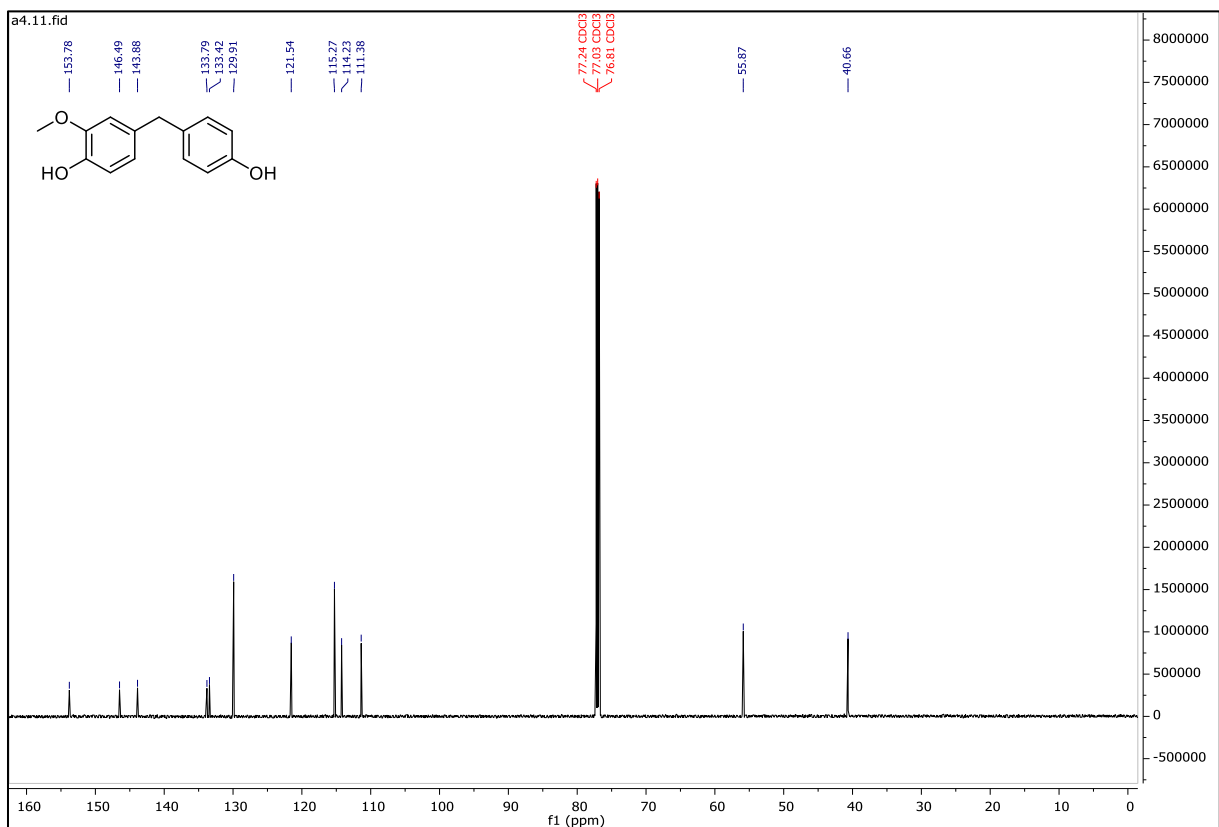


Figure S6. ¹³C NMR spectrum of *p, p'*-BGH

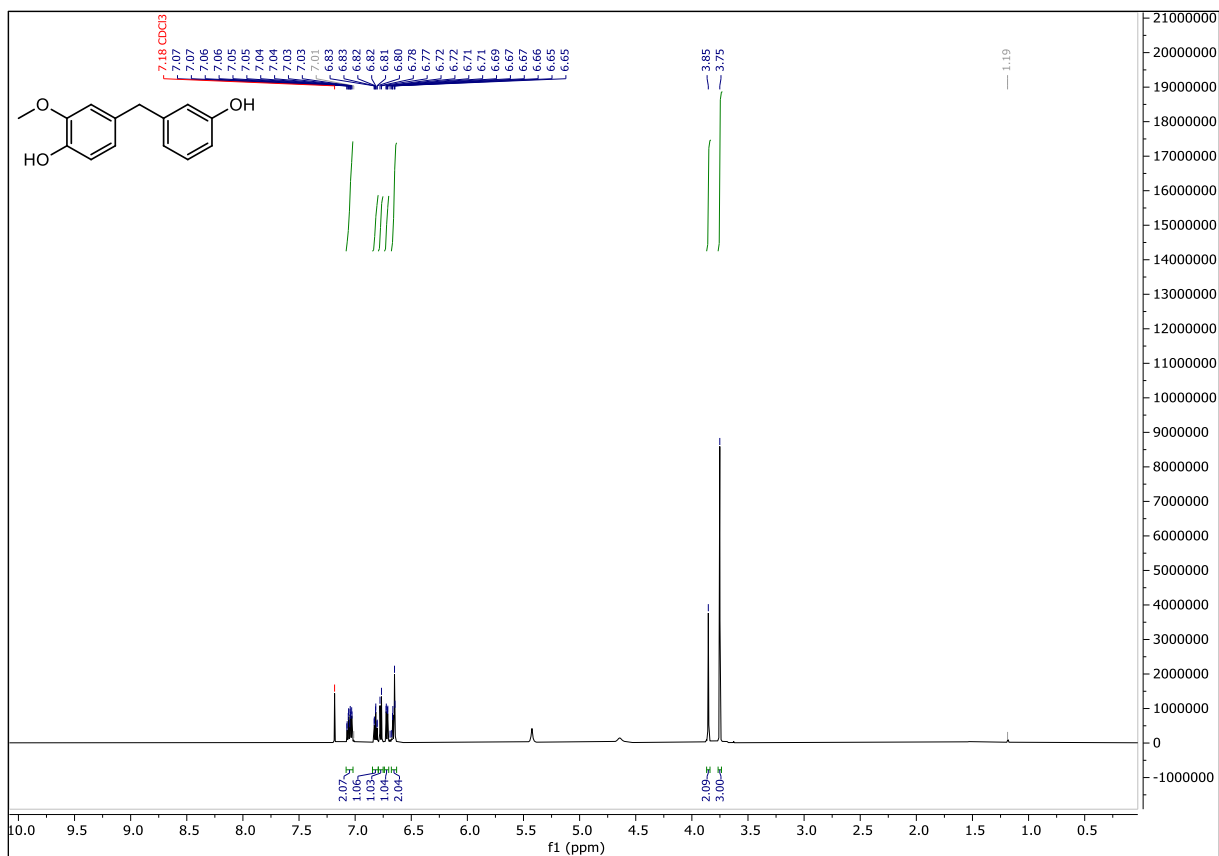


Figure S7. ¹H NMR spectrum of *m, p'*-BGH

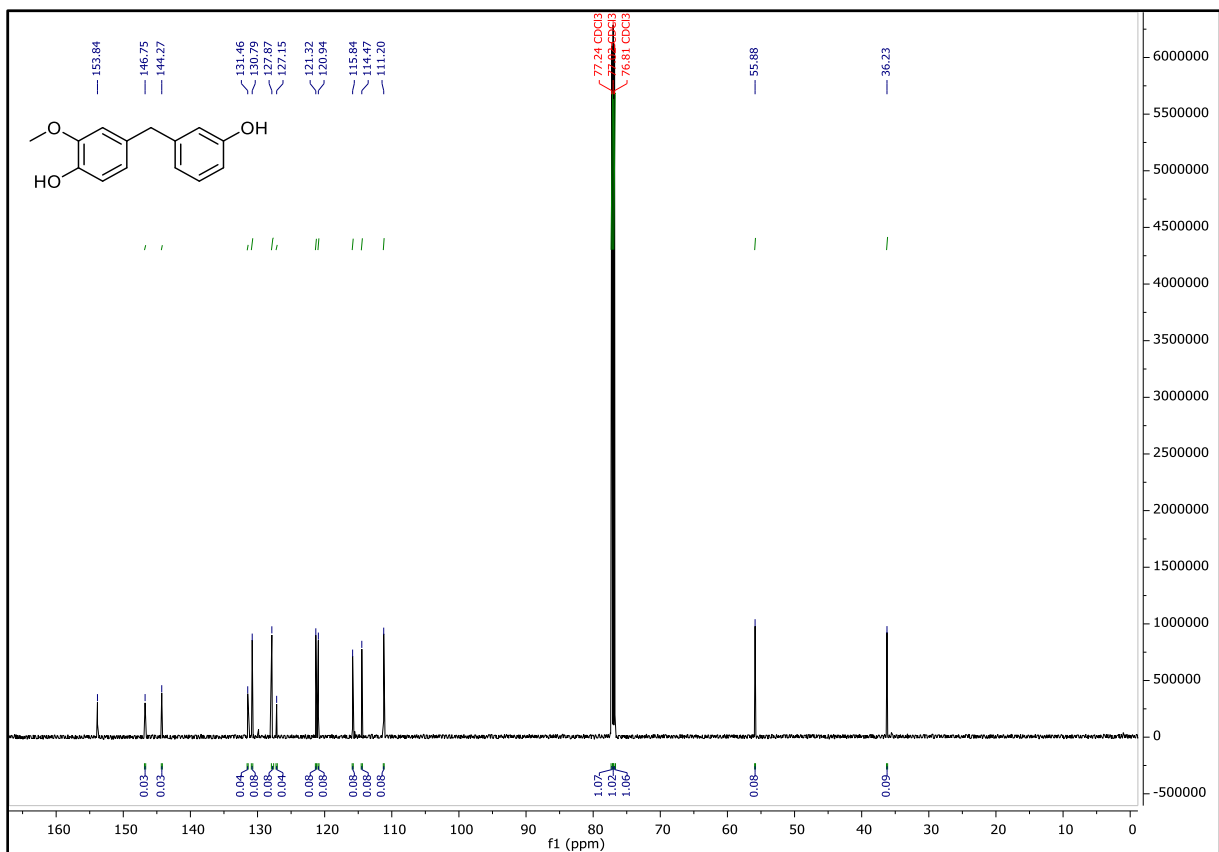


Figure S8. ¹³C NMR spectrum of *m, p'*-BGH

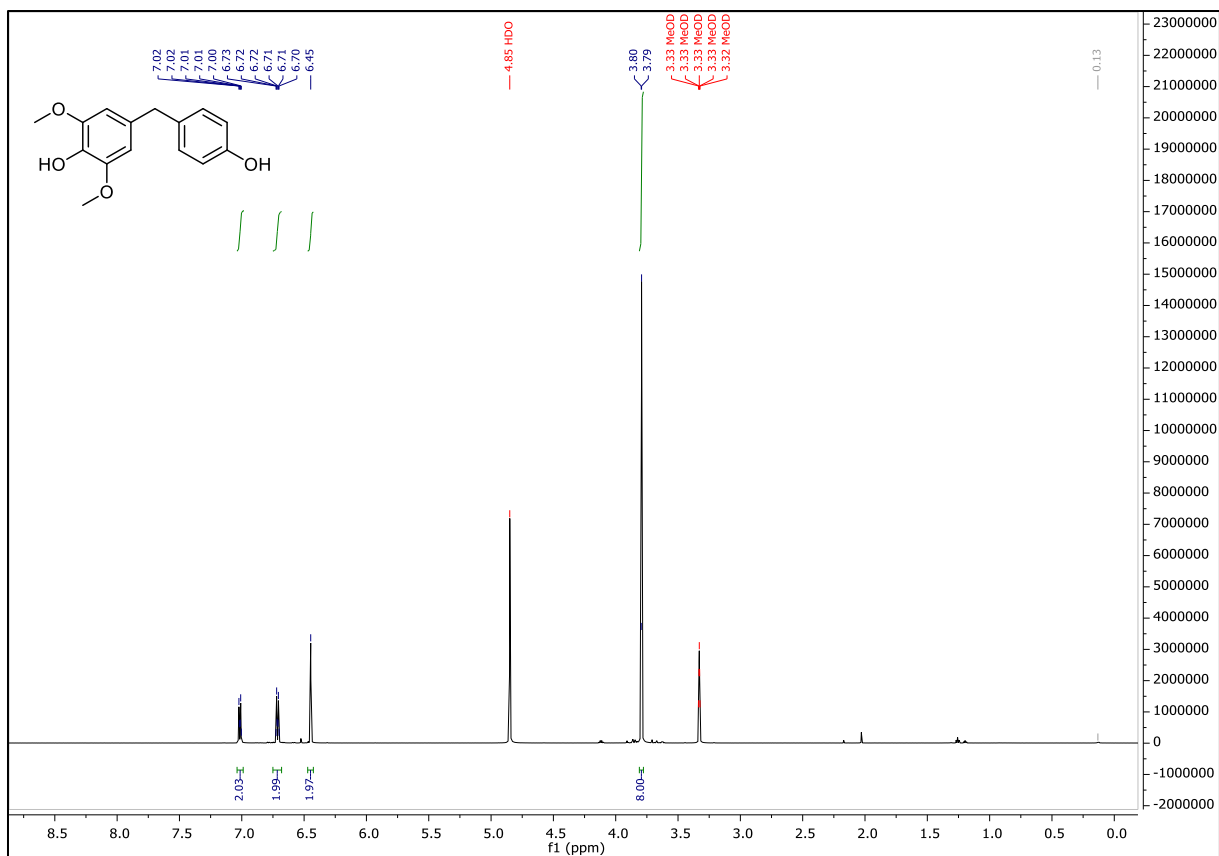


Figure S9. ¹H NMR spectrum of *p, p'*-BSH

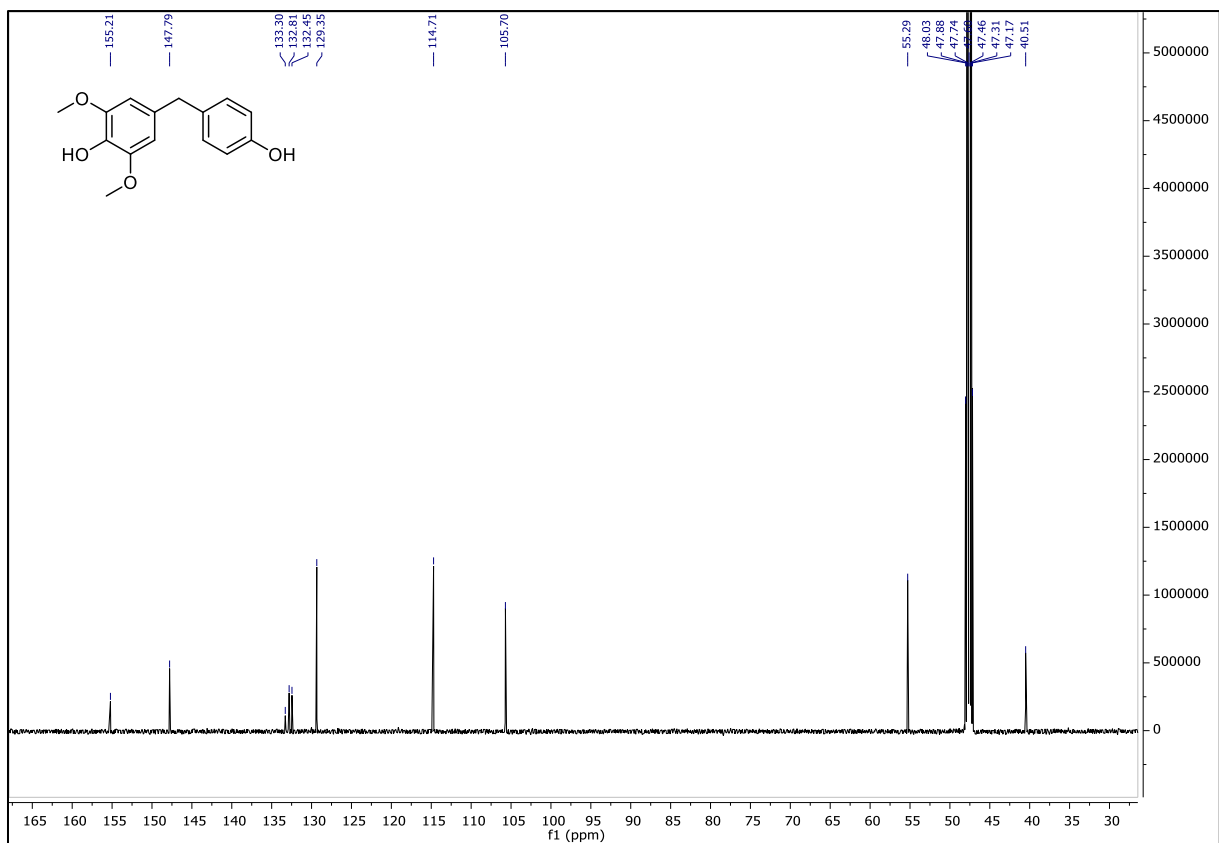


Figure S10. ¹³C NMR spectrum of *p, p'*-BSH

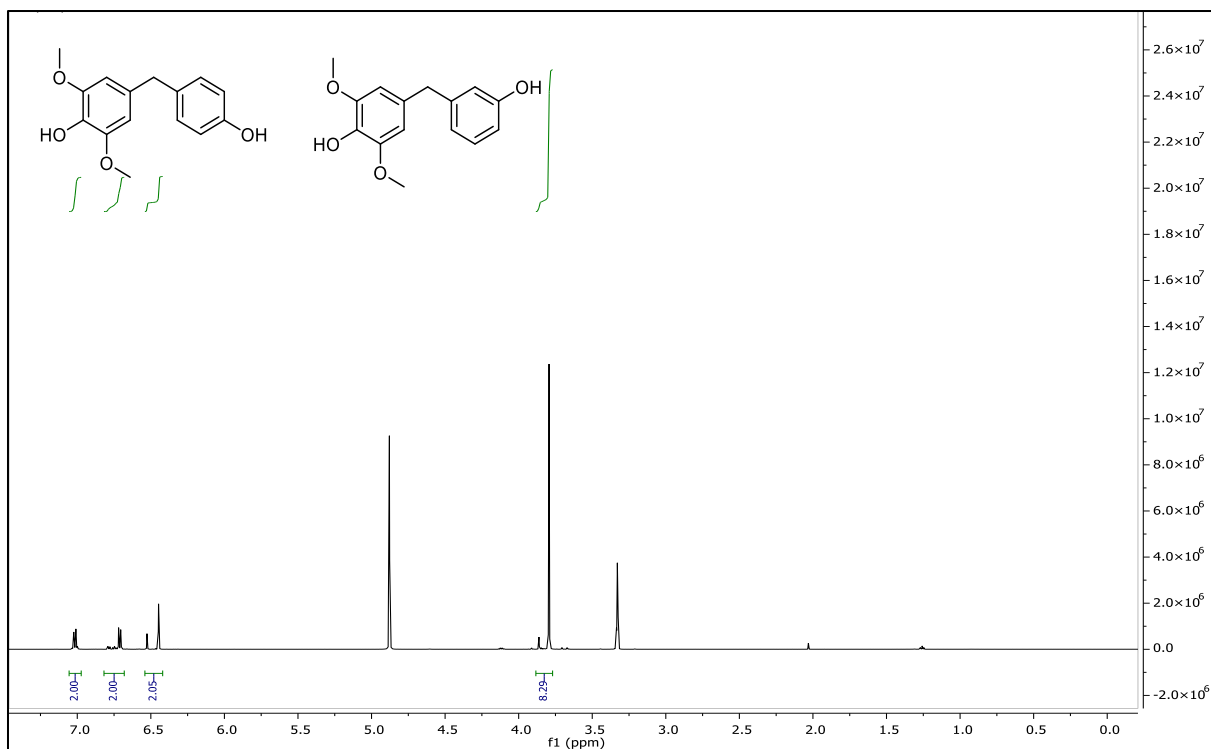


Figure S11. ^1H NMR spectrum of a mixture of *p*, *p'*-BSH and *m*, *p'*-BSH

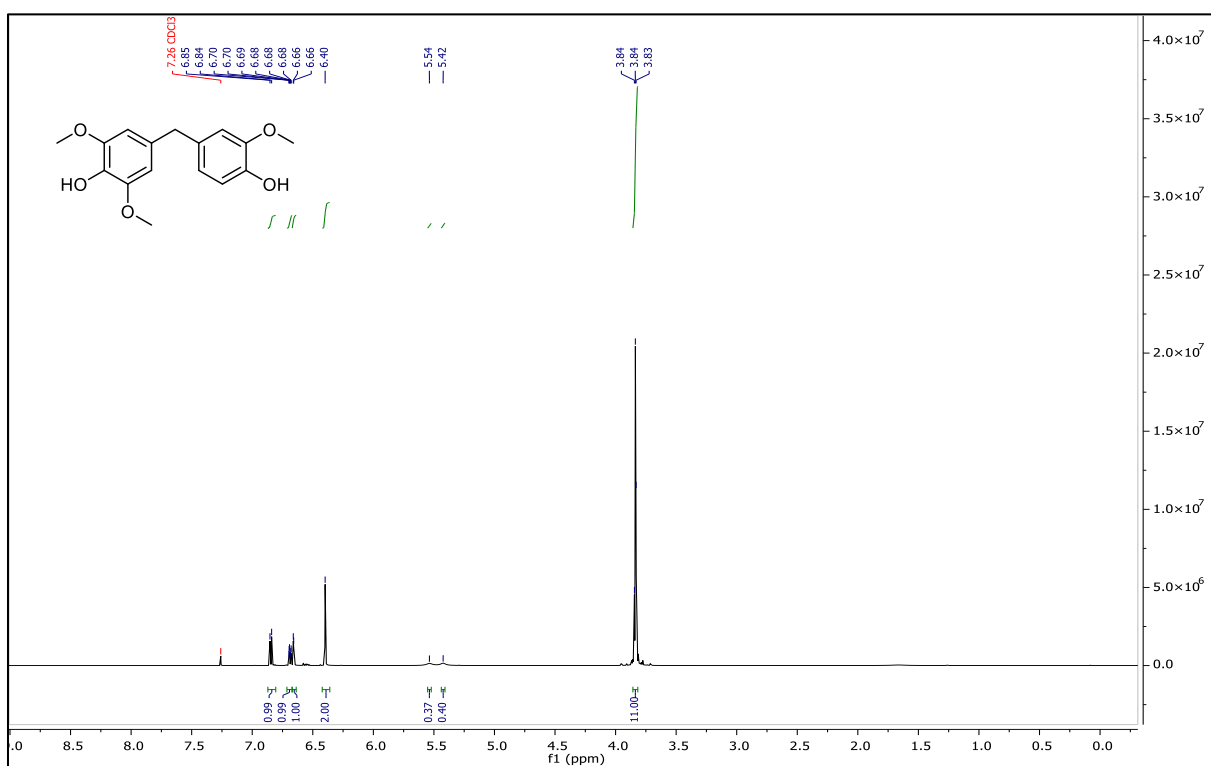


Figure S12. ^1H NMR spectrum of *p*, *p'*-BSG

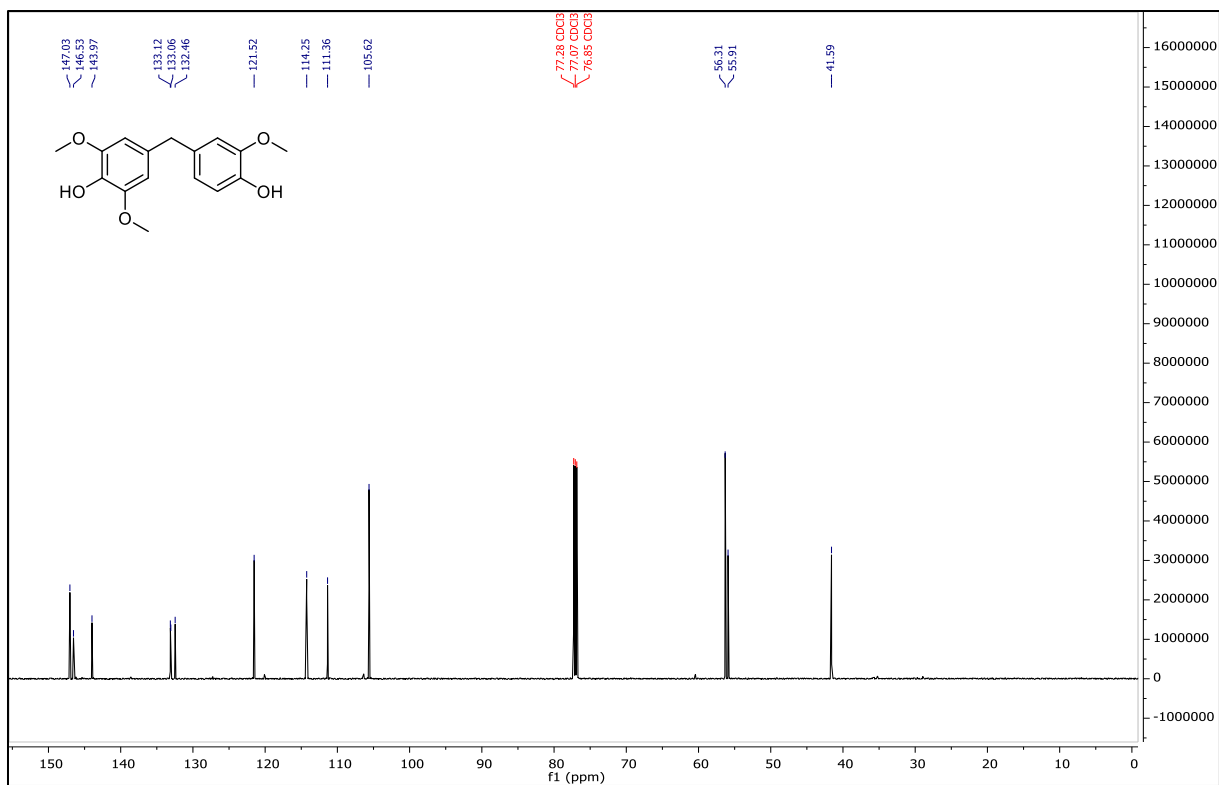


Figure S13. ¹³C NMR spectrum of *p, p'*-BSG

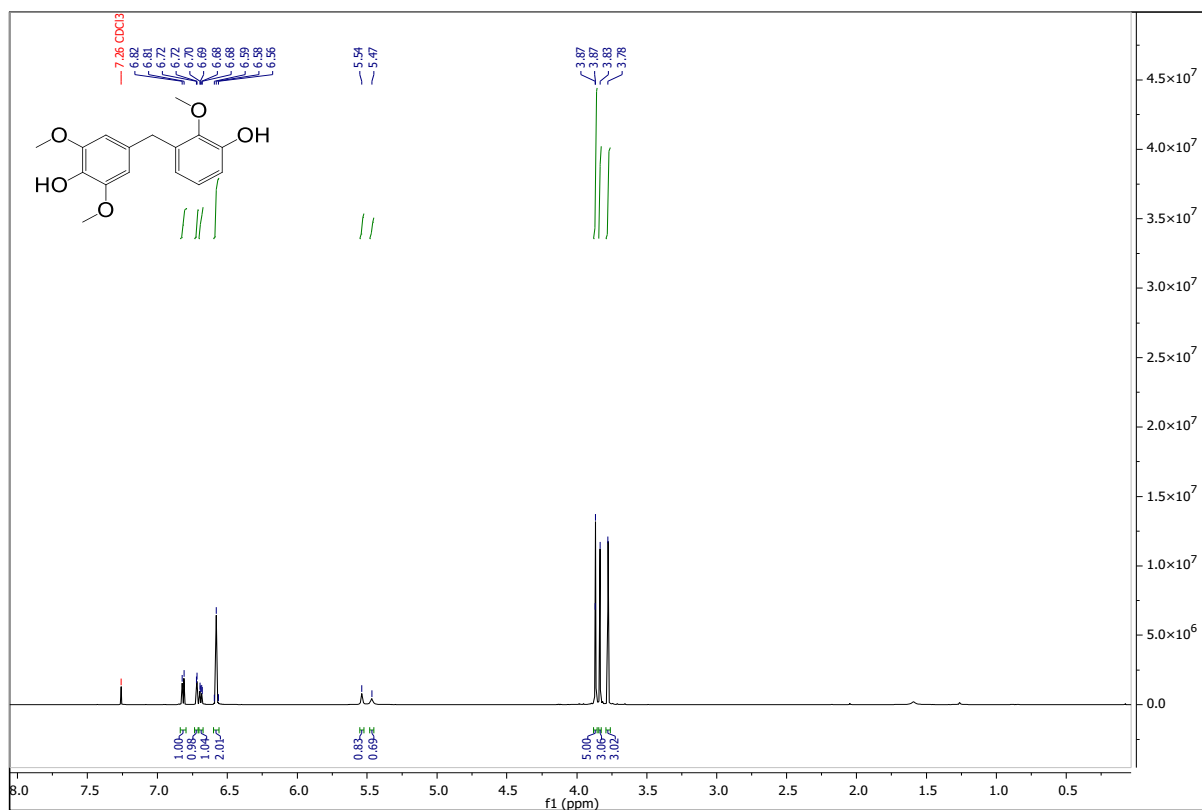


Figure S14. ¹H NMR spectrum of *m, p'*-BSG

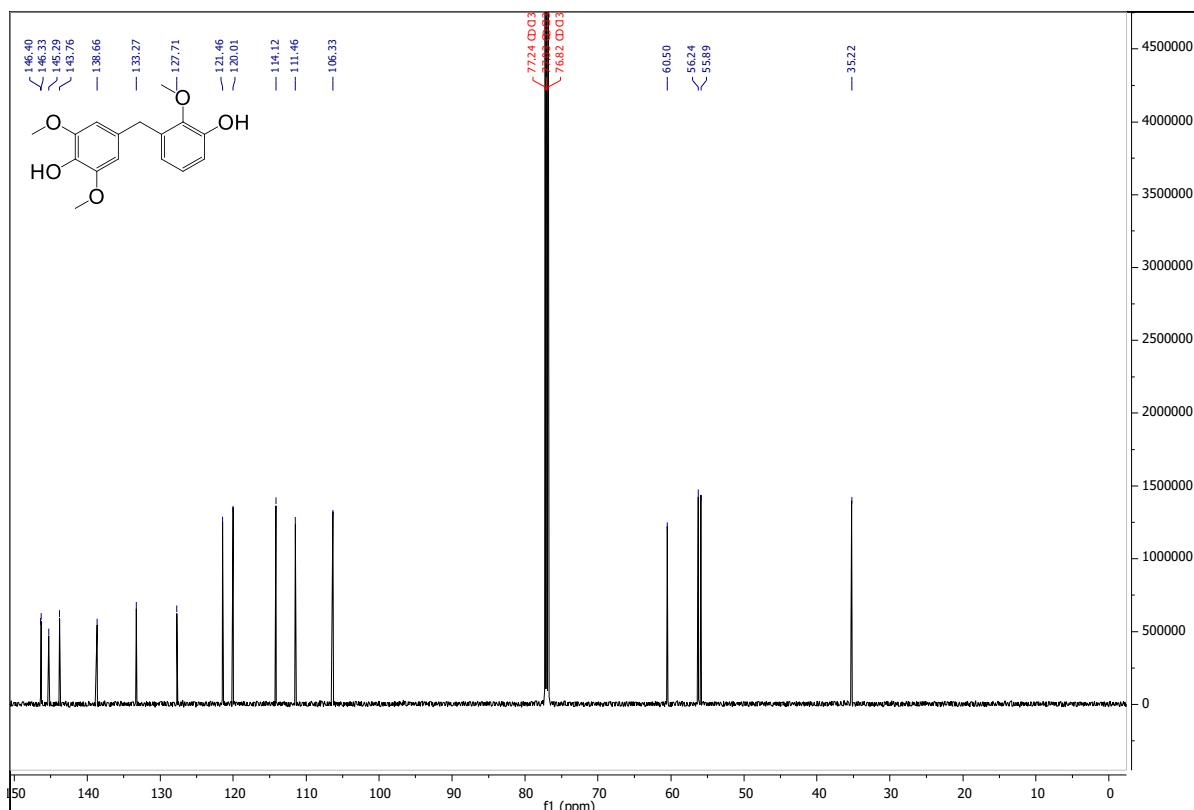


Figure S15. ¹³C NMR spectrum of *m, p'*-BSG

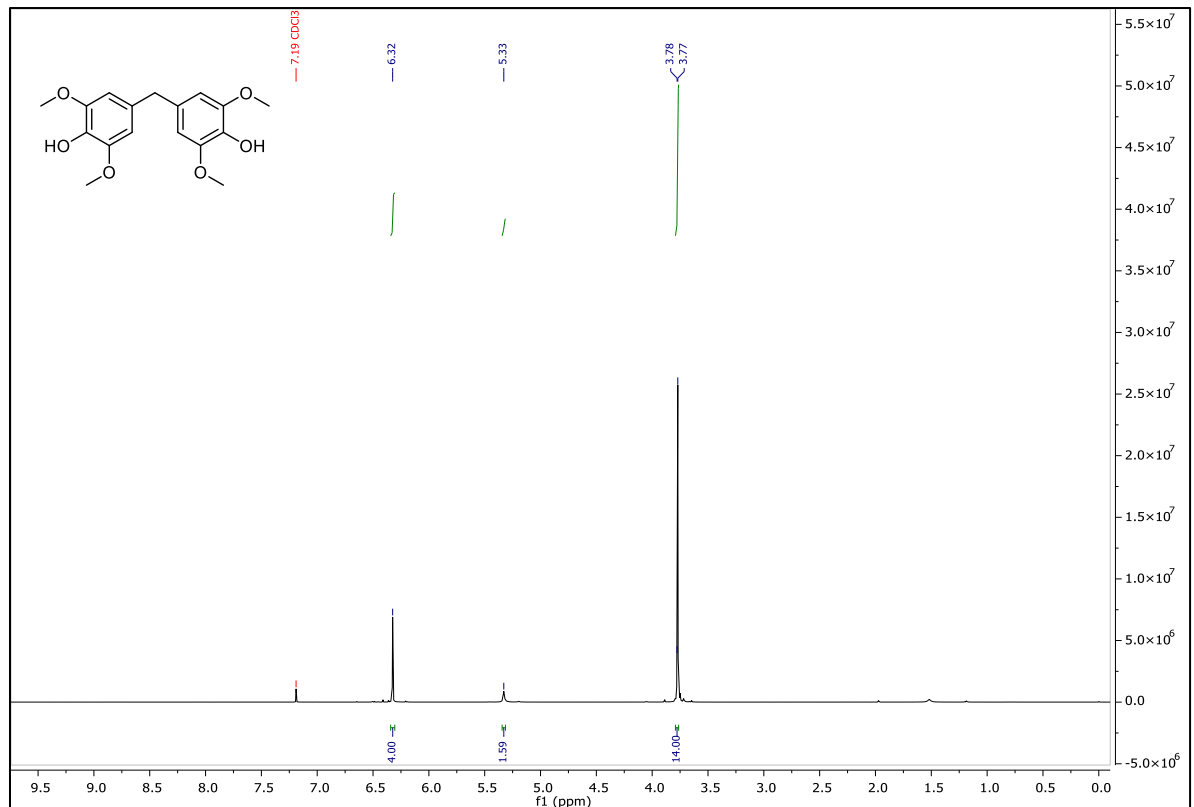


Figure S16. ¹H NMR spectrum of *p, p'*-BSS

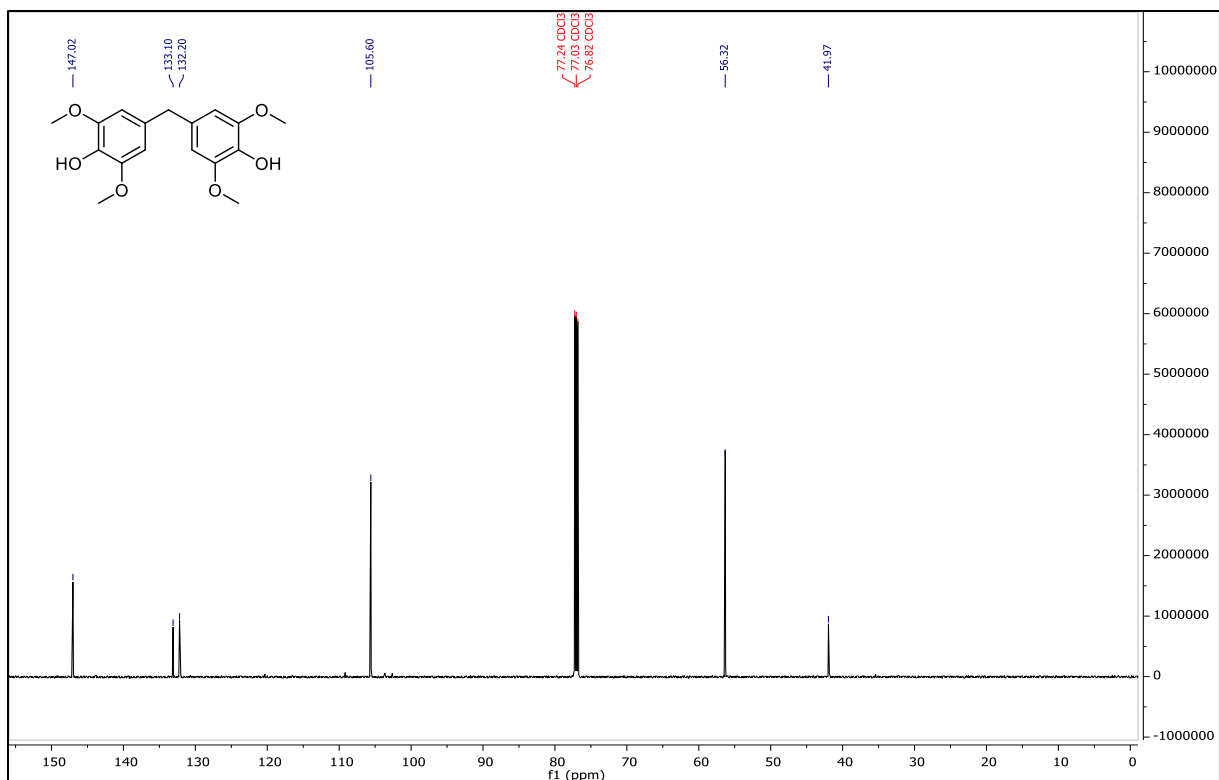


Figure S17. ¹³C NMR spectrum of *p, p'*-BSS

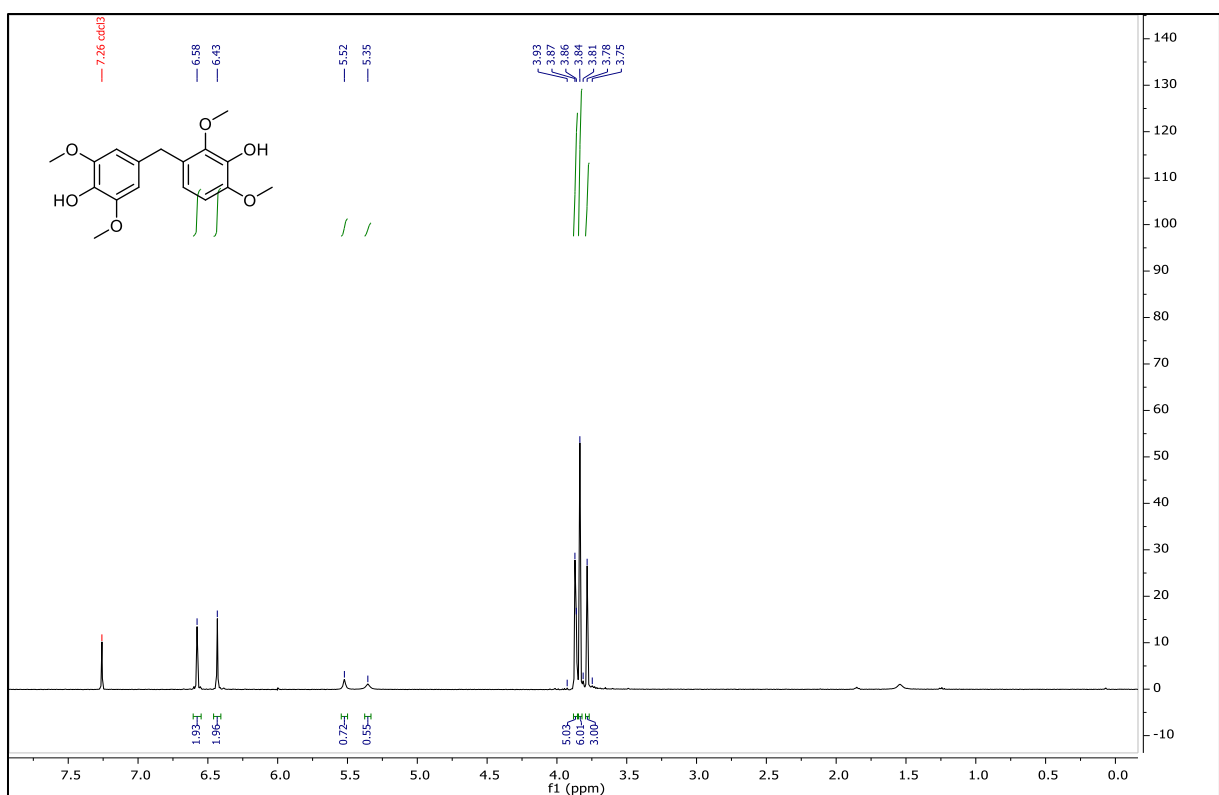


Figure S18. ¹H NMR spectrum of *m, p'*-BSS

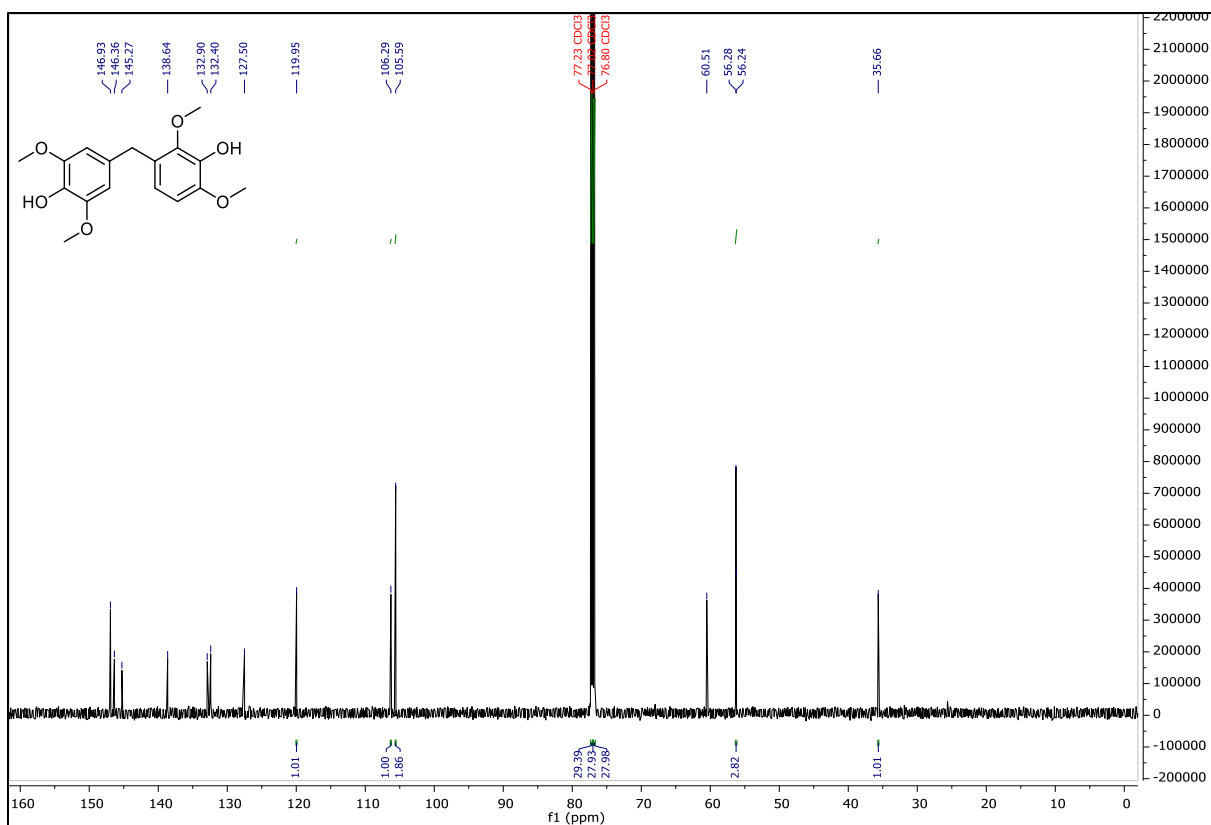


Figure S19. ^{13}C NMR spectrum of *m, p'*-BSS

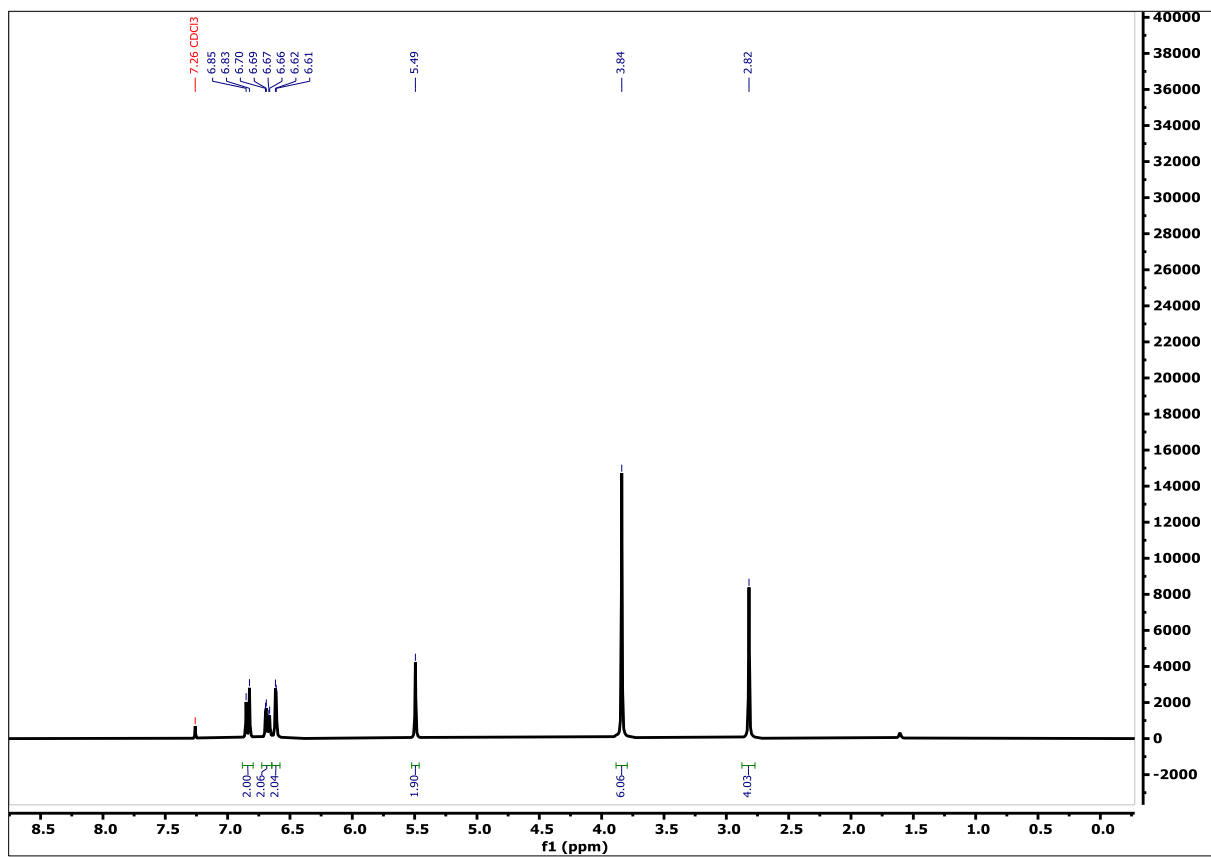


Figure S20. ^1H NMR spectrum of β -1

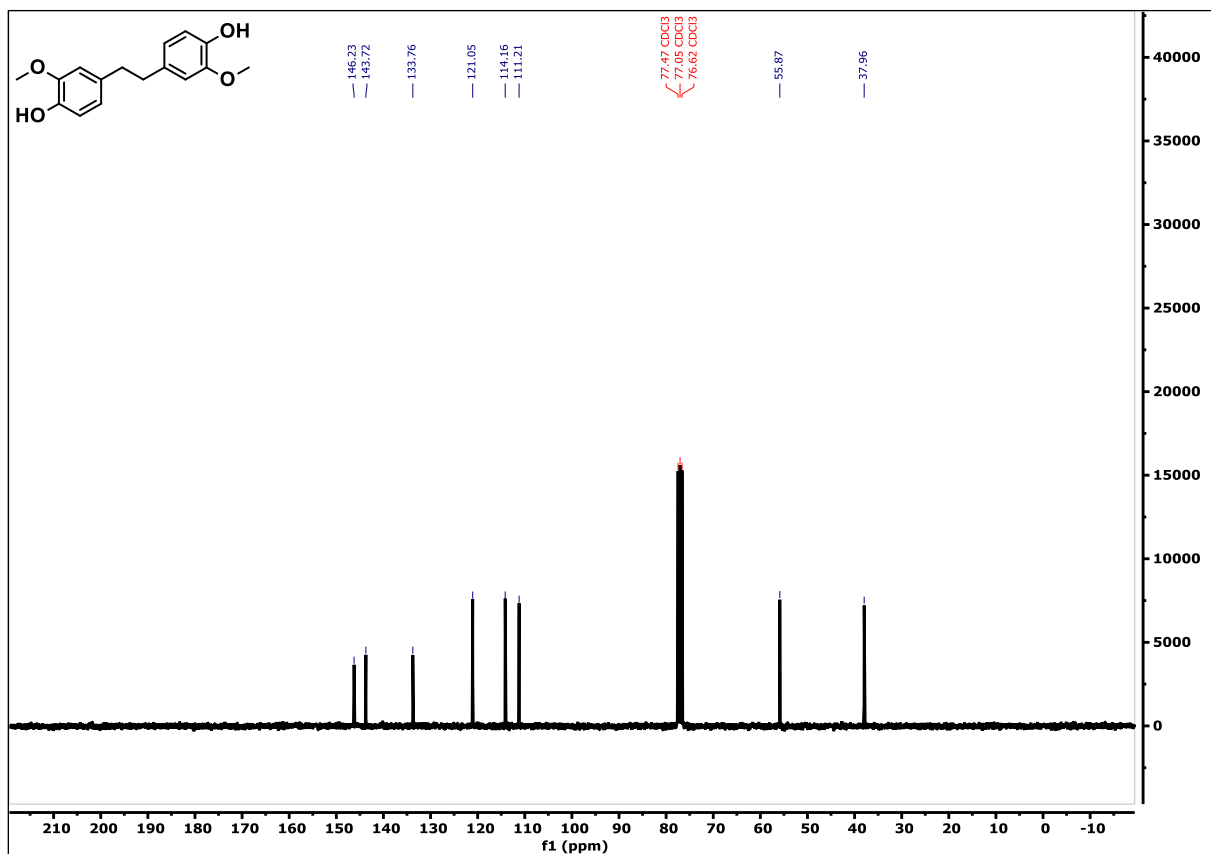


Figure S21. ^{13}C NMR spectrum of β -1

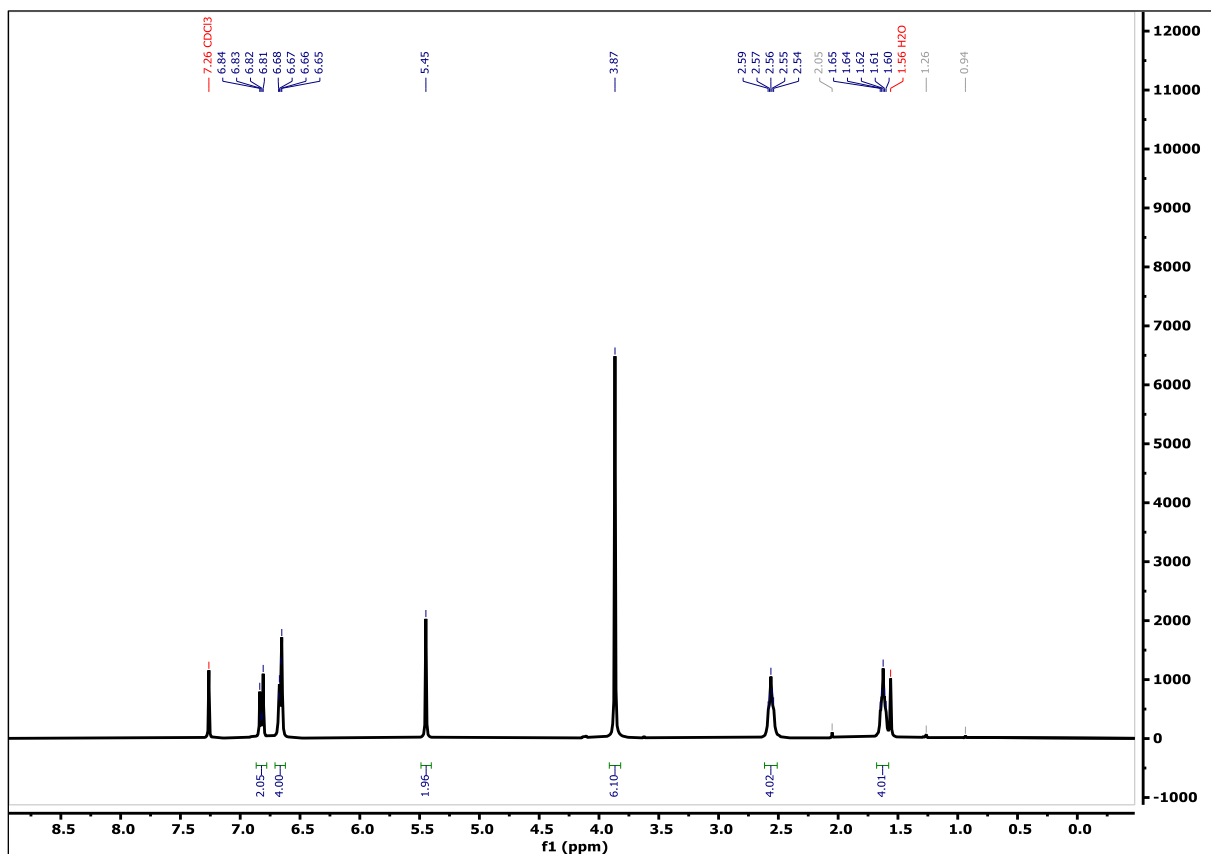


Figure S22. ^1H NMR spectrum of β - β

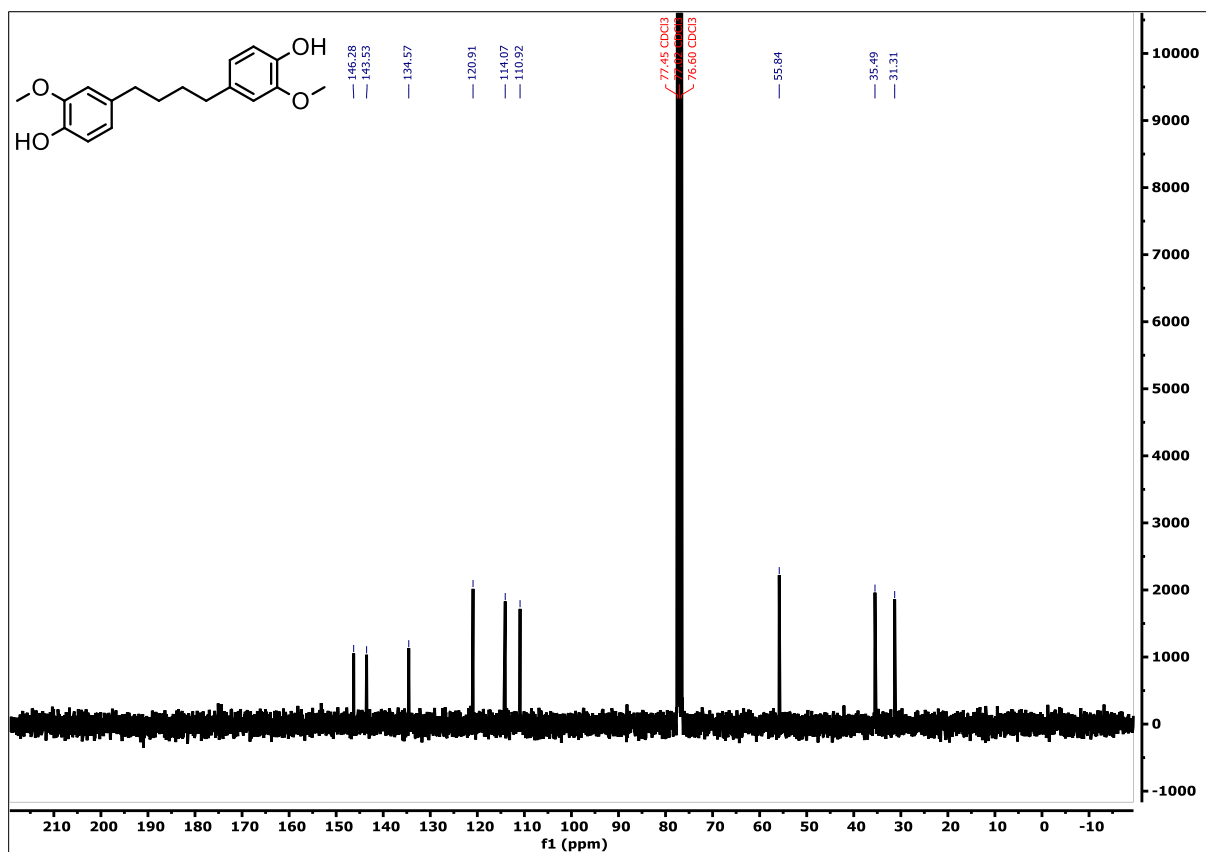


Figure S23. ^{13}C NMR spectrum of β - β

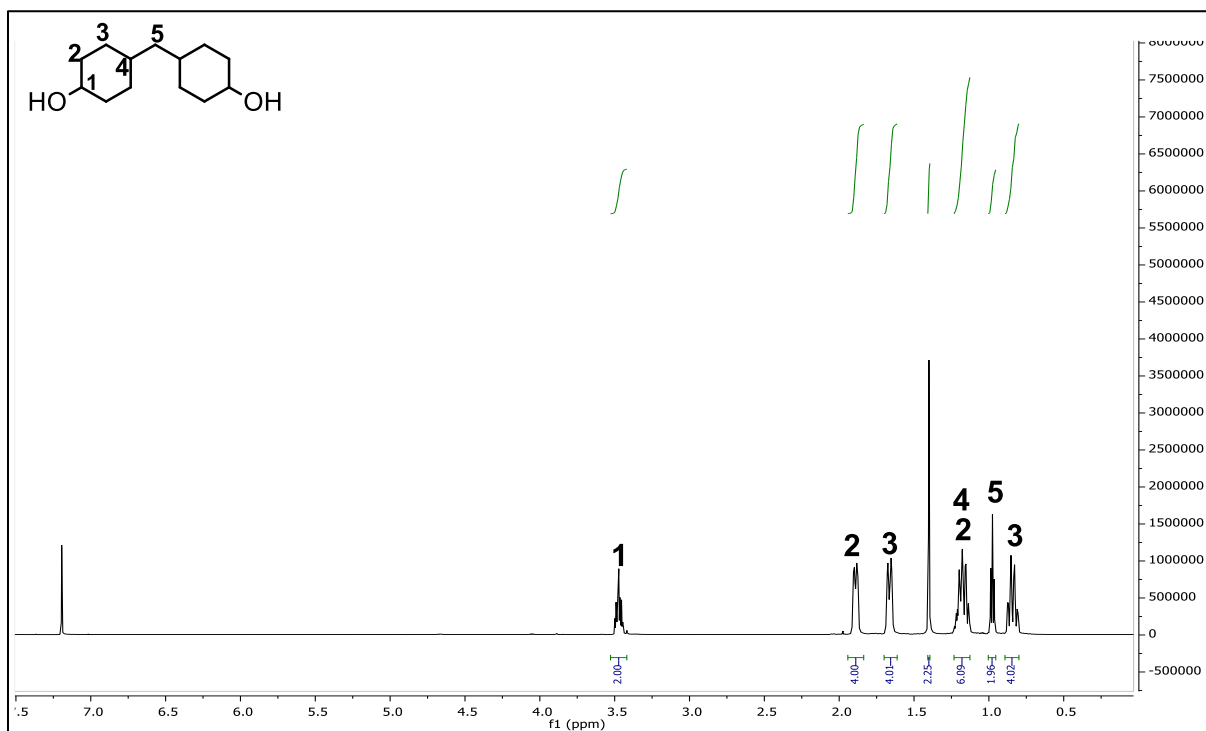


Figure S24. ^1H NMR spectrum of MBC (*trans-trans*)

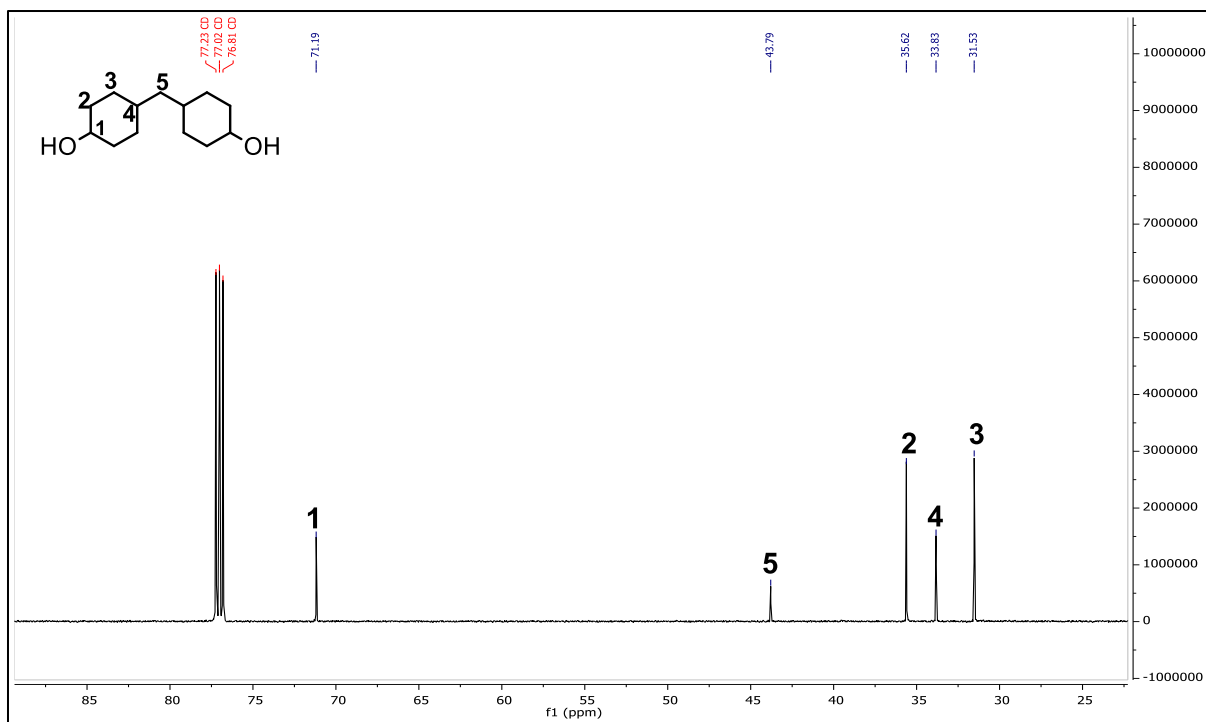


Figure S25. ^{13}C NMR spectrum of **MBC** (*trans-trans*)

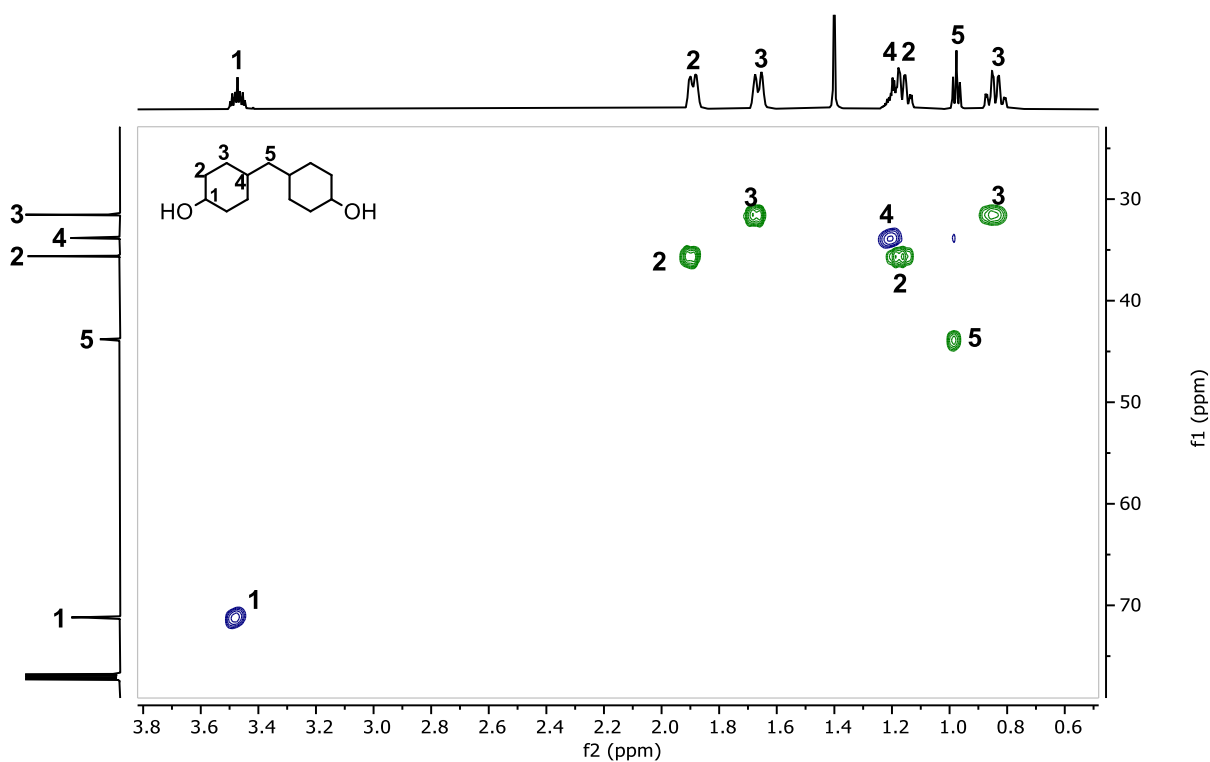


Figure S26. 2D-HSQC spectrum of **MBC** (*trans-trans*)

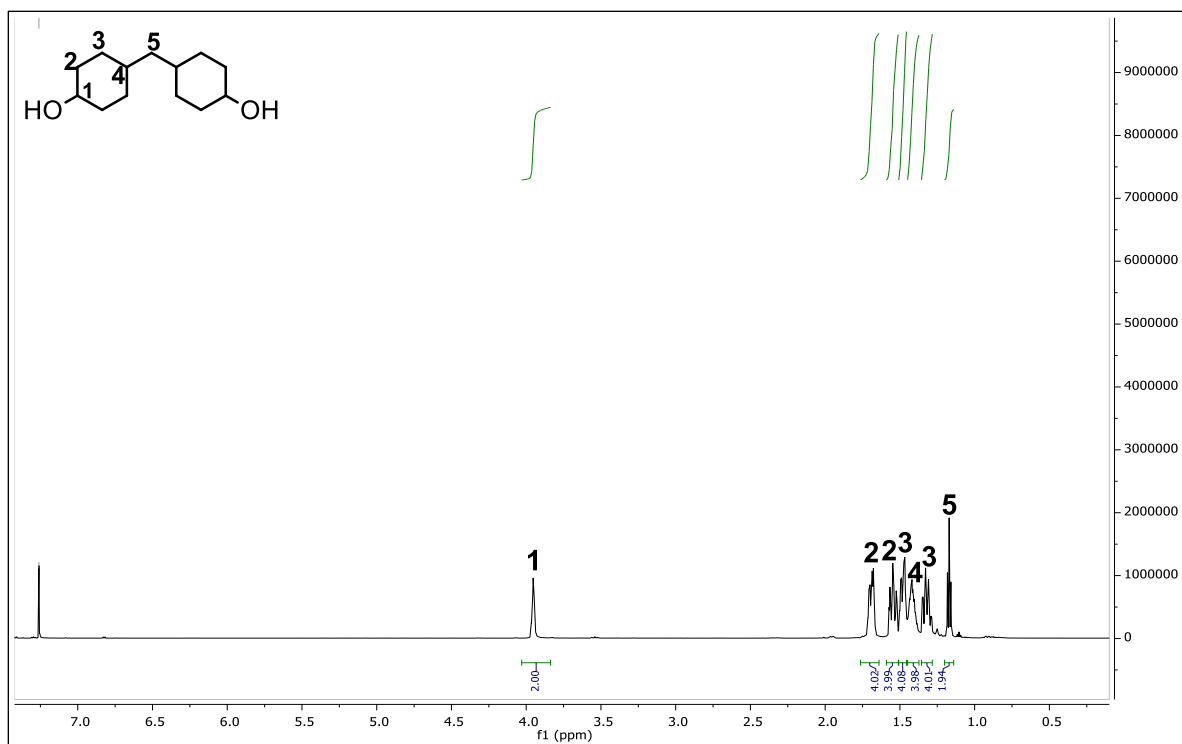


Figure S27. ¹H NMR spectrum of MBC (*cis-cis*)

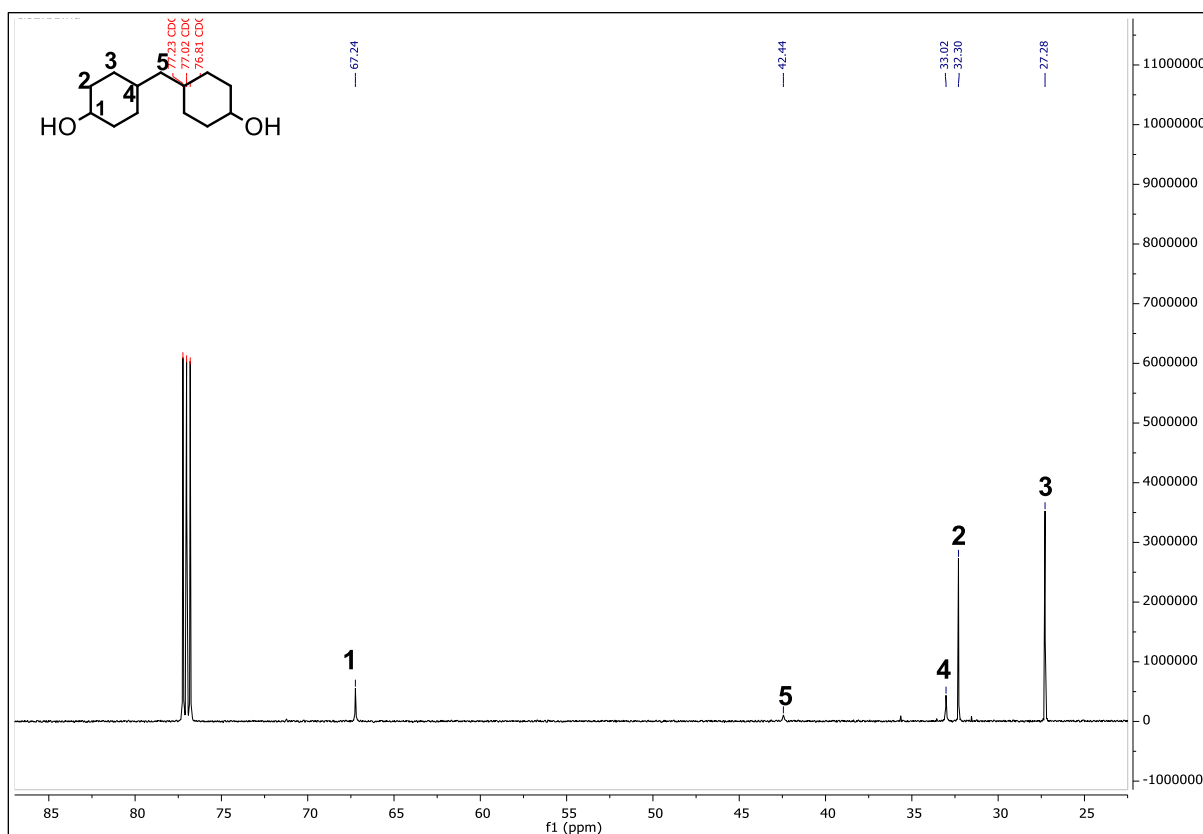


Figure S28. ¹³C NMR spectrum of MBC (*cis-cis*)

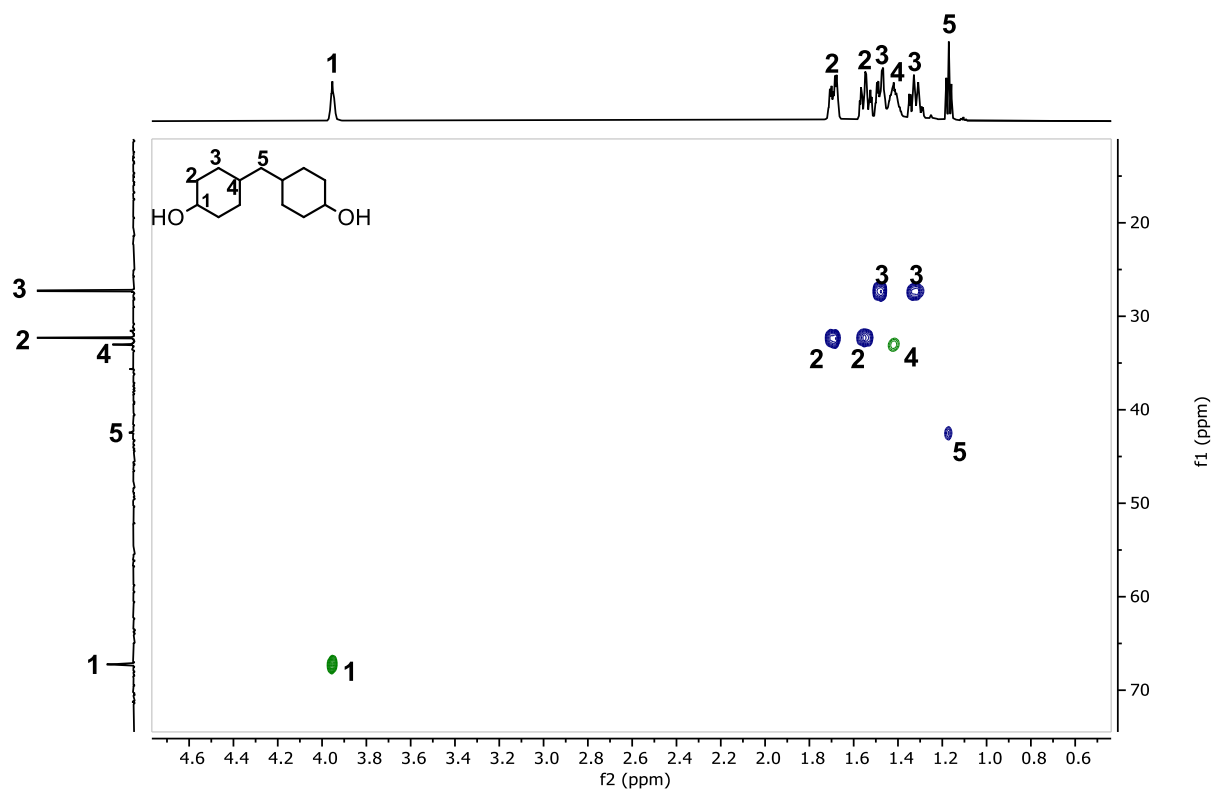


Figure S29. 2D-HSQC spectrum of **MBC** (*cis-cis*)

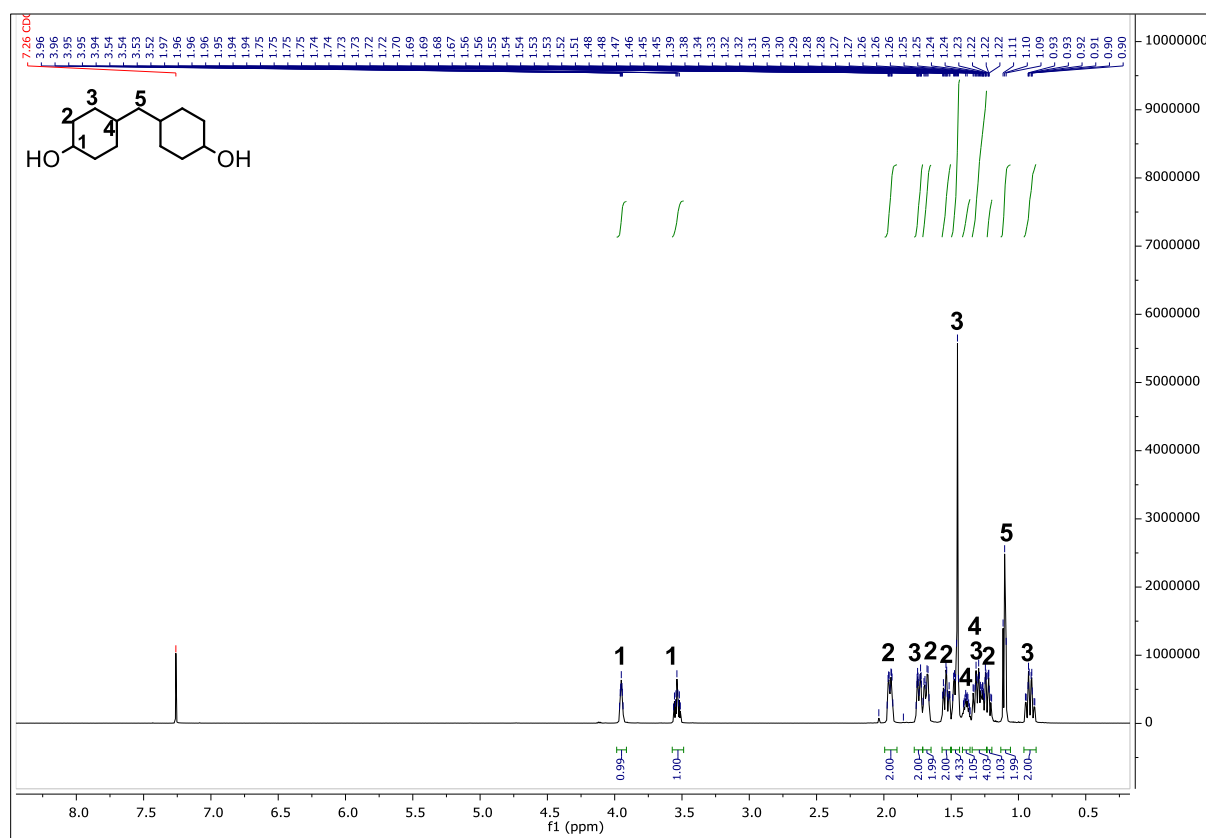


Figure S30. ^1H NMR spectrum of **MBC** (*cis-trans*)

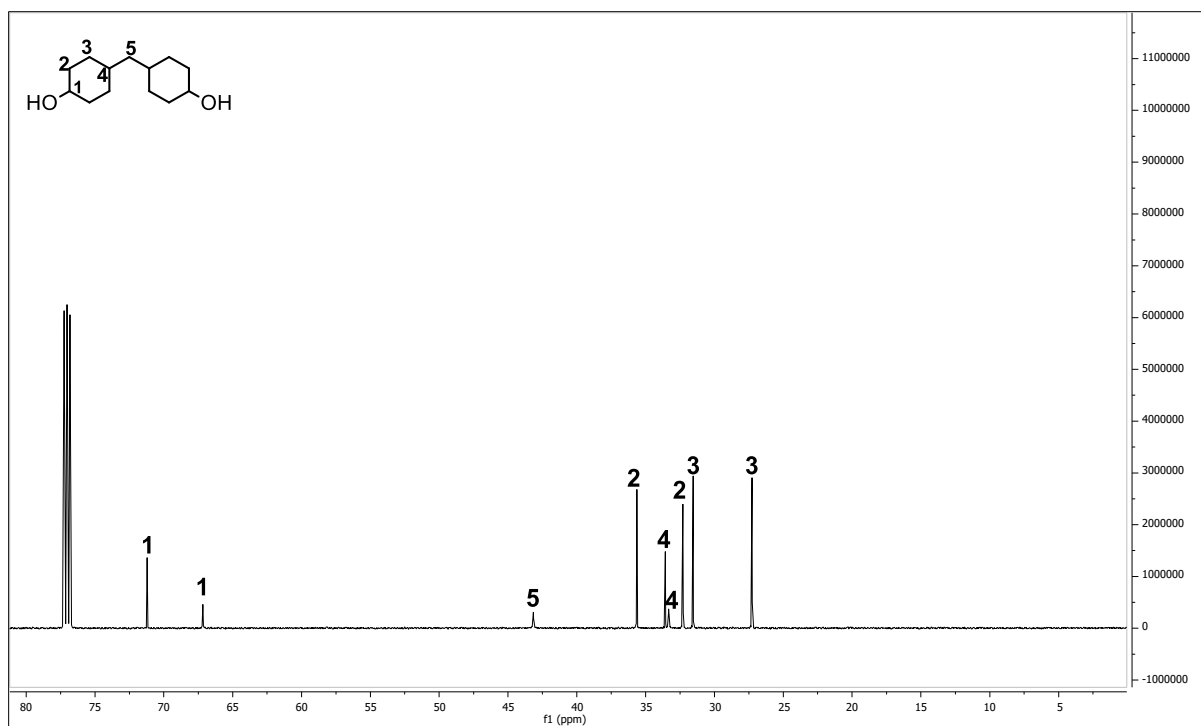


Figure S31. ¹³C NMR spectrum of **MBC** (*cis-trans*)

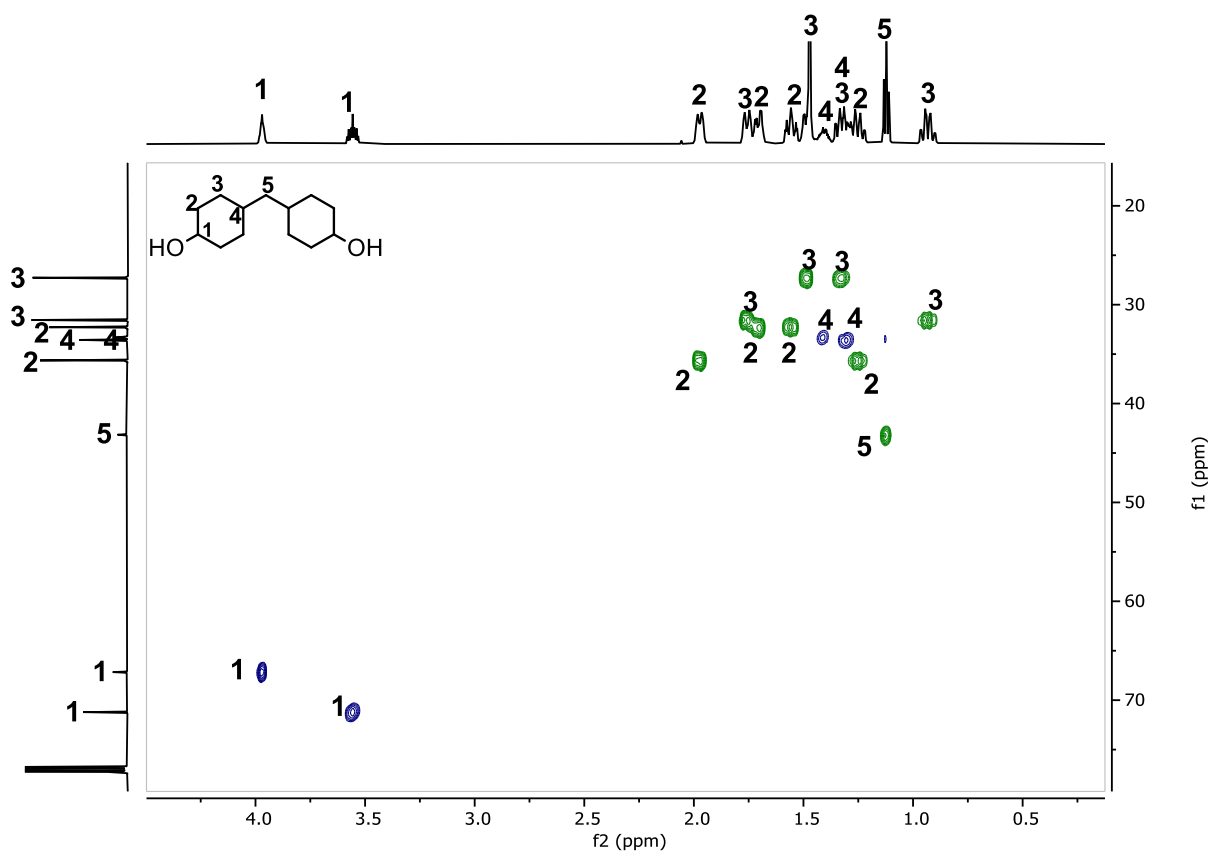


Figure S32. 2D HSQC spectrum of **MBC** (*cis-trans*)

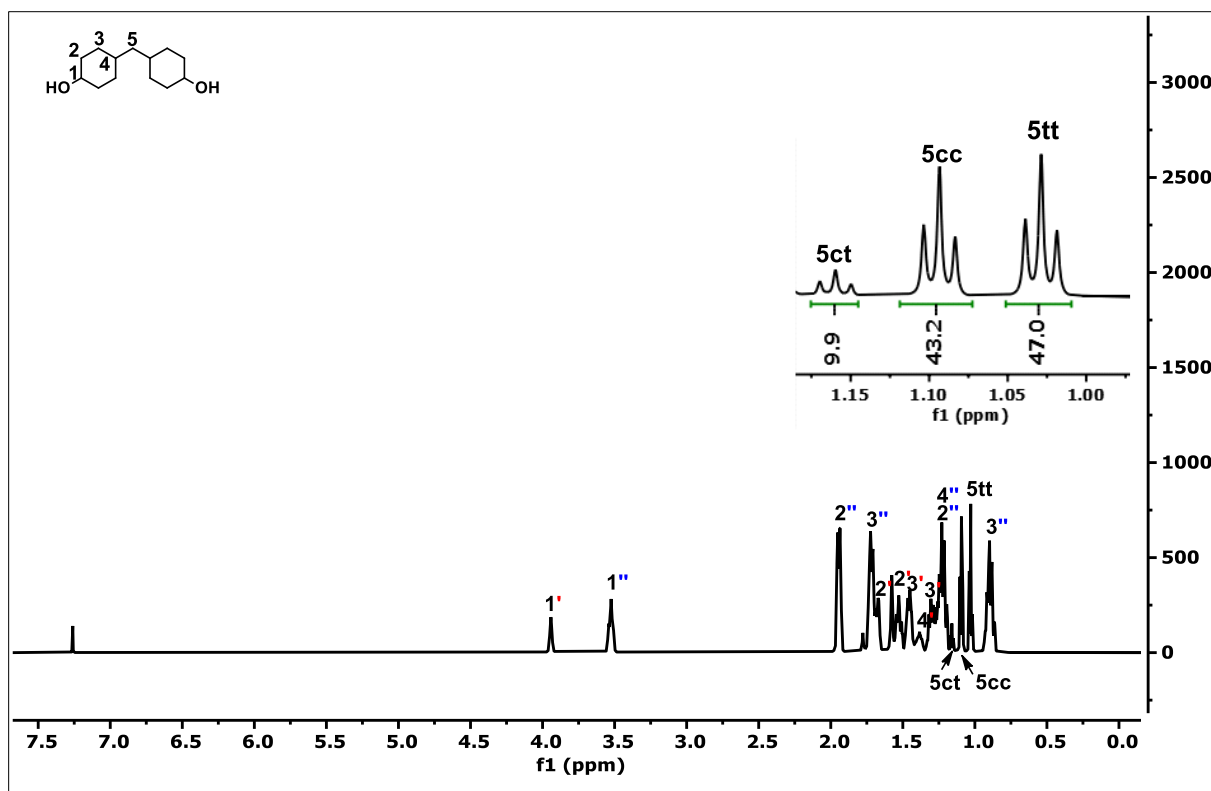


Figure S33. ¹H NMR spectrum of MBC (*cis-cis*, *cis-trans* and *trans-trans*)

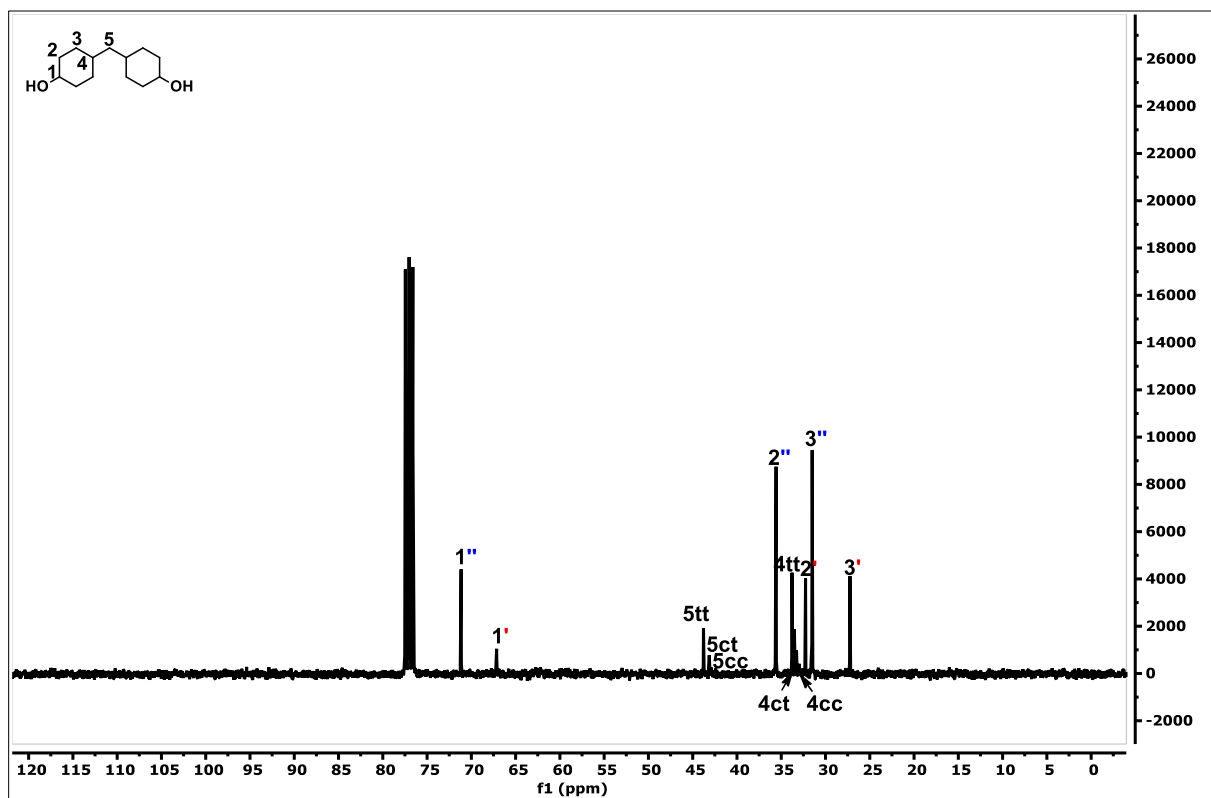


Figure S34. ¹³C NMR spectrum of MBC (*cis-cis*, *cis-trans* and *trans-trans*)

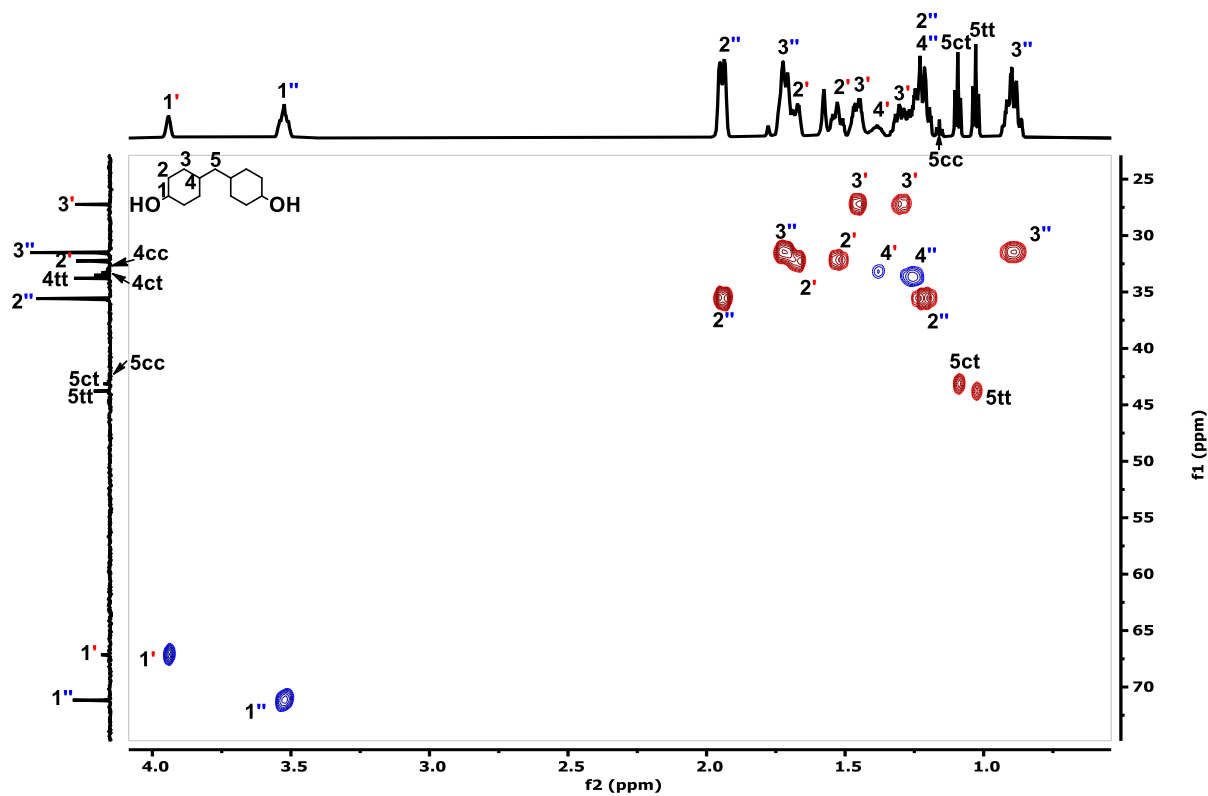


Figure S35. 2D HSQC spectrum of MBC (*cis-cis*, *cis-trans* and *trans-trans*)

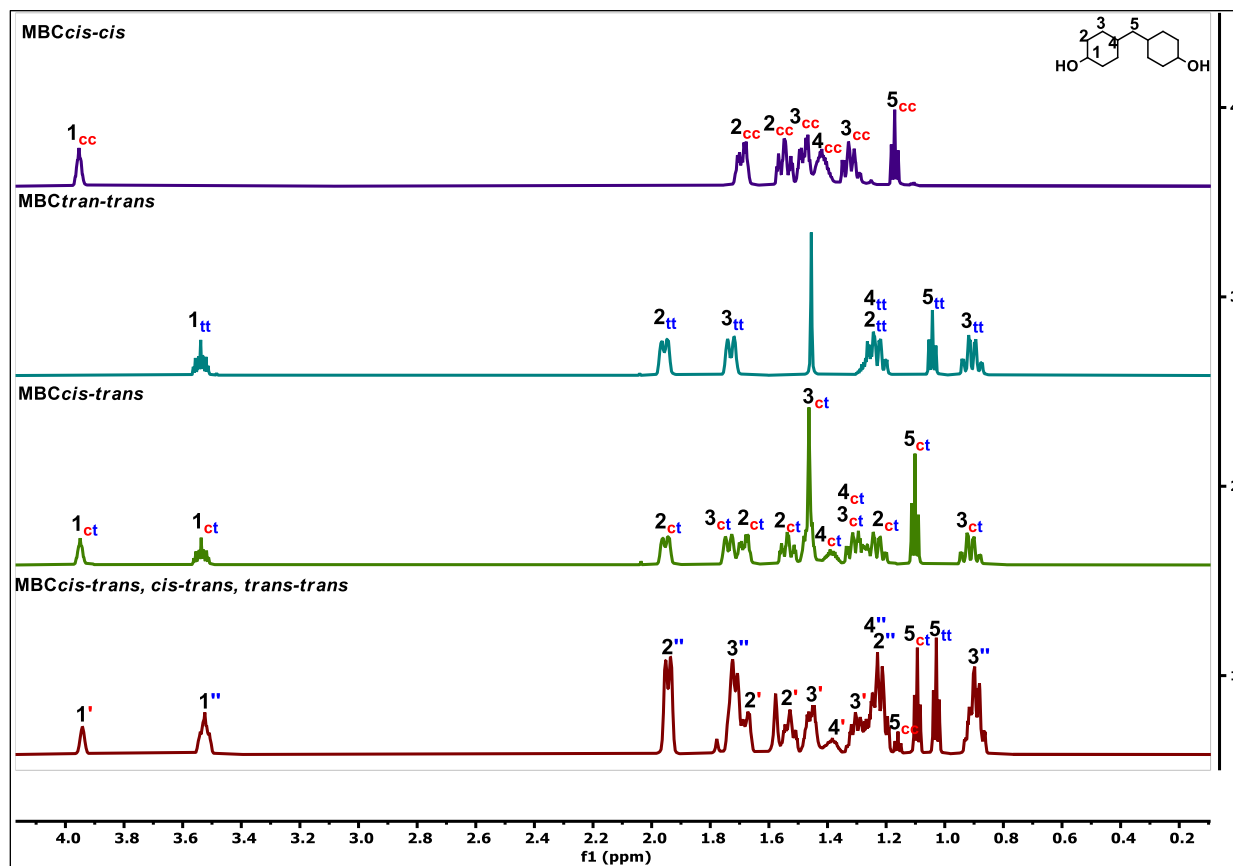


Figure S36. ¹H NMR spectra of MBC *cis-cis*, MBC *cis-trans*, MBC *trans-trans* and MBC *cis-cis*, *cis-trans*, *trans-trans*

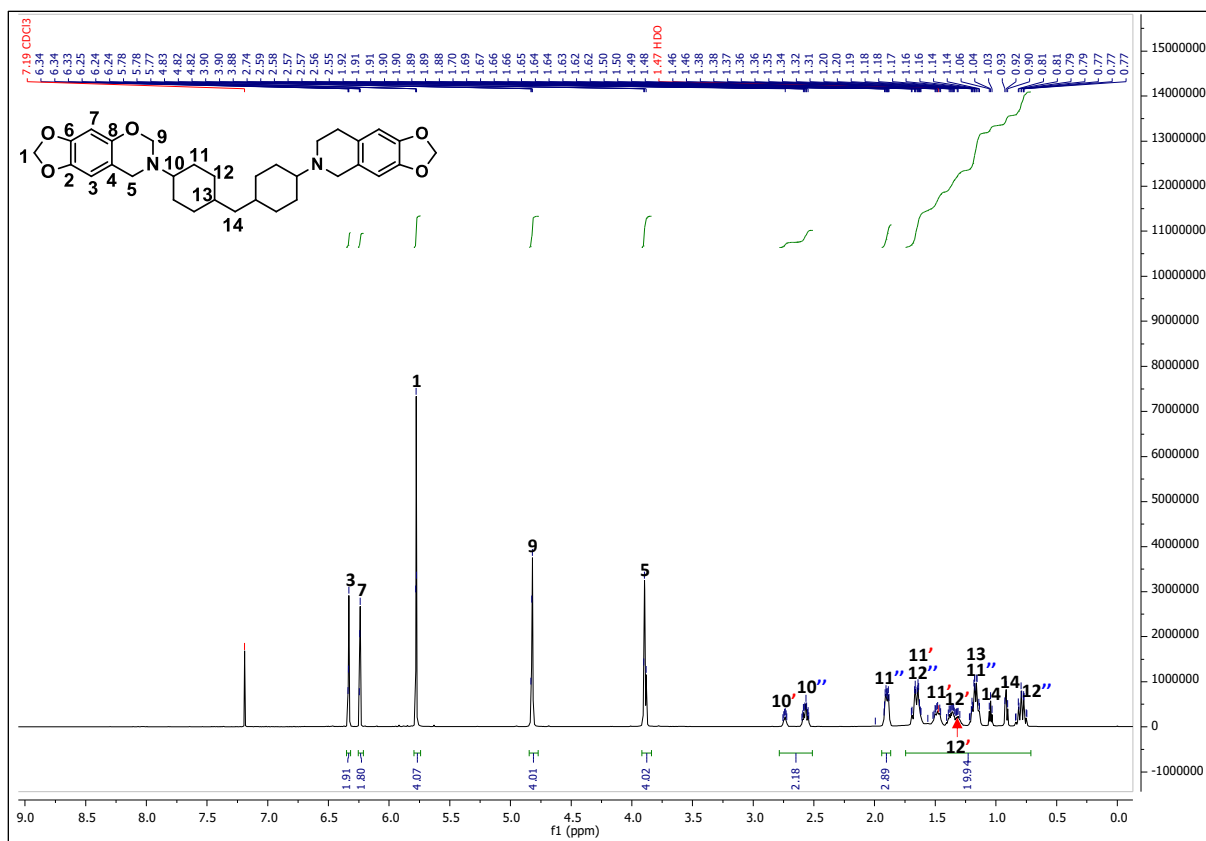


Figure S37. ¹H NMR spectrum of S-MBCA

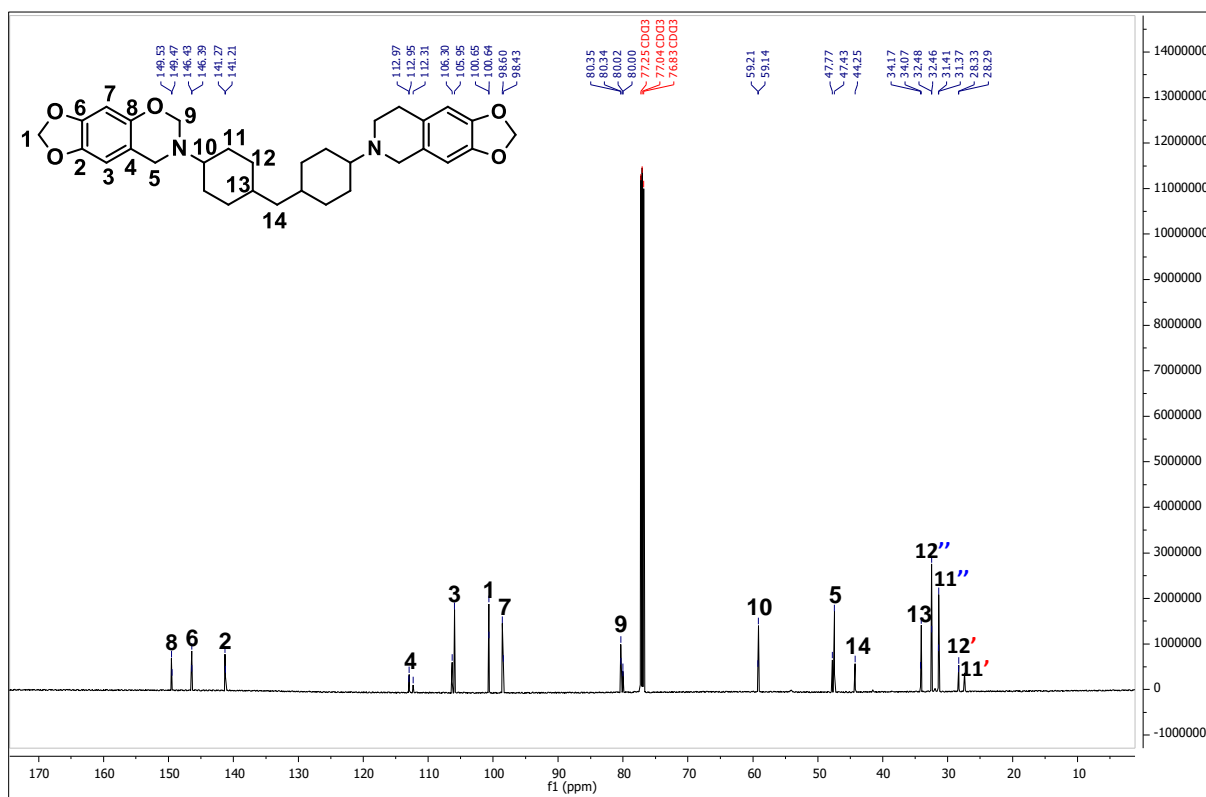


Figure S38. ¹³C NMR spectrum of S-MBCA

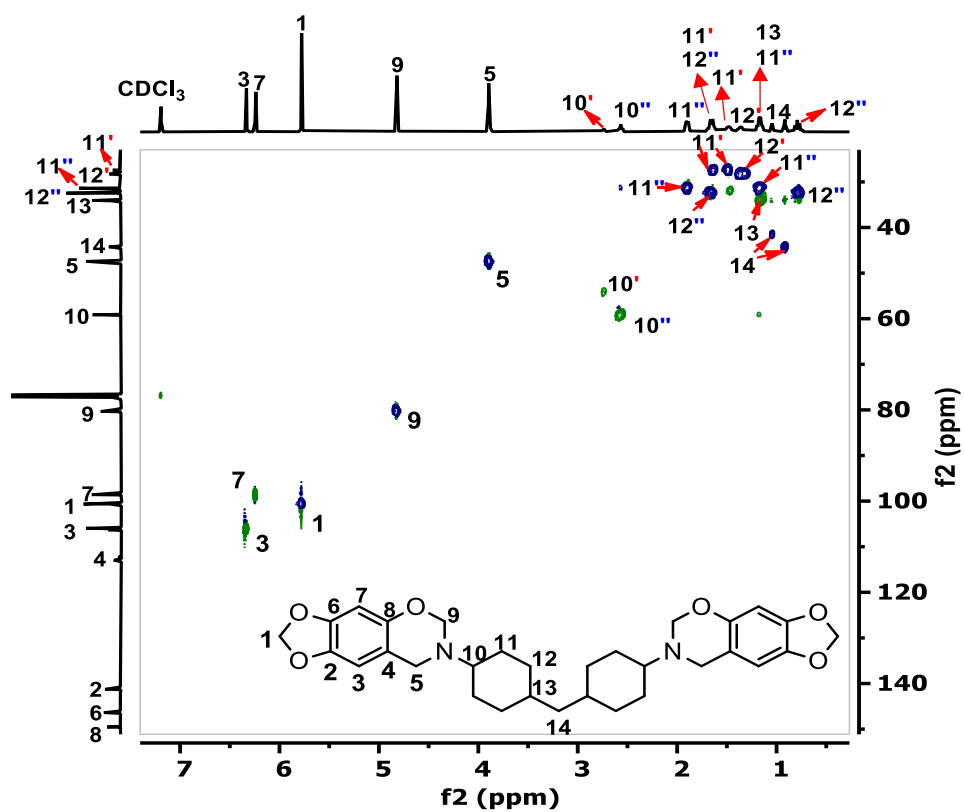


Figure S39. 2D HSQC spectrum of **S-MBCA**

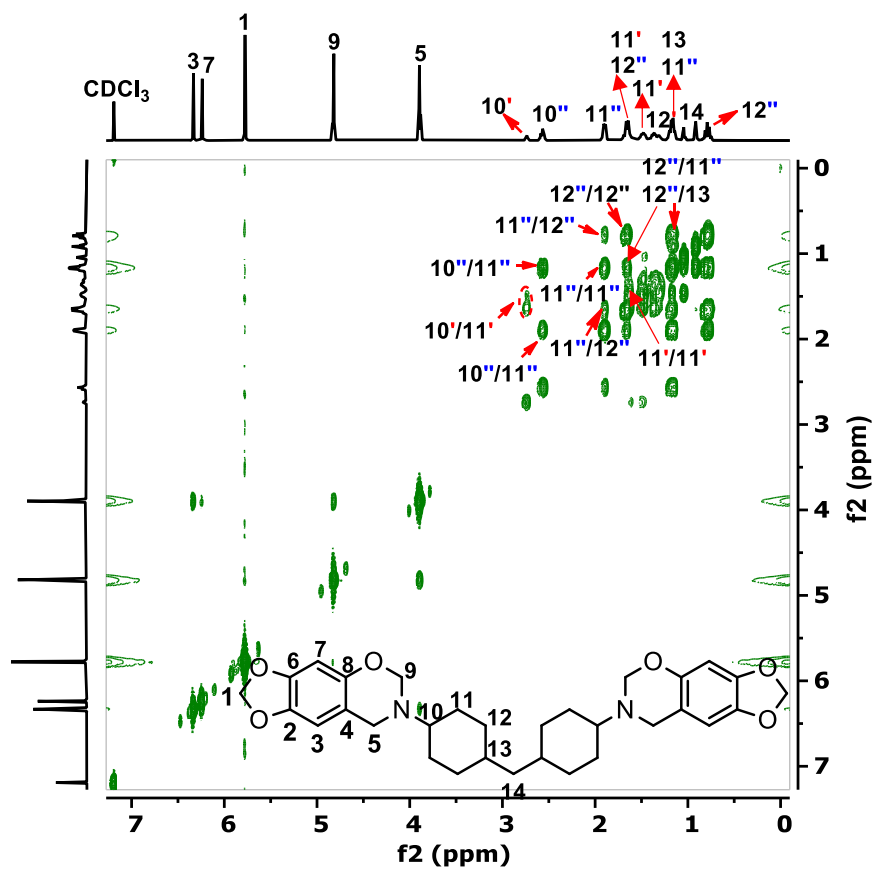


Figure S40. 2D COSY spectrum of **S-MBCA**

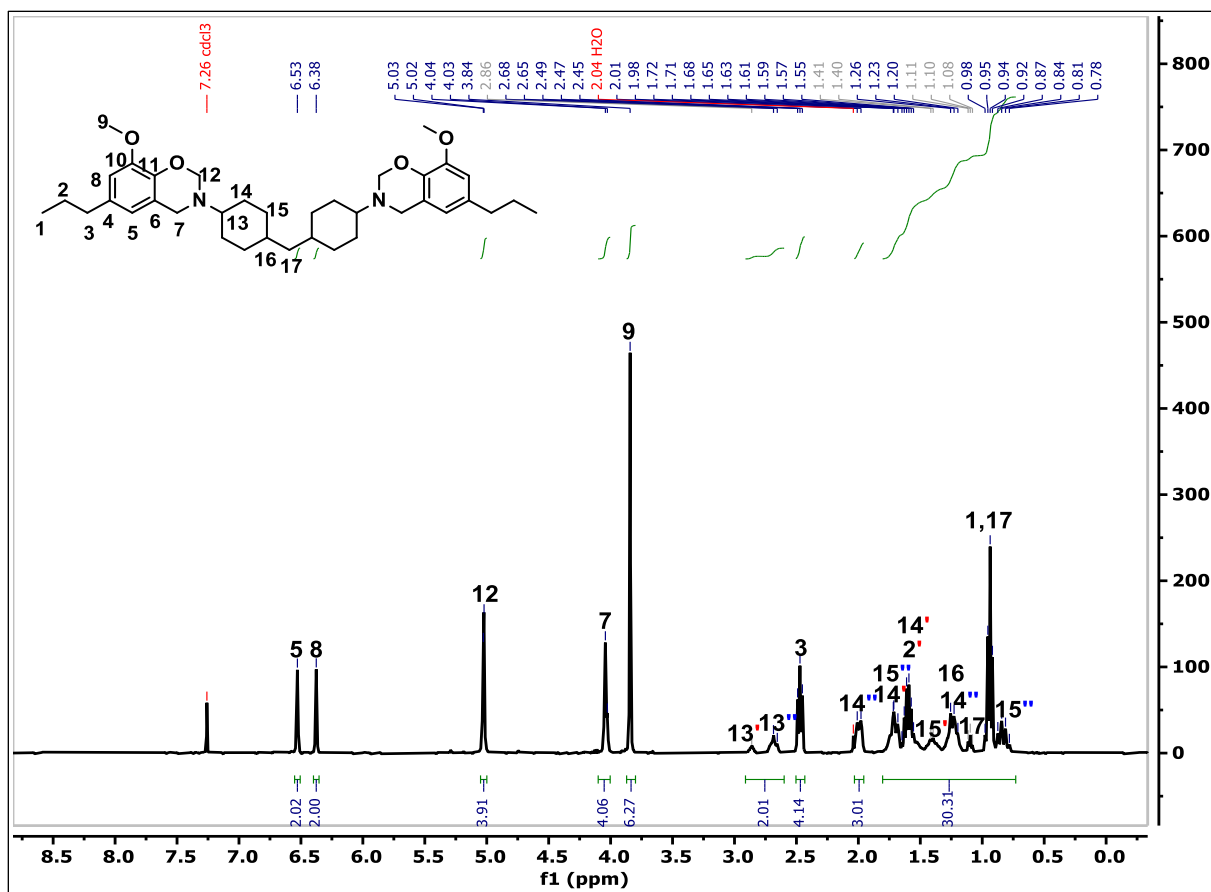


Figure S41. ¹H NMR spectrum of PG-MBCA

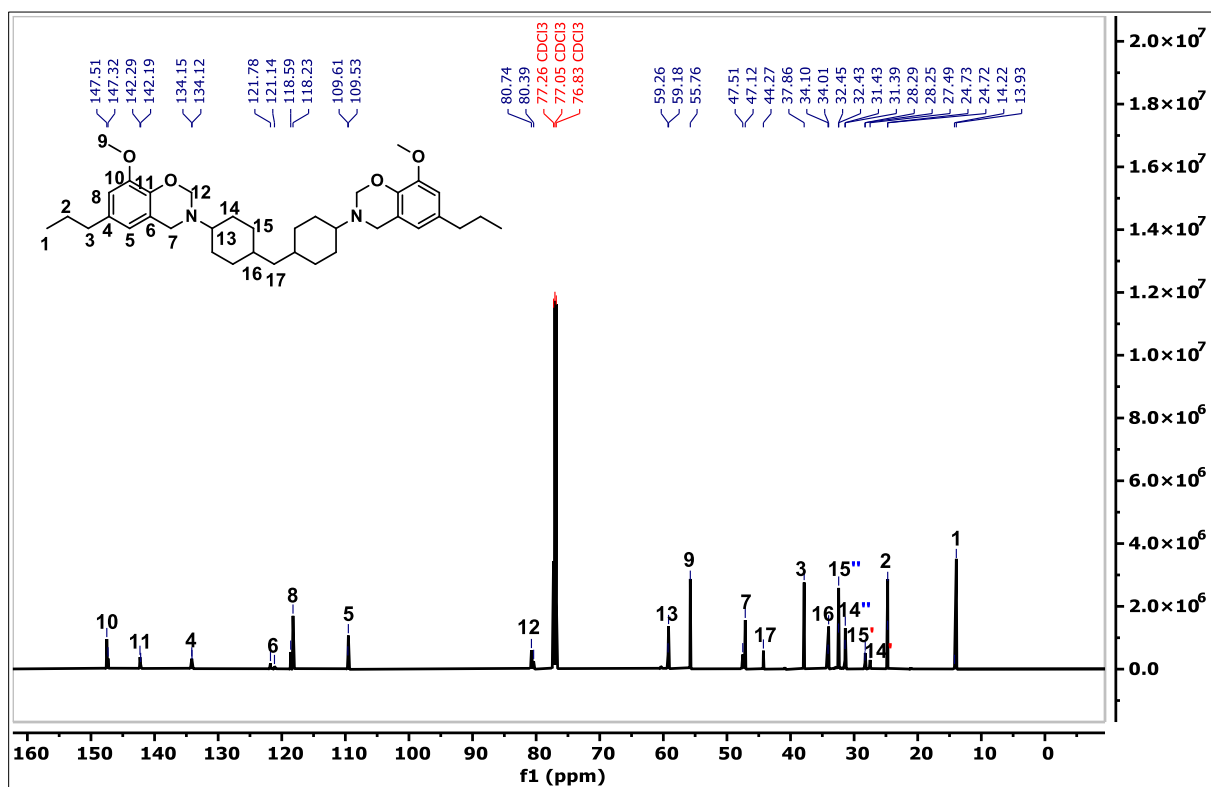


Figure S42. ¹³C NMR spectrum of PG-MBCA

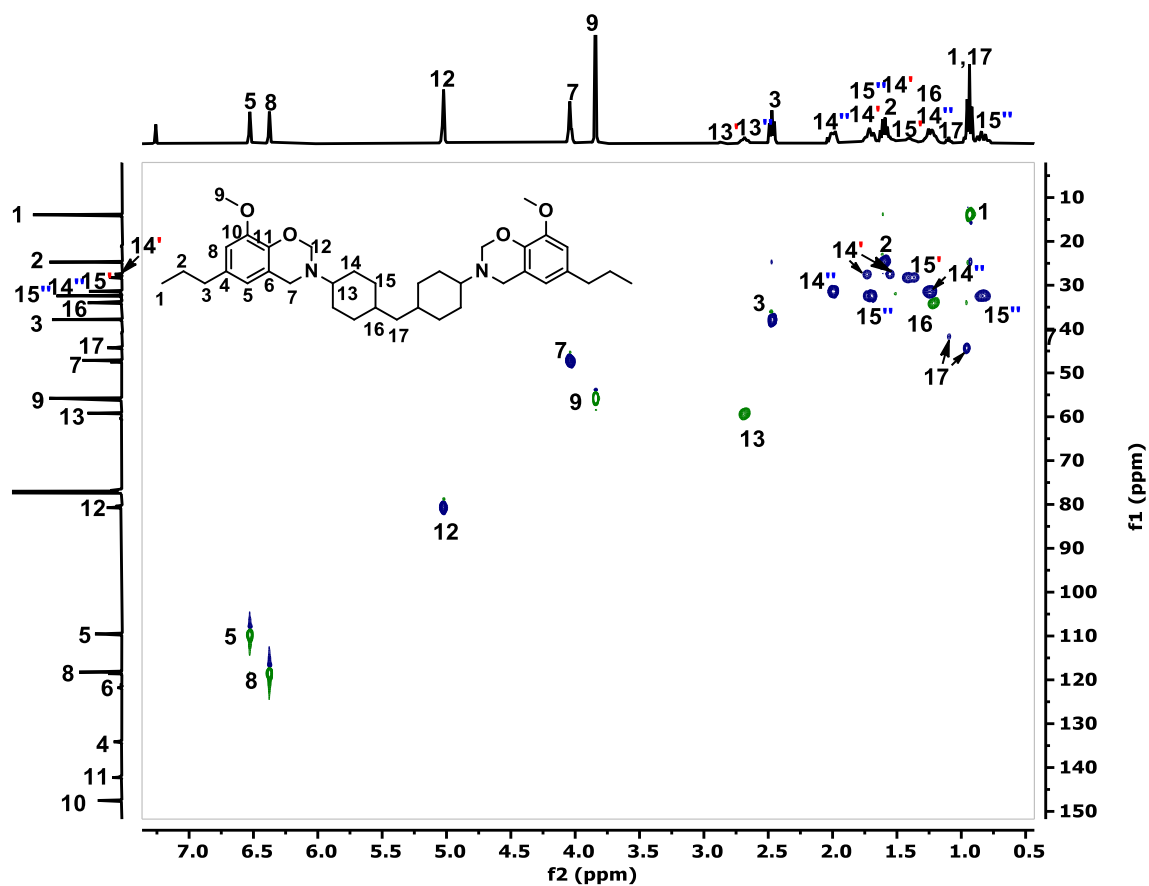


Figure S43. 2D HSQC spectrum of PG-MDCA

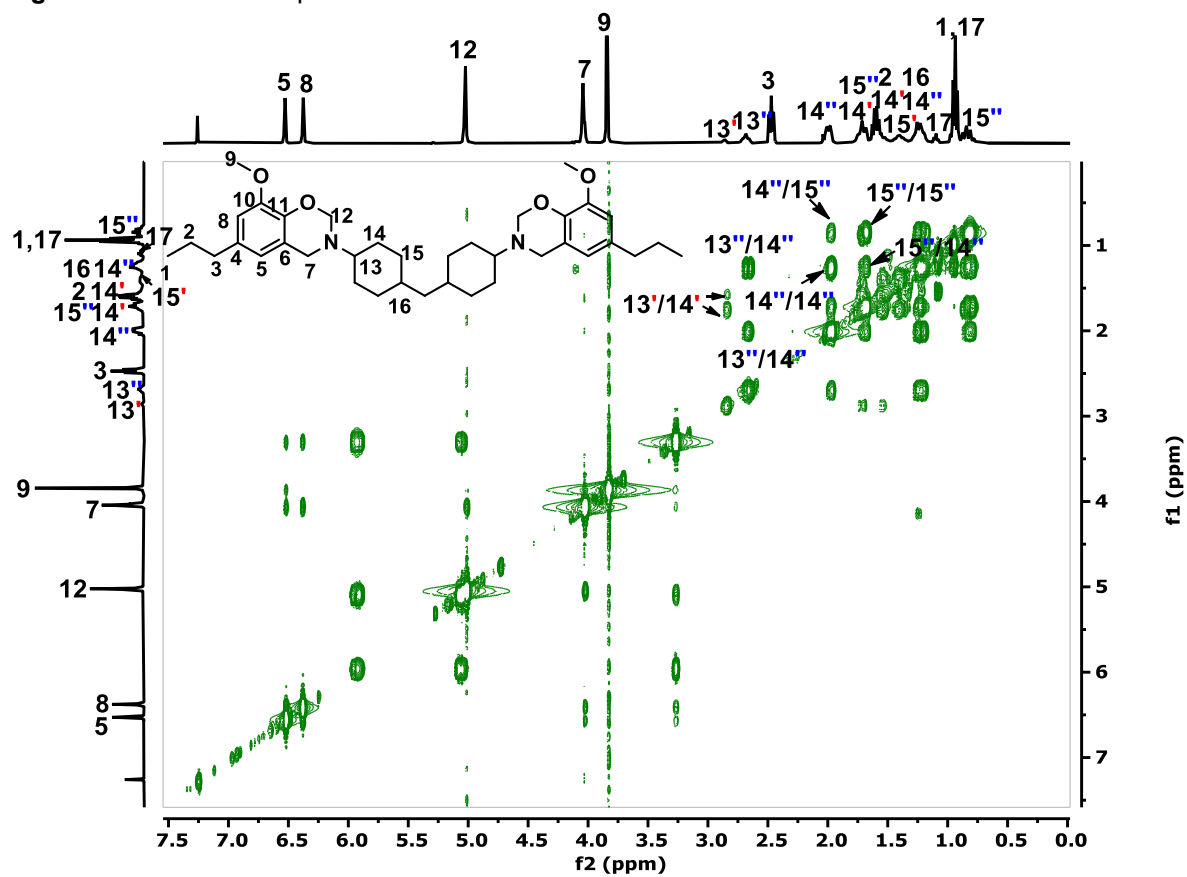


Figure S44. 2D COSY spectrum of PG-MDCA

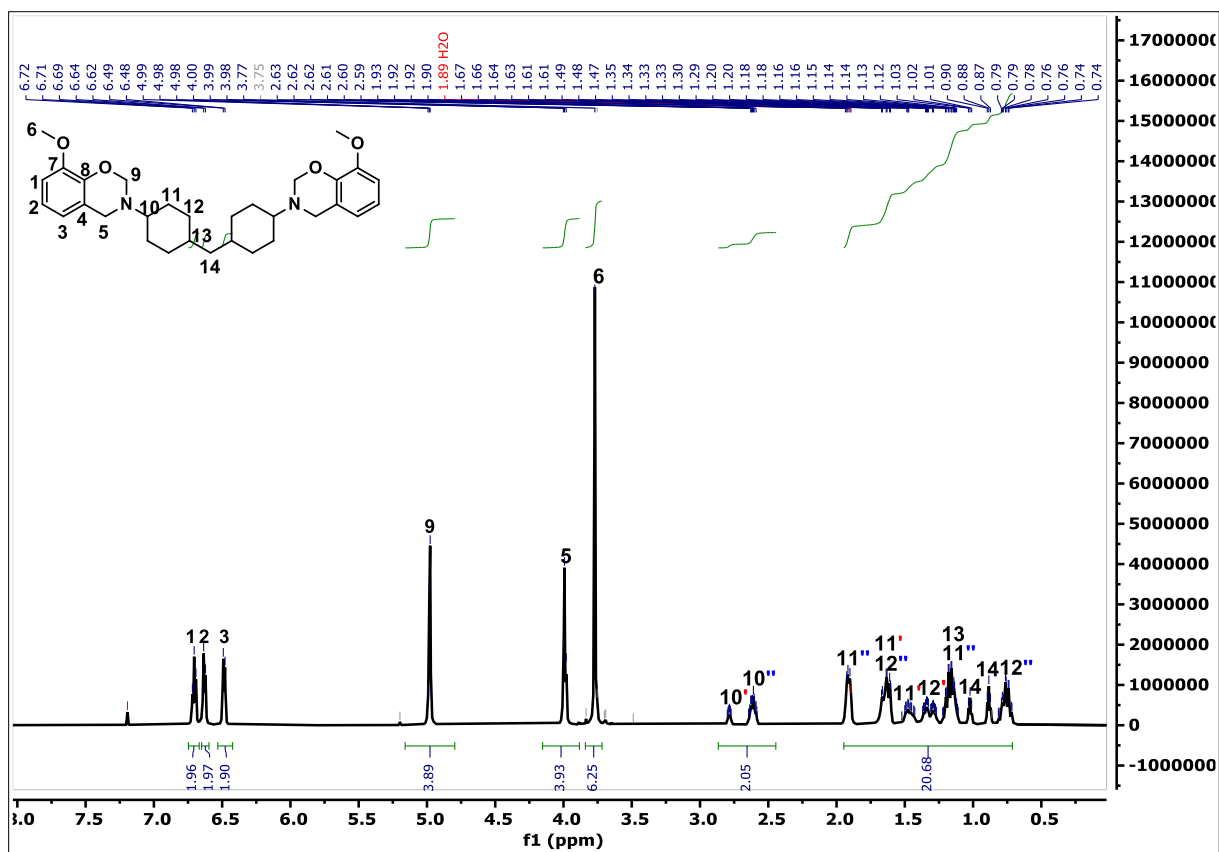


Figure S45. ^1H NMR spectrum of G-MBCA

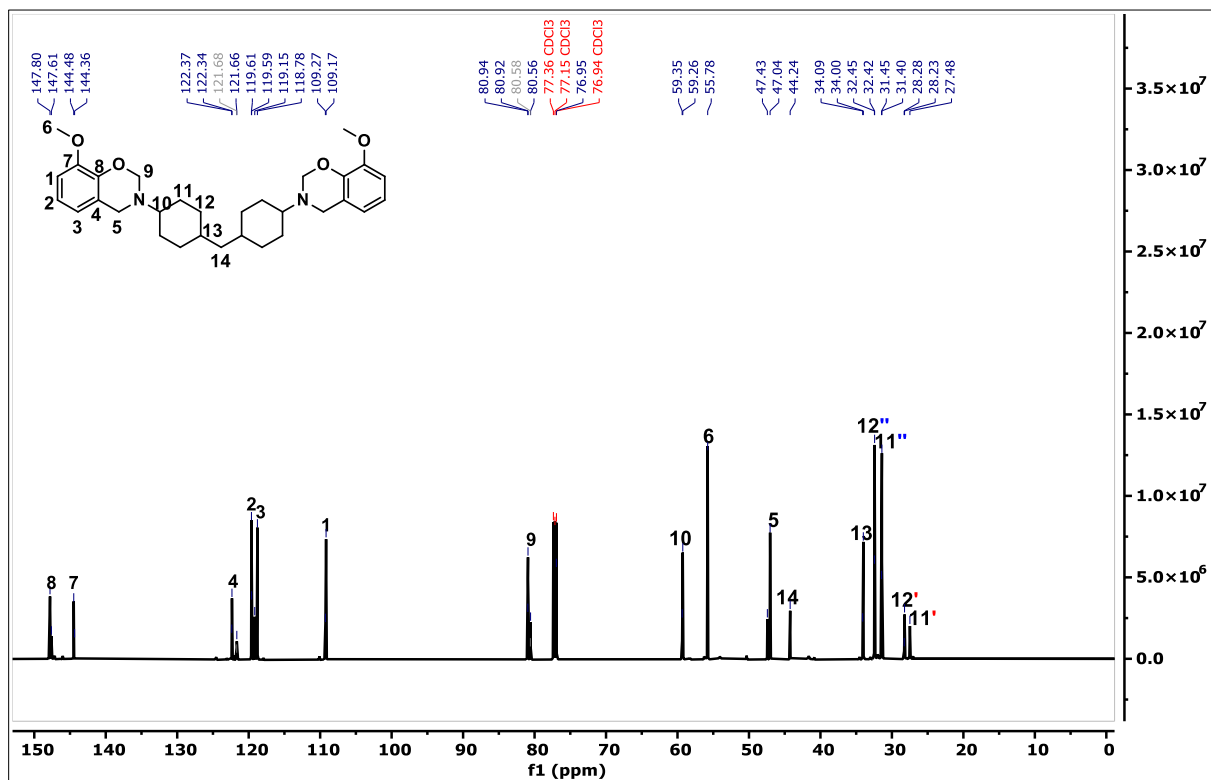


Figure S46. ^{13}C NMR spectrum of G-MBCA

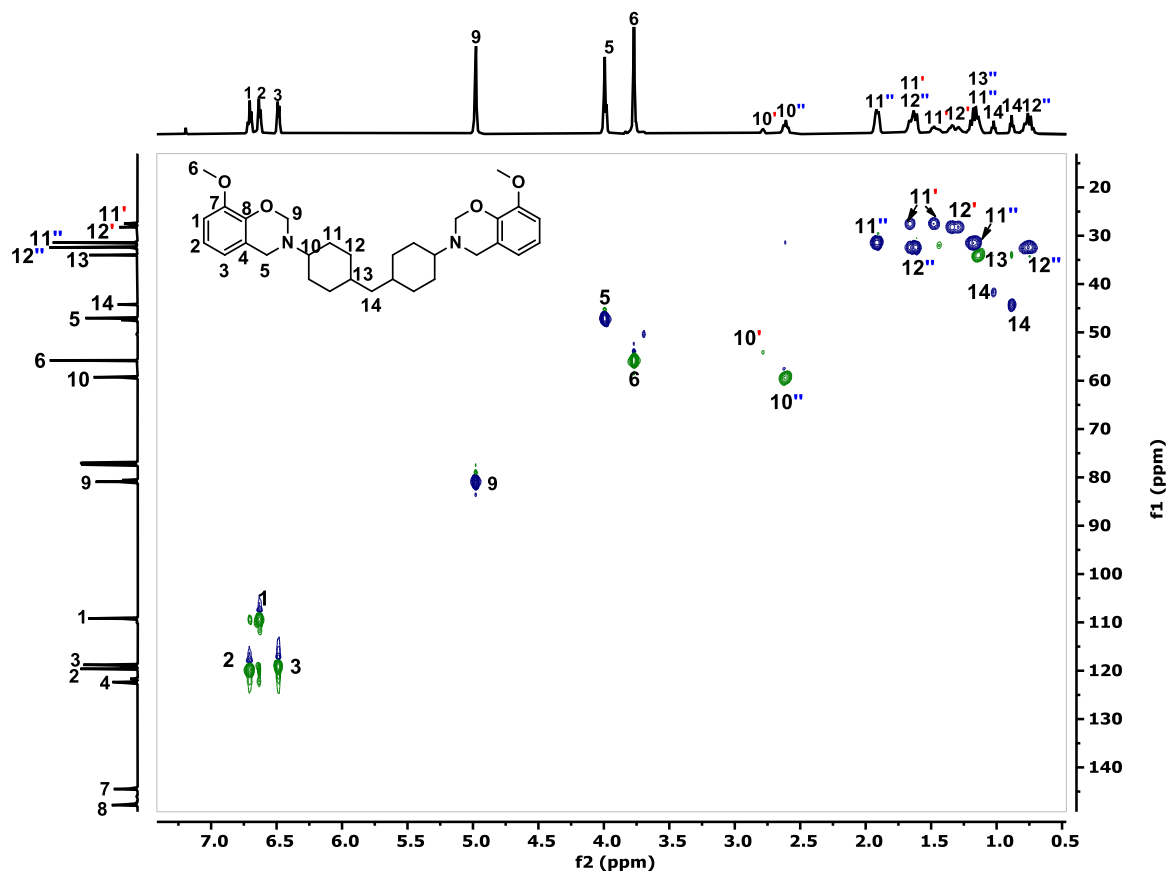


Figure S47. 2D HSQC spectrum of G-MDCA

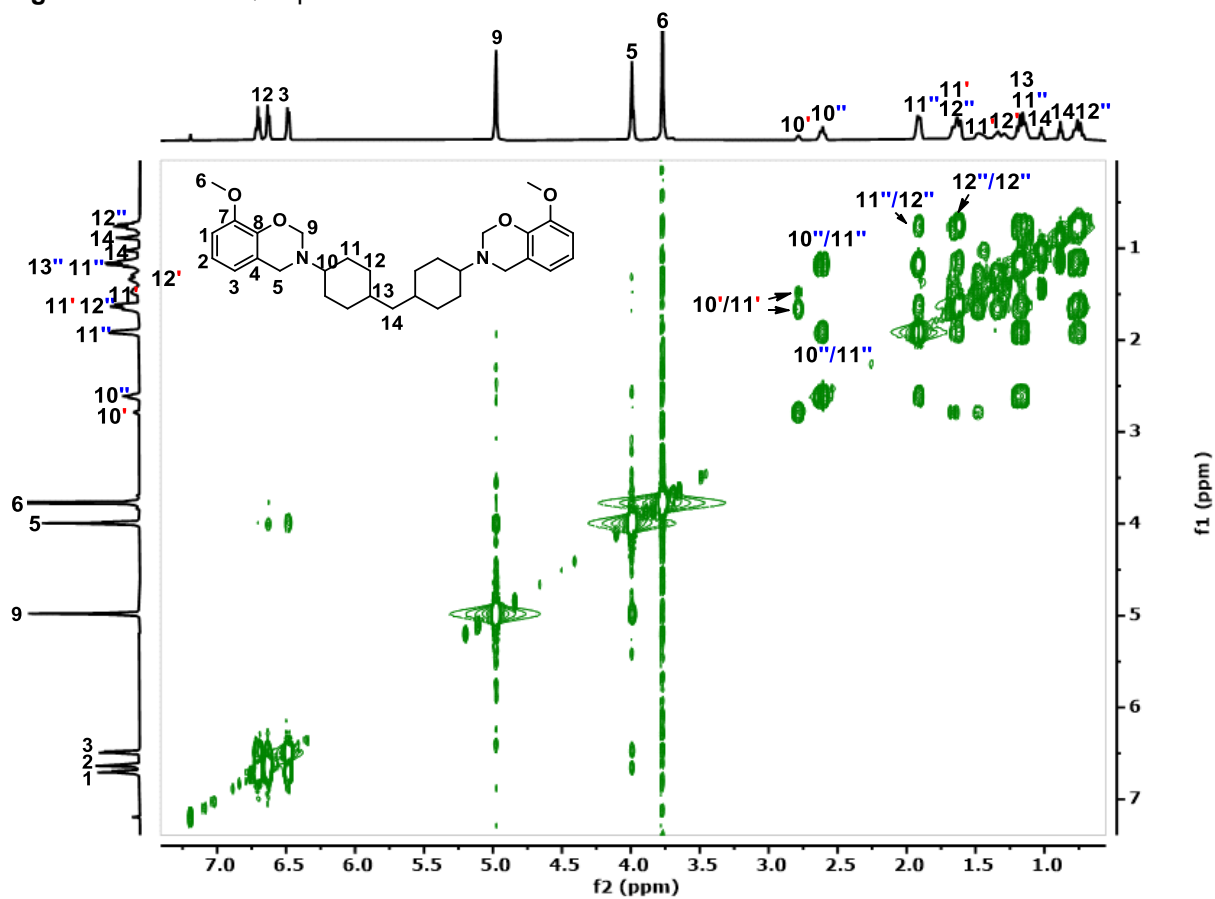


Figure S48. 2D COSY spectrum of G-MDCA

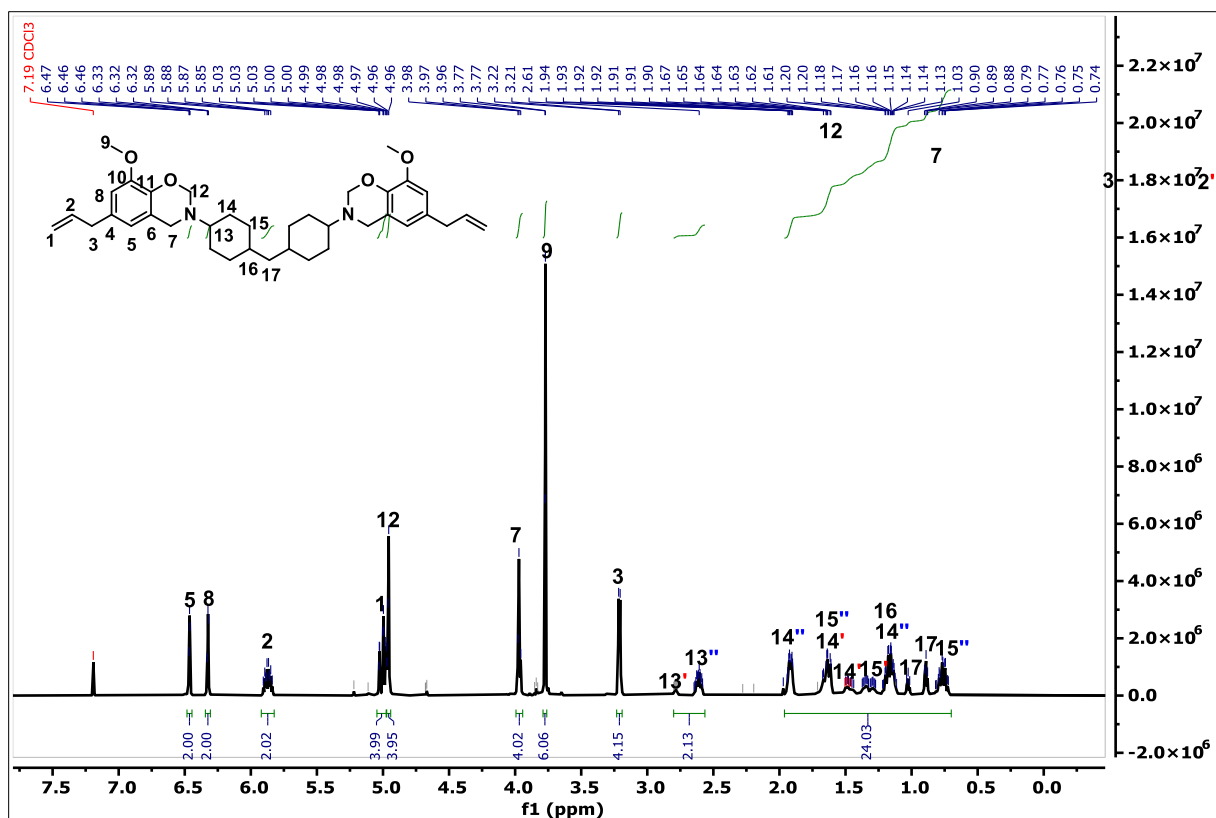


Figure S49. ¹H NMR spectrum of E-MBCA

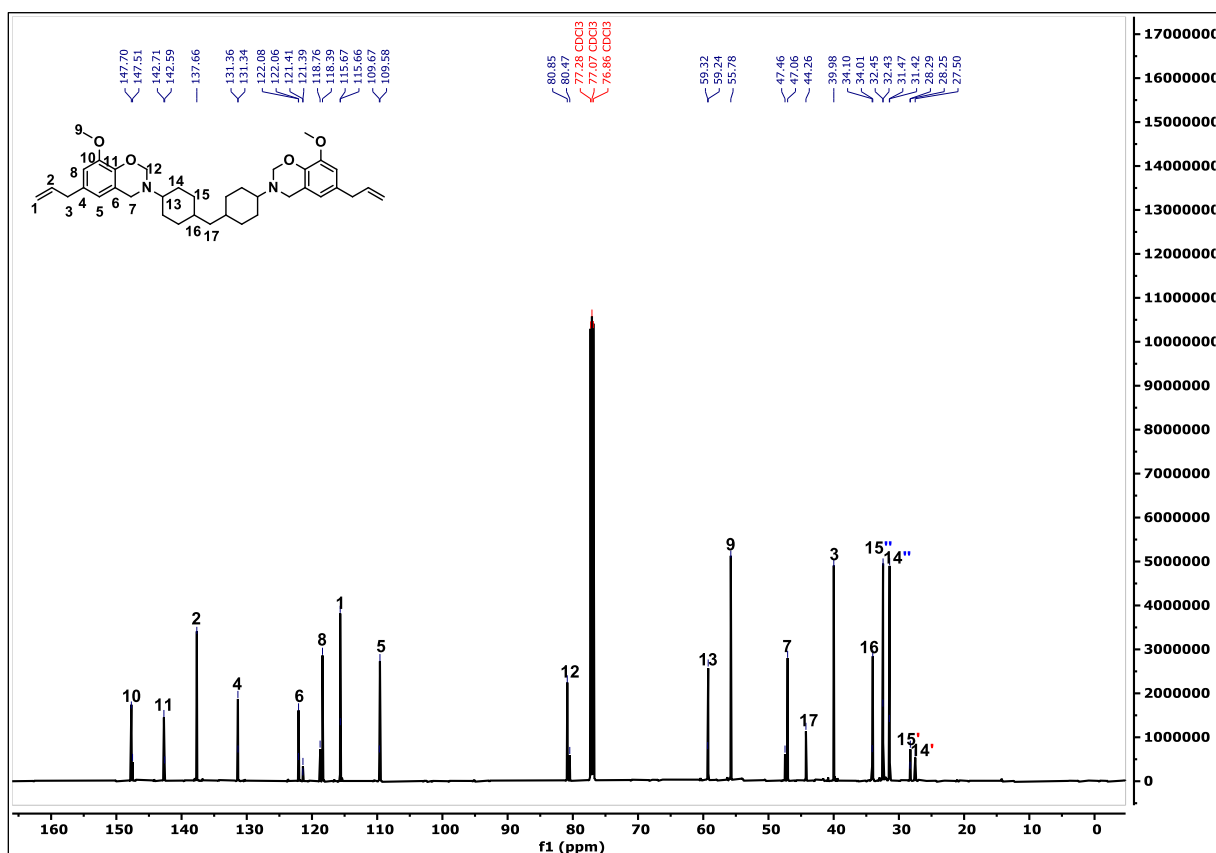


Figure S50. ¹³C NMR spectrum of E-MBCA

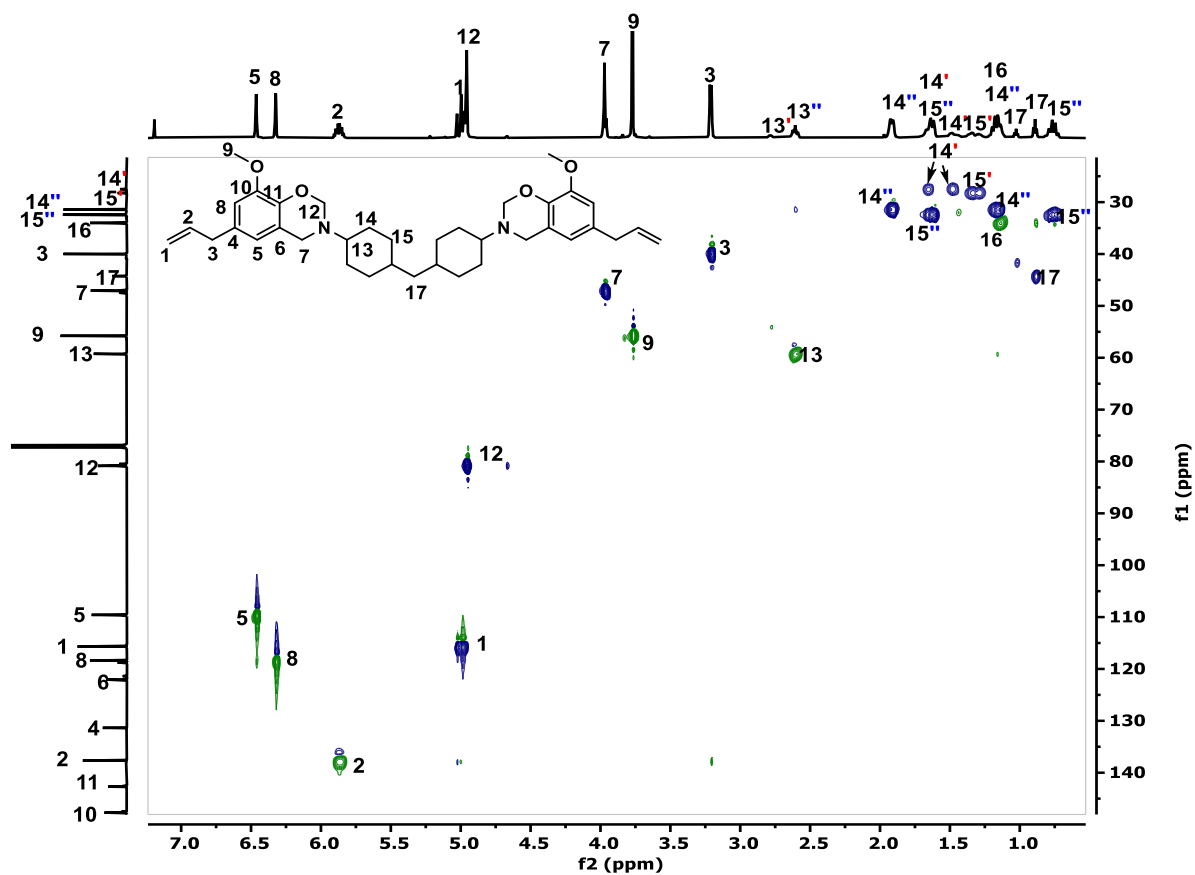


Figure S51. 2D HSQC spectrum of E-MBCA

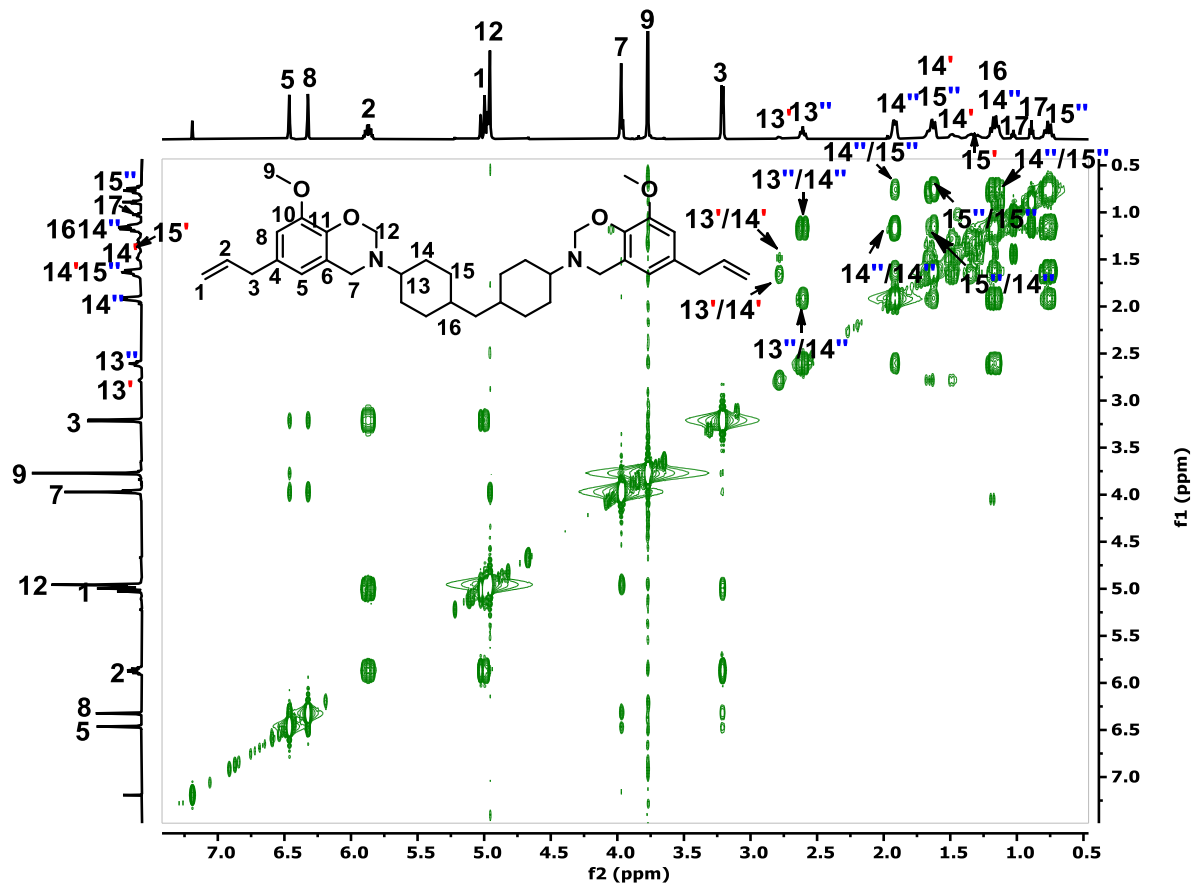


Figure S52. 2D COSY spectrum of E-MBCA

1.4 General experimental procedure

Catalytic demethoxylation and hydrogenation of methoxylated bisphenols into MBC: The demethoxylation/hydrogenation of methoxylated bisphenols was carried out in a 100 mL high-pressure Parr autoclave equipped with an overhead stirrer. Typically, the autoclave was charged with 100 mg Raney nickel catalyst, 0.5 mmol methoxylated bisphenols, 20 mL isopropanol and 10 mg dodecane as internal standard. The reactor was sealed and flushed with N₂ three times. The reactor was then heated and stirred at 400 rpm for 3-8 h. After the reaction was completed, the reactor was cooled down to RT. Then 0.1 mL solution was collected through a syringe and injected to GC-MS or GC-FID after filtration through a PTFE filter (0.45 μm).

The recycling test of Raney nickel catalyst: The reusability of Raney nickel catalyst was performed under the optimal reaction conditions: 100 mg Raney Nickel catalyst, 0.5 mmol **BGH**, 20 mL isopropanol, 20 mg dodecane, 150 °C, 3 h. After the first run, Raney nickel was washed with 10 mL isopropanol for 3 times with the assistance of magnet. Then 0.5 mmol **BGH**, 20 mg dodecane were introduced to carried out next run. After completion of several runs, the solution was combined and concentrated under reduced pressure. The crude mixture was characterized by ICP analysis to determine possible Ni leaching.

The catalytic direct amination of MBC into MBCA over Raney nickel catalyst with ammonia gas: The catalytic direct amination of **MBC** into **MBCA** was performed in 10 mL high pressure autoclave equipped with magnetic stirring bar. Typically, a 4 mL vial was charged with 50 mg Raney nickel catalyst, 0.5 mmol **MBC**, 2.5 mL *t*-amyl alcohol, 10 mg dodecane as an internal standard. Then the vial was sealed inside autoclave and pressurized with 7 bar NH₃. The reactor was heated and stirred at 400 rpm for 18 h. After completion of the reaction, the reactor was cooled down to RT. Then, 0.1 mL solution was collected through a syringe and injected to GC-MS or GC-FID after filtration through a PTFE filter (0.45 μm). The crude mixture was characterized by ¹H, ¹³C-NMR, 2D HSQC and COSY to confirm the structure.

The polymerization of benzoxazine monomers S-MBCA, PG-MBCA, G-MBCA and E-MBCA: The polybenzoxazine resins were prepared by thermally induced ring opening polymerizations of the obtained benzoxazine monomers. Typically, **S-MBCA** was transferred into a stainless-steel mold (50×5×1.5 mm), and then melted and degassed in a vacuum oven at 160 °C for 5 min. The product was step-cured in an air-circulating oven according to the following cycle: 1 h at 160 °C, 2 h at 180 °C, 2 h at 200 °C, and 2 h at 220 °C. Next, the cured sample was allowed slowly to cool down to RT and was removed carefully from the mold. Before property measurements, all the samples were left still at RT for 24 h.

2. Catalytic conversion of bisphenols to MBC over Raney nickel catalyst

2.1 Establishing the reaction conditions for bisphenols production

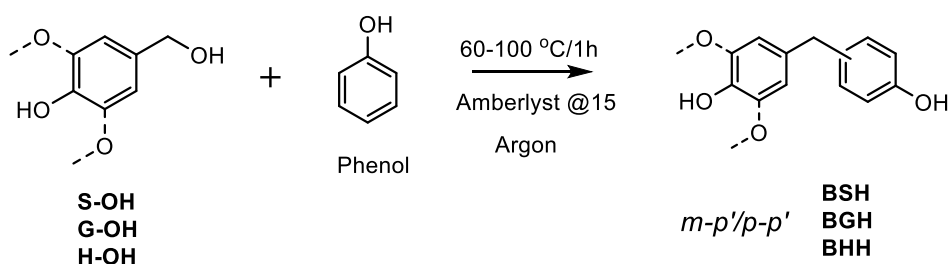


Table S1. Establishing the reaction conditions for bisphenols production

Entry	S-OH (mmol)	Phenol (mmol)	T (°C)	<i>t</i> (h)	<i>m-p': p-p'</i> ^[a]	BSH yield ^[b] (%)
1	1	10	60	1	15:85	36.4
2	1	10	60	3	15:85	37.2
3	1	10	80	1	22:78	46.9
4	1	10	100	1	26:74	73.8
Entry	G-OH (mmol)	Phenol (mmol)	T (°C)	<i>t</i> (h)	<i>m-p': p-p'</i>	BGH yield (%)
5	1	2.5	60	1	13: 87	34.2
6	1	5	60	1	13: 87	70.4
7	1	10	60	1	13: 87	90.8
Entry	H-OH (mmol)	Phenol (mmol)	T (°C)	<i>t</i> (h)	<i>m-p': p-p'</i>	BHH yield (%)
8	1	10	60	1	14: 86	86.2
Entry	S/G/H-OH (mmol)	Phenol (equiv.)	T (°C)	<i>t</i> (h)	<i>m-p': p-p'</i>	BSH/BGH/BHH yield (%)
9	1:1:1	10	60	1	17: 83	81.9
10	1:1:1	10	100	1	28: 72	89.8
11	0.5:1:0.5	10	60	1	17: 83	85.0

[a]. *m-p': p-p'* was determined by GC-FID ratio; [b]. isolated yield.

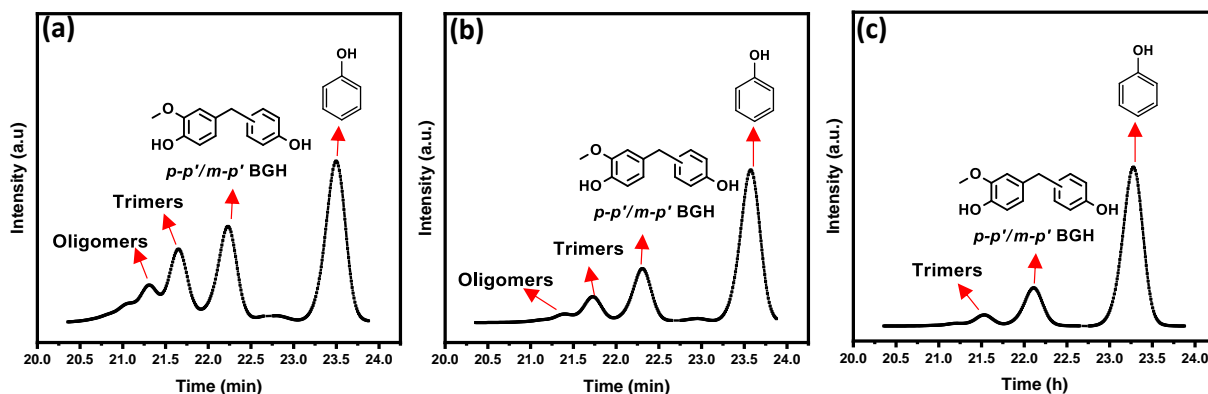


Figure 53. GPC traces of crude mixture obtained by acid catalyzed coupling of phenol with vanillyl alcohol. Reaction conditions: 1 mmol vanillyl alcohol, 2.5-10 equiv. phenol (a, 2.5 mmol, b, 5 mmol and c, 10 mmol), 30 wt.% Amberlyst 15 catalyst based vanillyl alcohol, 60 °C, 1h under Argon.

2.2 GC-MS traces of catalytic demethoxylation/hydrogenation of BGH to MBC over Raney nickel catalyst

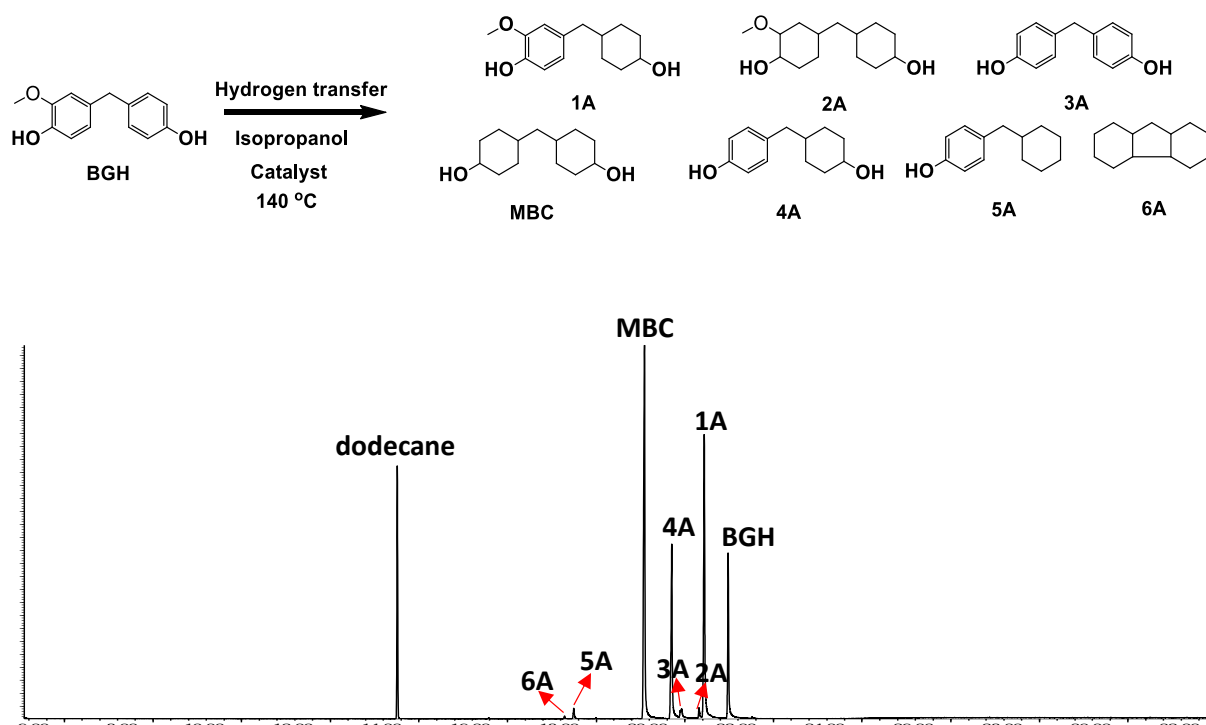
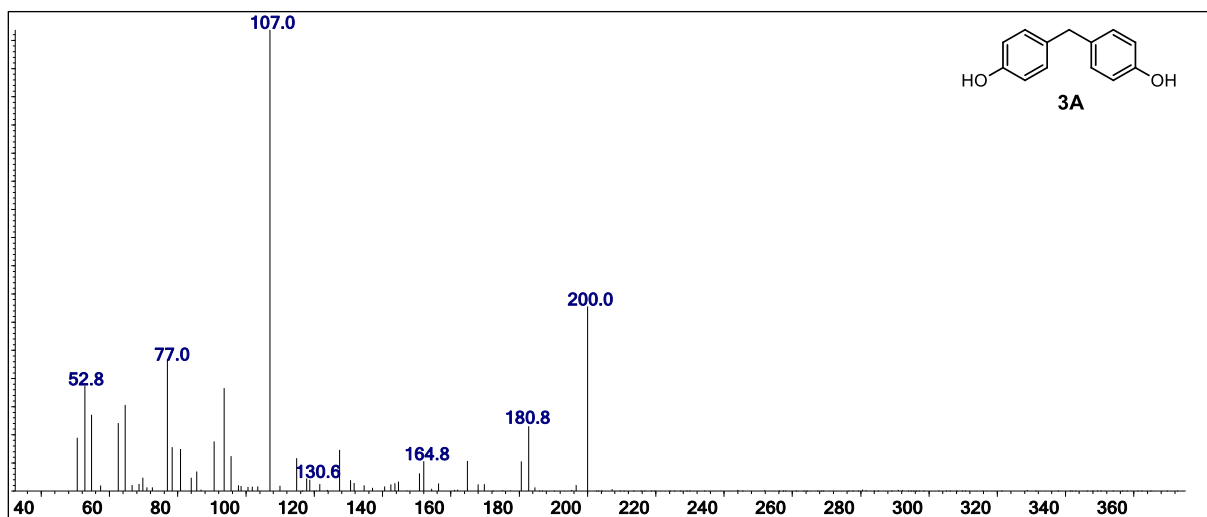
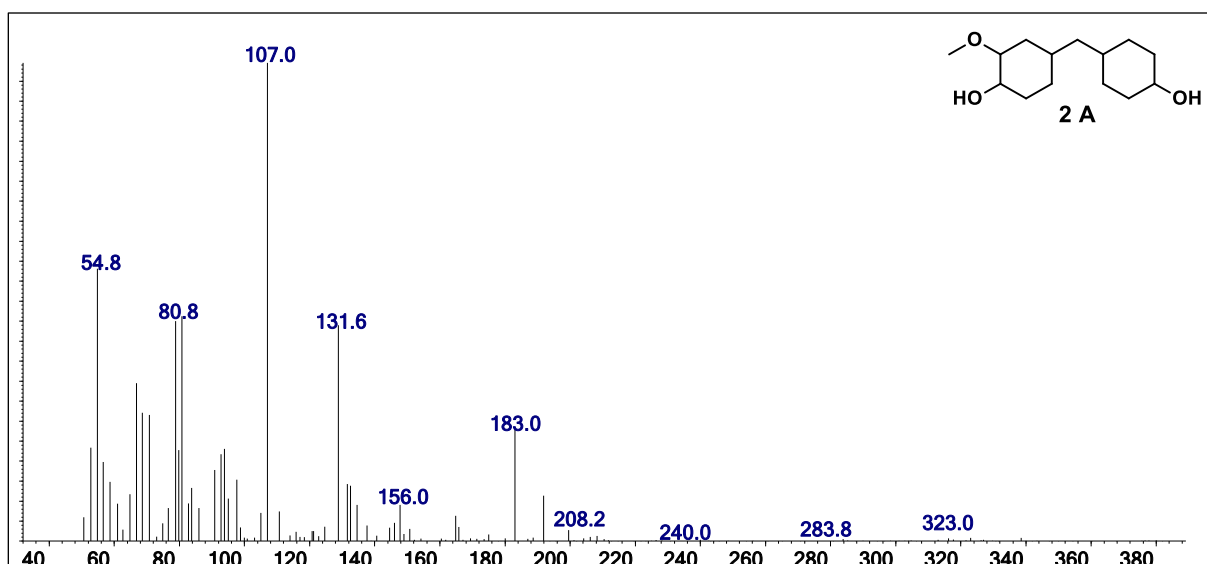
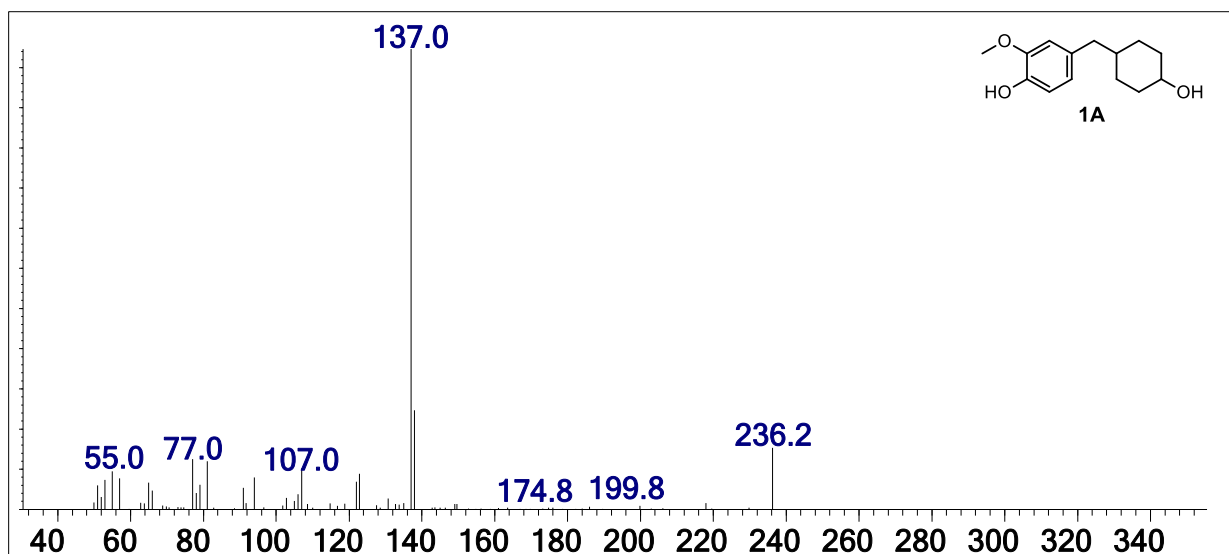
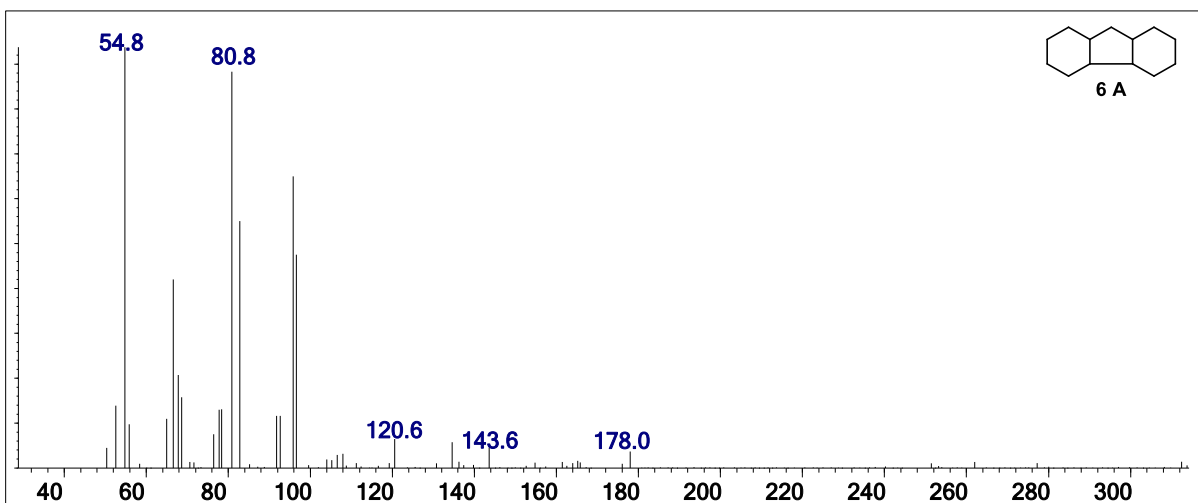
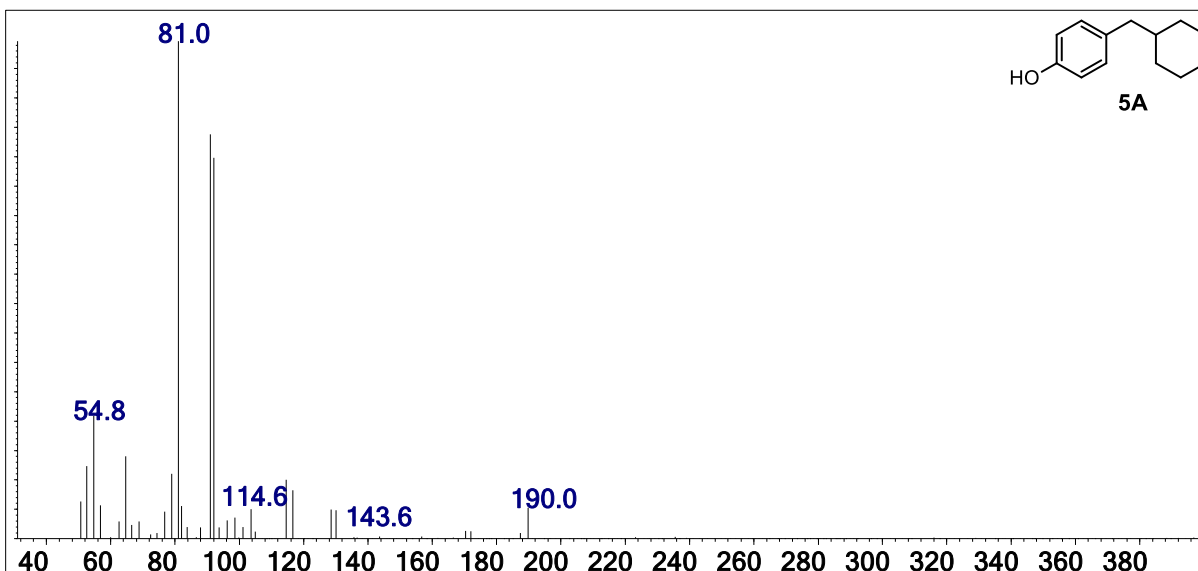
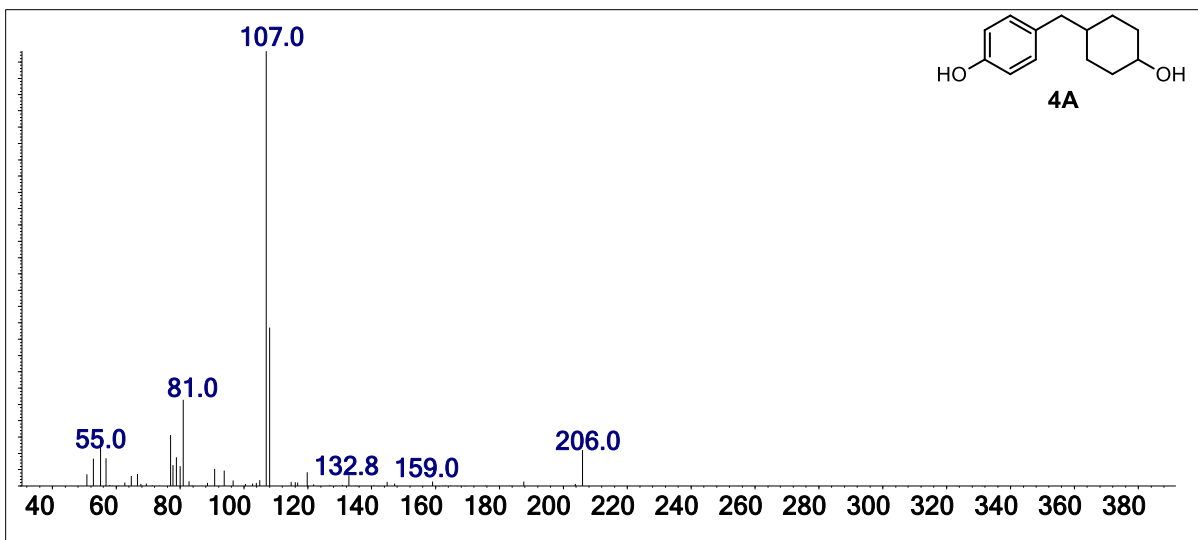
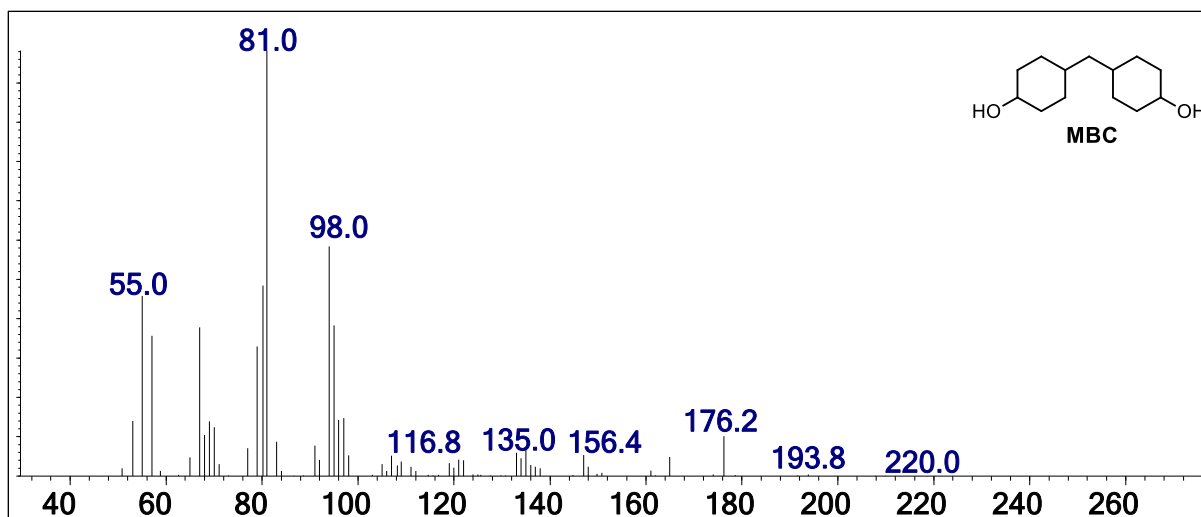


Figure S54. GC-MS trace of the product mixture obtained upon catalytic demethoxylation and hydrogenation of BGH to MBC over Raney nickel catalyst. Reaction conditions: 100 mg Raney nickel catalyst, 110 °C, 3 h, 15 mL isopropanol, 10 mg dodecane.

Mass spectra of 1A, 2A, MBC, 3A, 4A, 5A, 6A.







2.3 Recycling test for catalytic demethoxylation and hydrogenation of BGH to MBC over Raney nickel catalyst

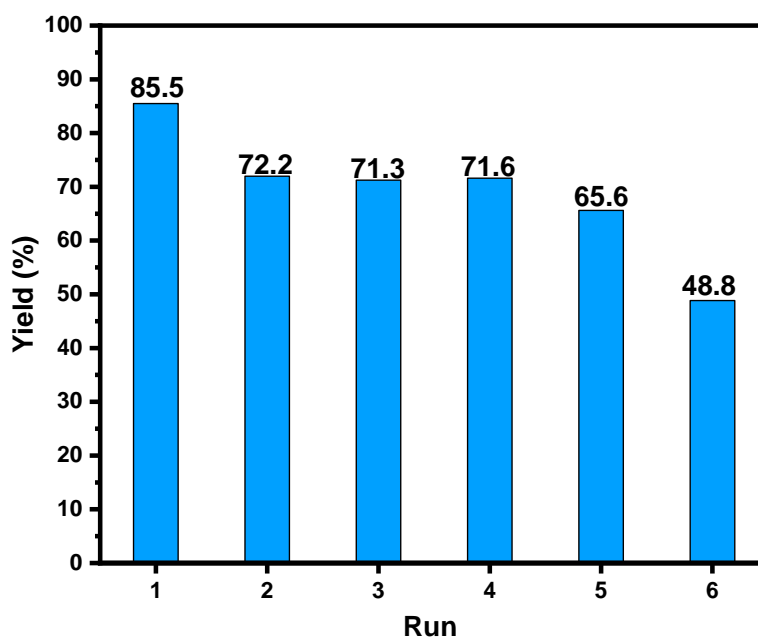


Figure S55. Recycling test for catalytic demethoxylation and hydrogenation of **BGH** to **MBC** over Raney nickel catalyst; Reaction conditions: 0.5 mmol **BGH**, 100 mg catalyst, 15 mL isopropanol, 140 °C, 3h, 10 mg dodecane. Yield was determined by calibration curve using dodecane as internal standard.

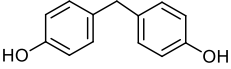
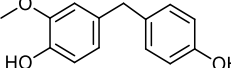
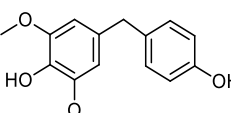
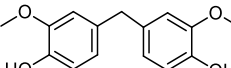
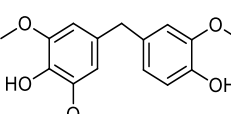
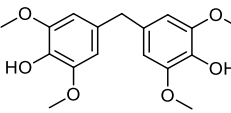
The Ni leaching contents in the liquid solution (filtrate) was analyzed by Inductively coupled Plasma Mass Spectrometry mass (ICP-MS). As shown in **Table S2**, there is no obvious Ni leaching after six runs, indicating good stability of the employed catalytic systems.

Table S2. Ni leaching content was analyzed by ICP-MS

Catalytic system	Leached Ni from the catalyst/%	Ni concentration in filtrate/ppm (mg/kg)	Ni amount in the filtrate/mg
Raney Ni (100 mg, 20 % water)	0.24	288	0.198

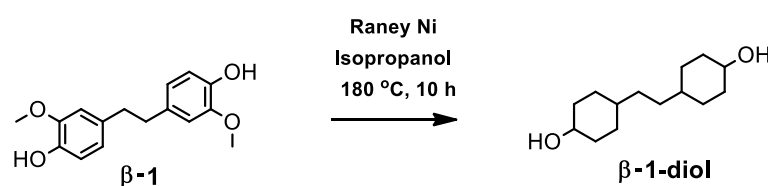
2.4 Catalytic demethoxylation and hydrogenation of lignin-derived bisphenols.

Table S3. Catalytic demethoxylation and hydrogenation of lignin-derived **H**-, **G**-, and **S**-, bisphenols^[a]

Entry	Substrates	T/t (°C /h)	Selectivity ^[b] (%)					Yield ^[c] (%)
			MBC	1A	2A	3A	4A	
1-BHH		140/3	95.0	-	1.5		3.5	94.6
2-BGH		150/3	83.1	5.5	4.8		5.9	84.8
3-BSH		160/6	84.2	2.6	2.9		8.2	83.5
4-BGG		160/6	74.6	10.3	3.6		11.7	73.3
5-BSG		170/6	72.4	9.9	3.7		12.0	71.2
6-BSS		170/8	66.1	6.6	3.4	6.8	14.0	64.1
7	BHH: BGH: BSH 2:2:1	160/6	87.2	3.7	0.8		8.7	86.3

[a]. Reaction conditions: 0.5 mmol substrates, 100 mg Raney nickel, 15 mL isopropanol, 10 mg dodecane. [b]. Selectivity was determined by GC-FID. [c]. Yield was determined by calibration curve using dodecane as internal standard.

2.5 Catalytic demethoxylation and hydrogenation of lignin-derived dimers β -1 and β - β



The demethoxylation/hydrogenation of 4,4'-(ethane-1,2-diyl) dicyclohexanol (β -1) was prepared in 100 mL high-pressure Parr autoclave, equipped with an overhead stirrer. In a typical procedure, the autoclave was charged with 100 mg Raney nickel catalyst, 0.5 mmol (137 mg) β -1, and 20 mL isopropanol. The reactor was purged with N₂ three times. The reactor was sealed and heated to 170 °C and stirred at 400 rpm for 10 h. After completion of the reaction, the reactor was cooled to RT. Then 0.1 mL solution was collected through a syringe and injected to GC-FID (GC selectivity: 76.8%). The Raney nickel was separated from the solution by centrifugation and isopropanol soluble fractions were subjected to purification by column chromatography on silica gel, using methanol: dichloromethane (1:99-5:95) as eluent. 82.16 mg, 0.36 mmol solid was obtained in a yield of 72.7% as the isomers of *cis-cis*: *cis-trans*: *trans-trans* of 10: 46: 44. (GC ratio).

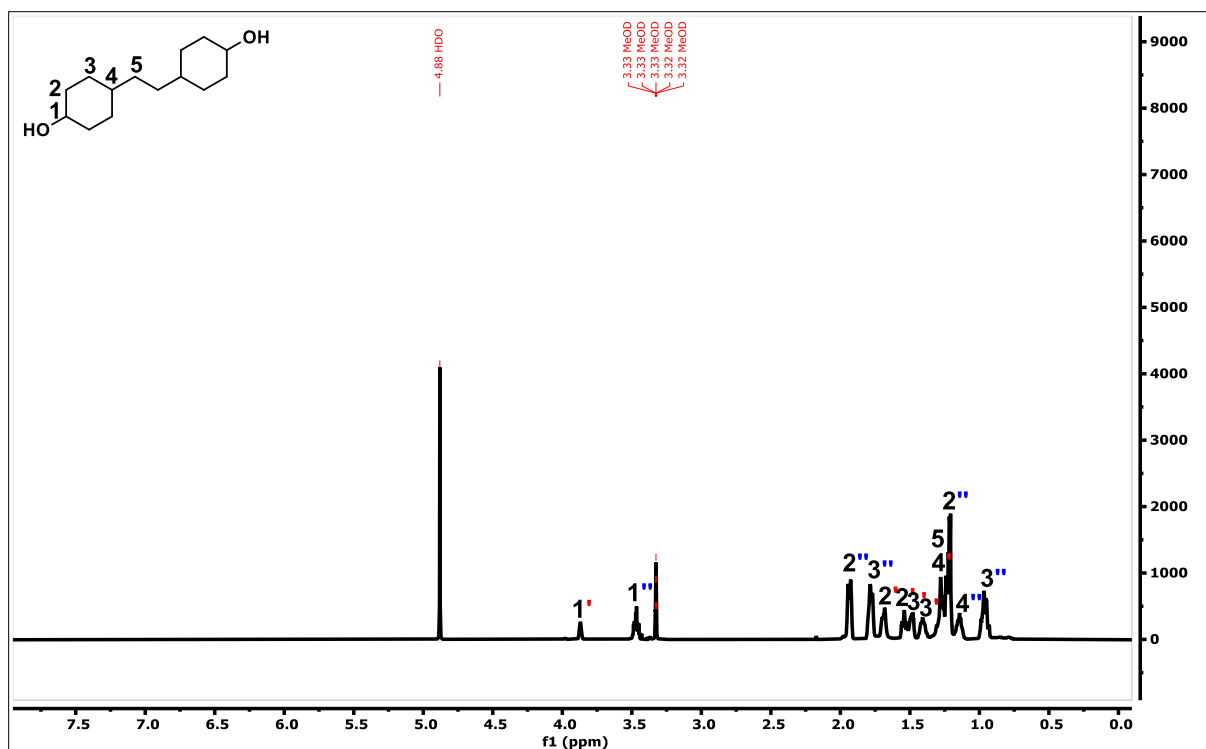


Figure S56. ¹H NMR spectrum of β -1-diol

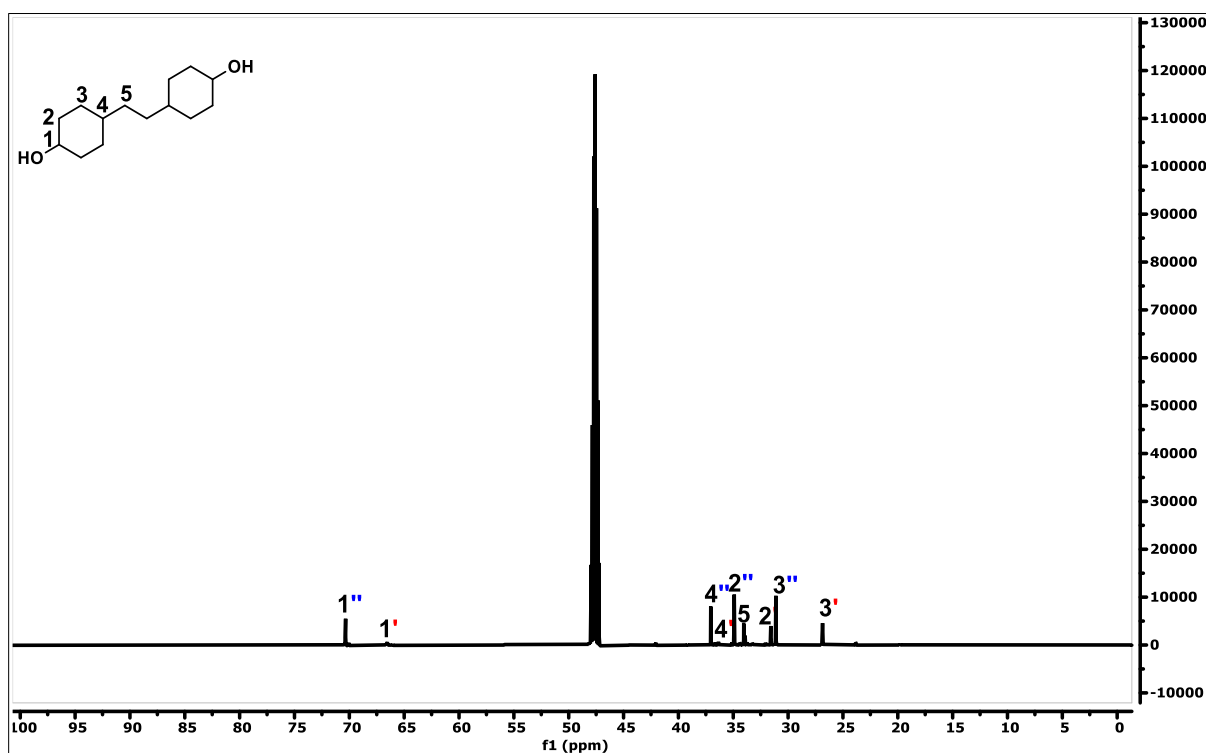


Figure S57. ¹³C NMR spectrum of β -1-diol

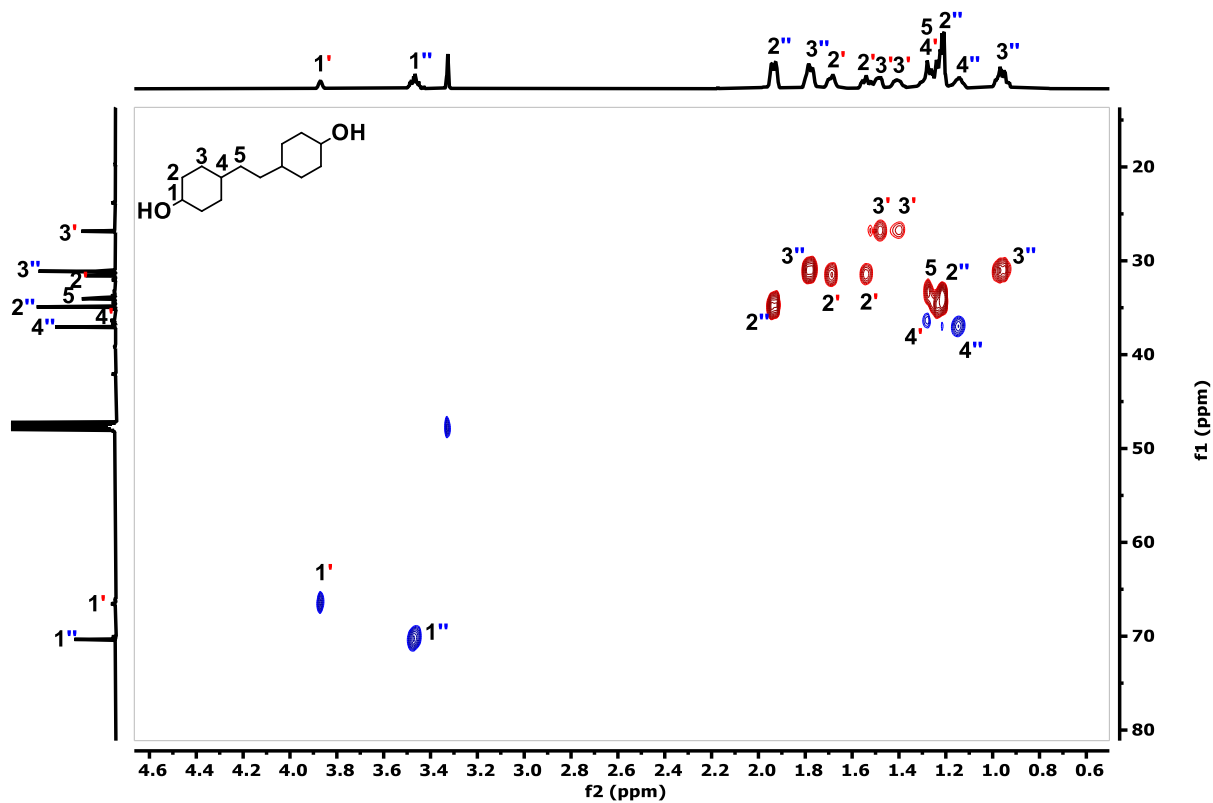


Figure S58. 2D HSQC spectrum of β -1-diol

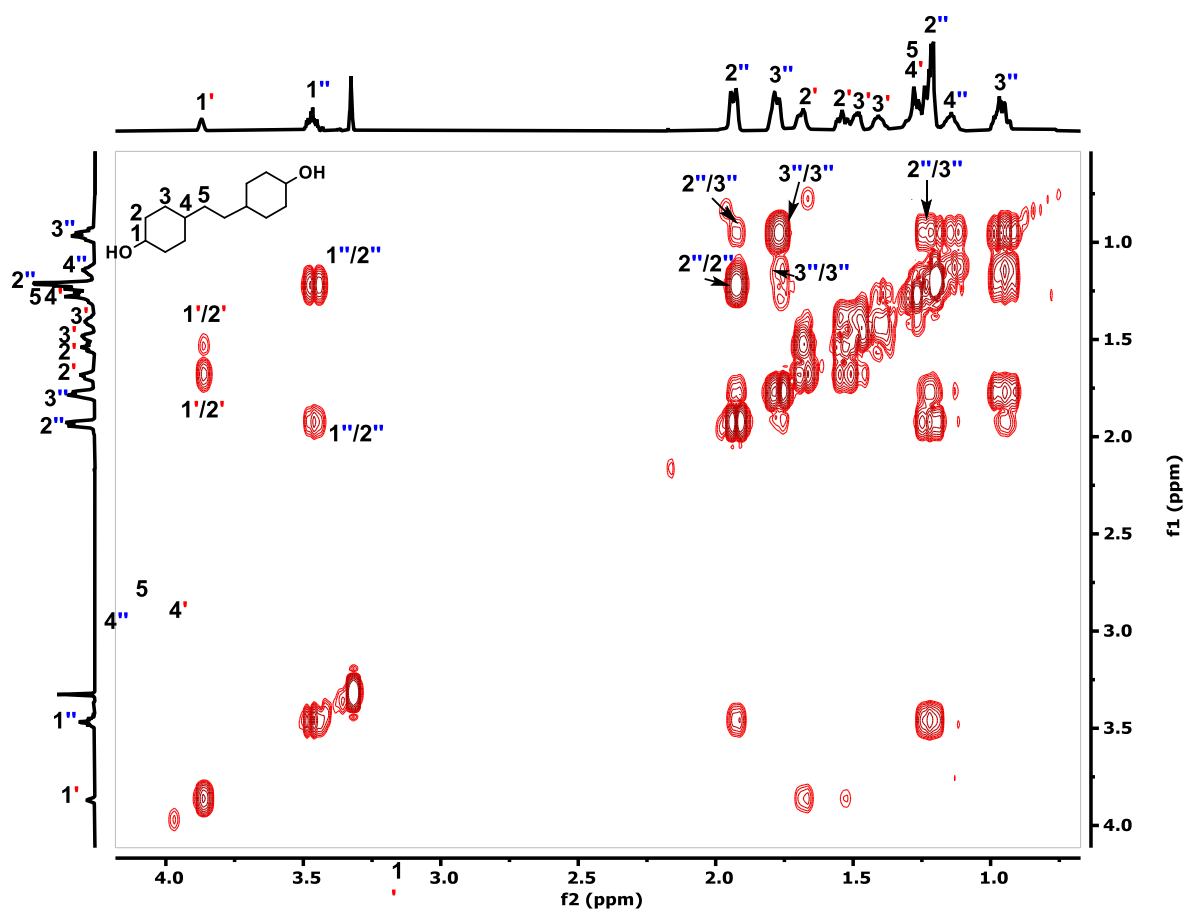
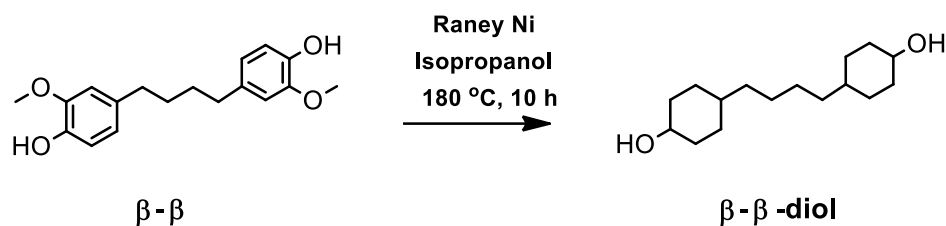


Figure S59. 2D COSY spectrum of β -1-diol



The demethoxylation/hydrogenation of **4,4'-(butane-1,4-diyl) bis(2-methoxyphenol) $\beta\text{-}\beta$** was prepared in 100 mL high-pressure Parr autoclave, equipped with an overhead stirrer. In a typical procedure, the autoclave was charged with 100 mg Raney nickel catalyst, 0.5 mmol (151 mg $\beta\text{-}\beta$), and 20 mL isopropanol. The reactor was purged with N_2 three times. The reactor was sealed and heated to 180 °C and stirred at 400 rpm for 10 h. After completion of the reaction, the reactor was cooled to RT. Then 0.1 mL solution was collected through a syringe and injected to GC-FID (GC selectivity: 77.9%). The Raney nickel was separated from the solution by centrifugation and isopropanol soluble fractions were subjected to purification by column chromatography on silica gel, using methanol: dichloromethane (1:99-5:95) as eluent. Solid product (87.5 mg, 0.345 mmol) was obtained in a yield of 68.9% as the isomers of *cis-cis*: *cis-trans*: *trans*: *trans* of 8:45:47 (GC ratio).

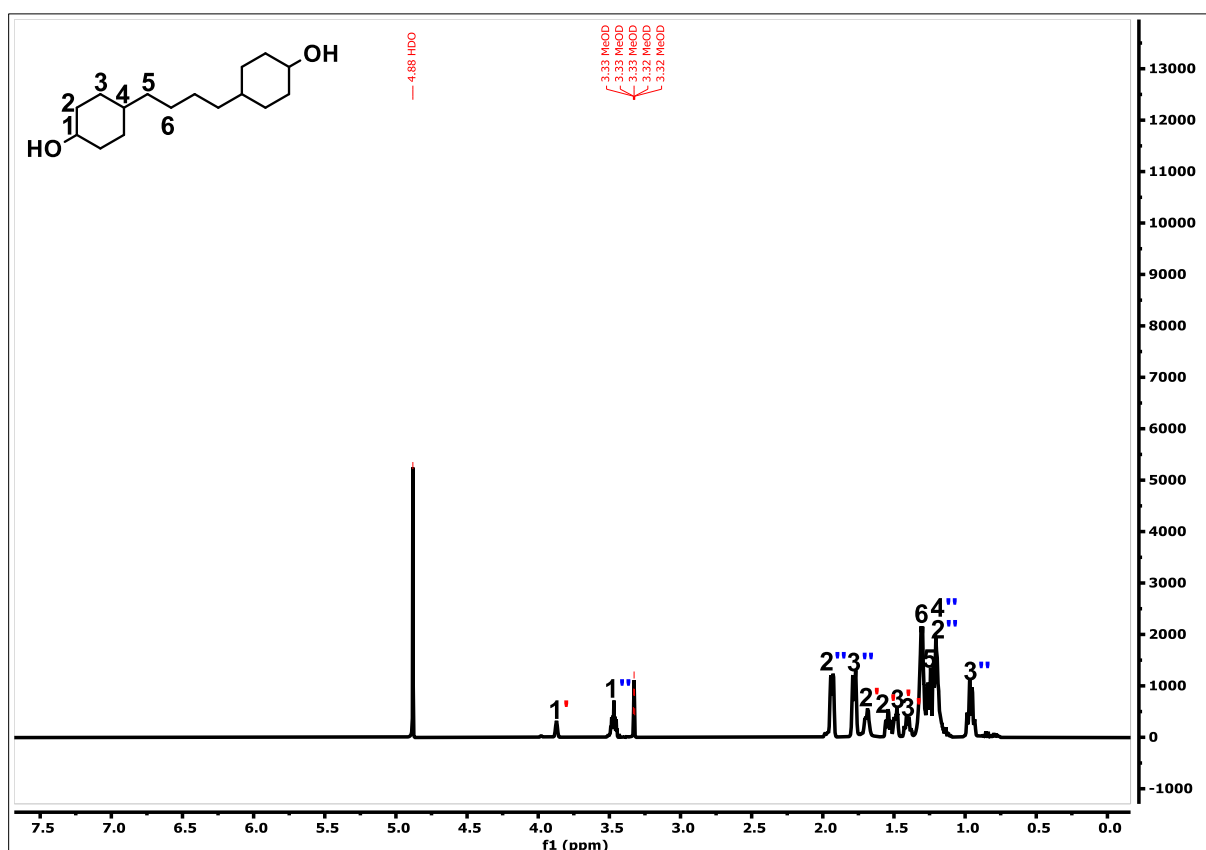


Figure S60. ^1H NMR spectrum of $\beta\text{-}\beta\text{-diol}$

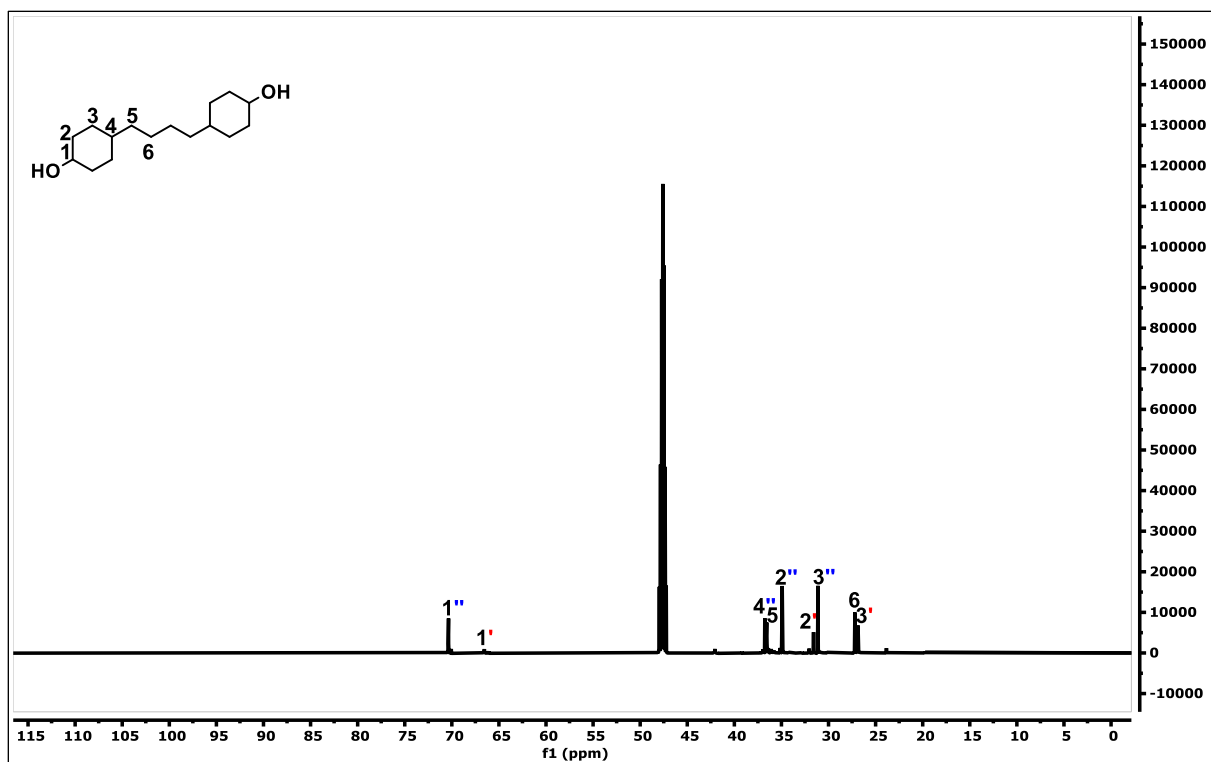


Figure S61. ^{13}C NMR spectrum of β - β -diol

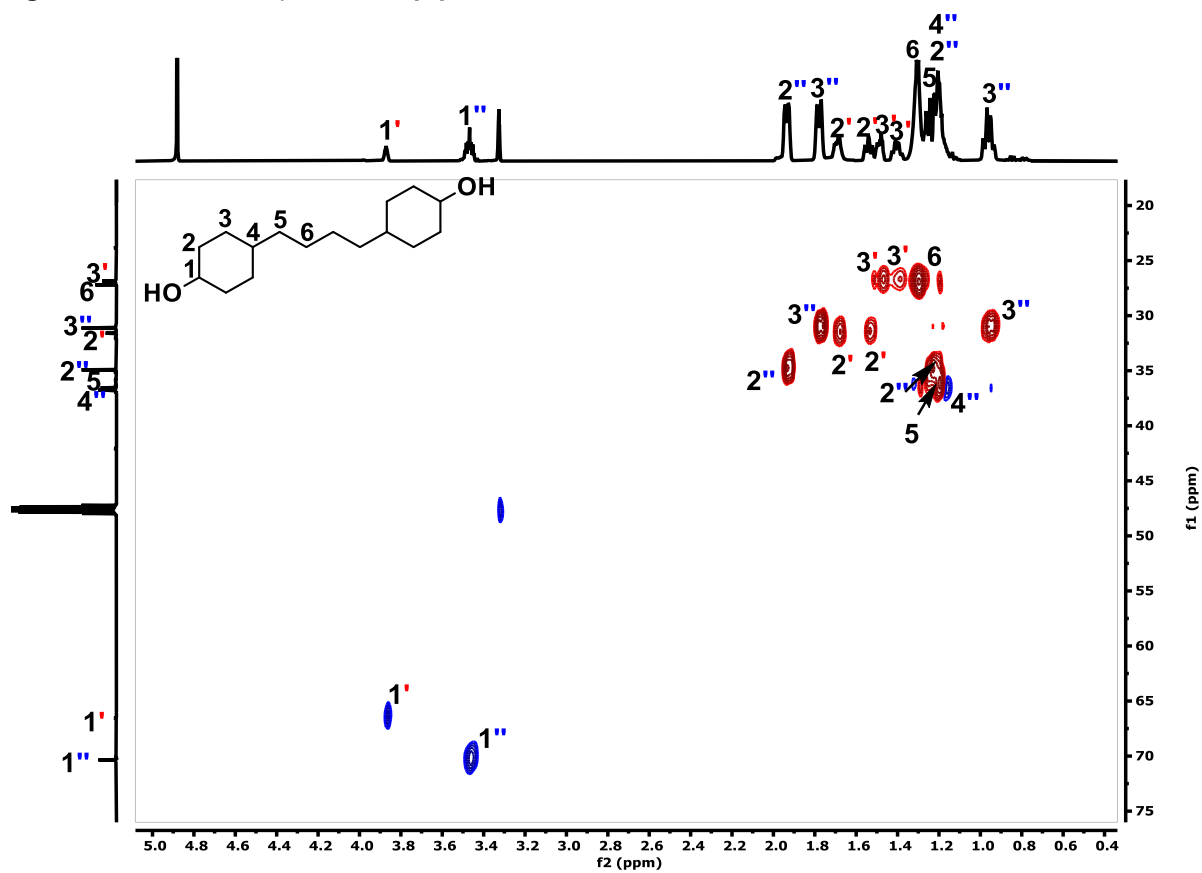


Figure S62. 2D HSQC spectrum of β - β -diol

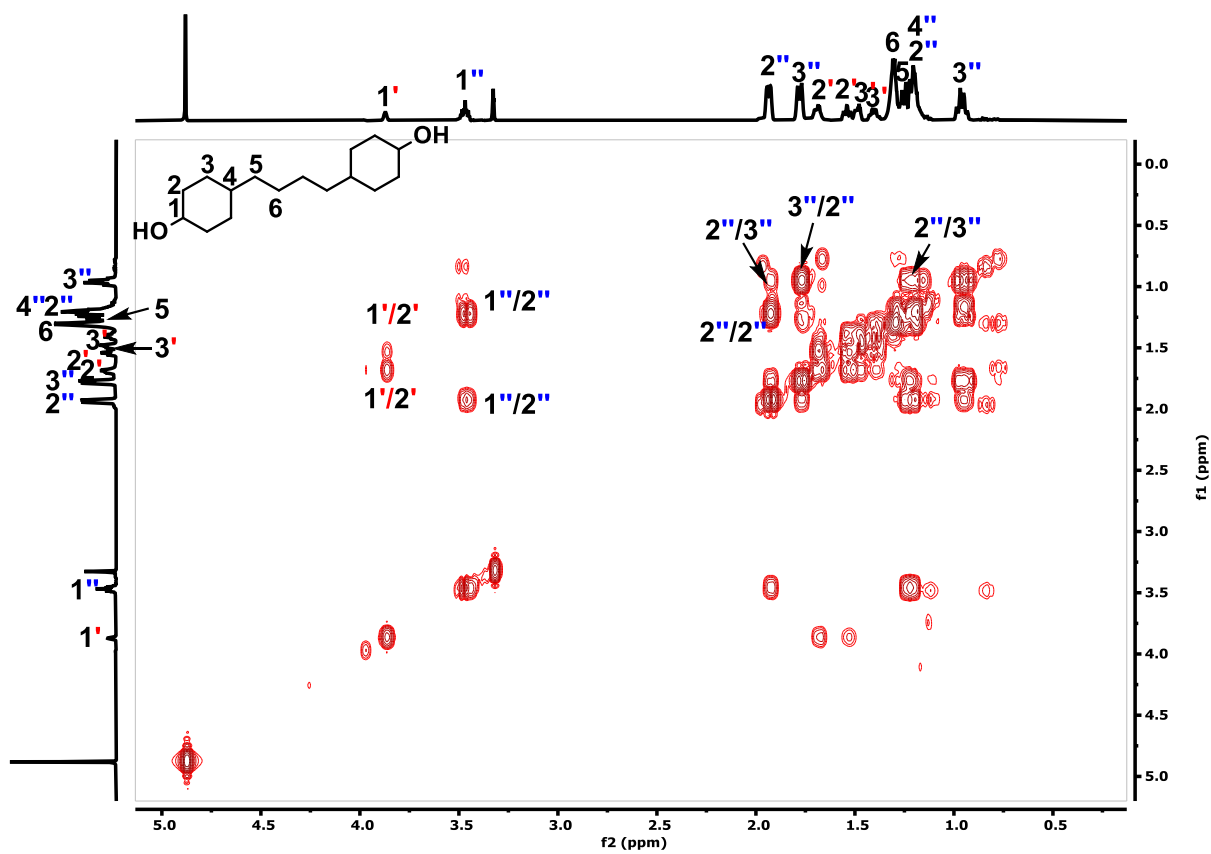


Figure S63. 2D COSY spectrum of β - β -diol

2.6 GC FID traces toward the production of MBC diol based on lignin to vanillin process

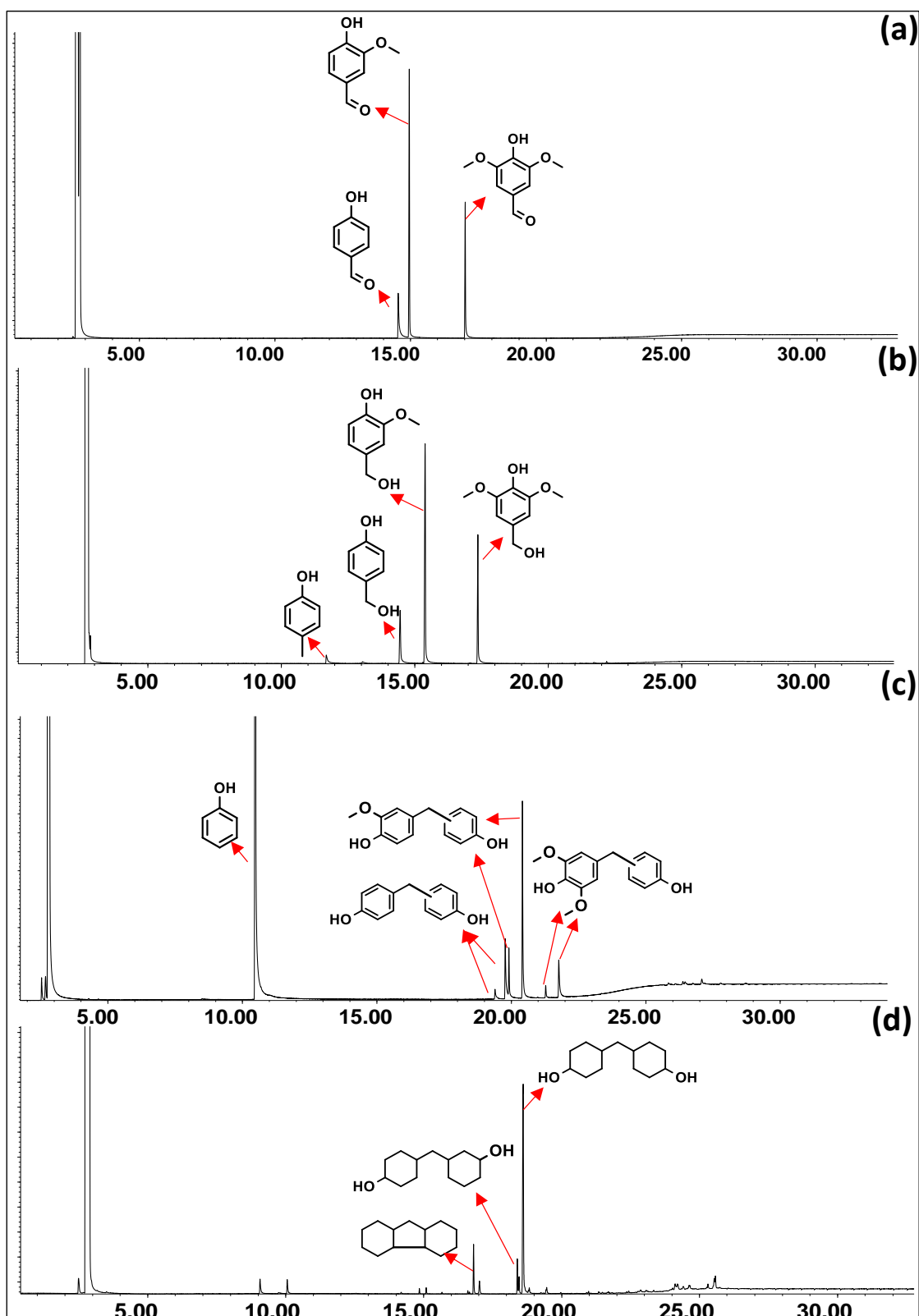
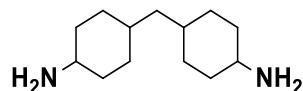


Figure S64. Gas Chromatographic analysis of respective product mixtures, for the reaction sequence from aldehyde mixtures to **MBC** diol. a) Catalytic hydrogenation: 0.5 mmol 4-hydroxybenzaldehyde, 0.5 mmol syringaldehyde and 1 mmol vanillin, 30 mg Pd/Al₂O₃, 5 bar H₂, 30 mL ethanol, RT, overnight; b) Acid mediated aromatic electrophilic substitution: 150 mg Amberlyst 15 catalyst, 10 equiv. phenol, 60 °C, 1h; c) Catalytic funneling by demethoxylation/hydrogenation: 500 mg Raney nickel catalyst, 30 mL isopropanol, 160 °C, 6 h.

3. Catalytic direct amination of MBC with ammonia to obtain MBCA over Raney nickel catalyst

3.1 Detailed analysis of the crude MBCA obtained from the amination of MBC

4,4'-methylenebiscyclohexanamine (**MBCA**)



Reaction conditions: 0.5 mmol **MBC** (106 mg) diol, 50 mg Raney nickel catalyst, 2.5 mL *t*-amyl alcohol, 170 °C, 18 h, 10 mg dodecane as internal standard (for GC yield). After the reaction, the solvent *t*-amyl alcohol was removed under reduced pressure and white solid (100.8 mg) was obtained in an isolated yield of 96%. The crude mixture was characterized by GC-FID, ¹H, ¹³C NMR, and 2D HSQC, COSY NMR.

¹H NMR (300 MHz, CDCl₃): δ = 2.89 (s, 0.41 H), 2.52 (tt, *J* = 10.9, 3.9 Hz, 1.59 H), 1.83 – 0.72 (m, 22 H).

¹³C NMR (75 MHz, CDCl₃): δ = 50.87, 47.61, 44.35, 42.20, 36.86, 33.90, 32.51, 32.35, 27.76.

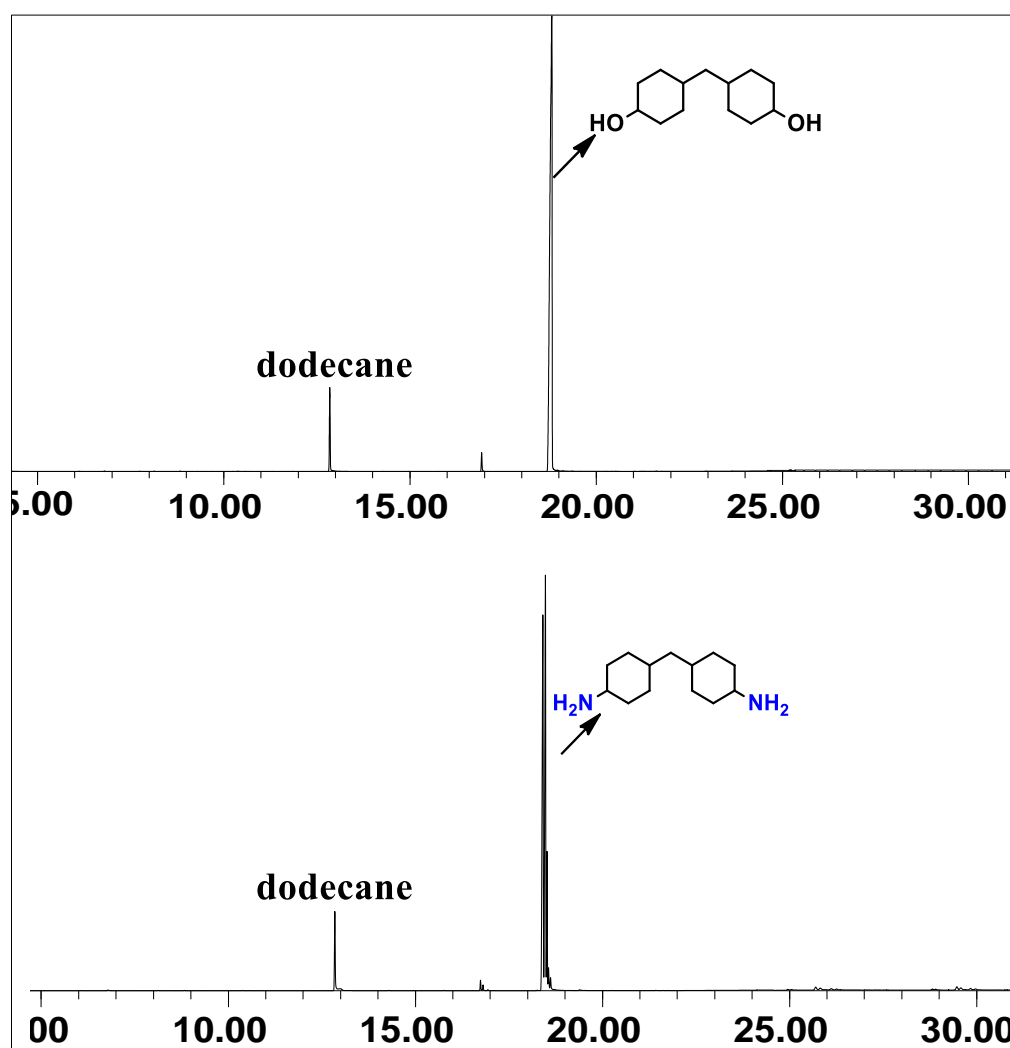


Figure S65. GC traces of (a) **MBC** and (b) crude **MBCA** after reaction

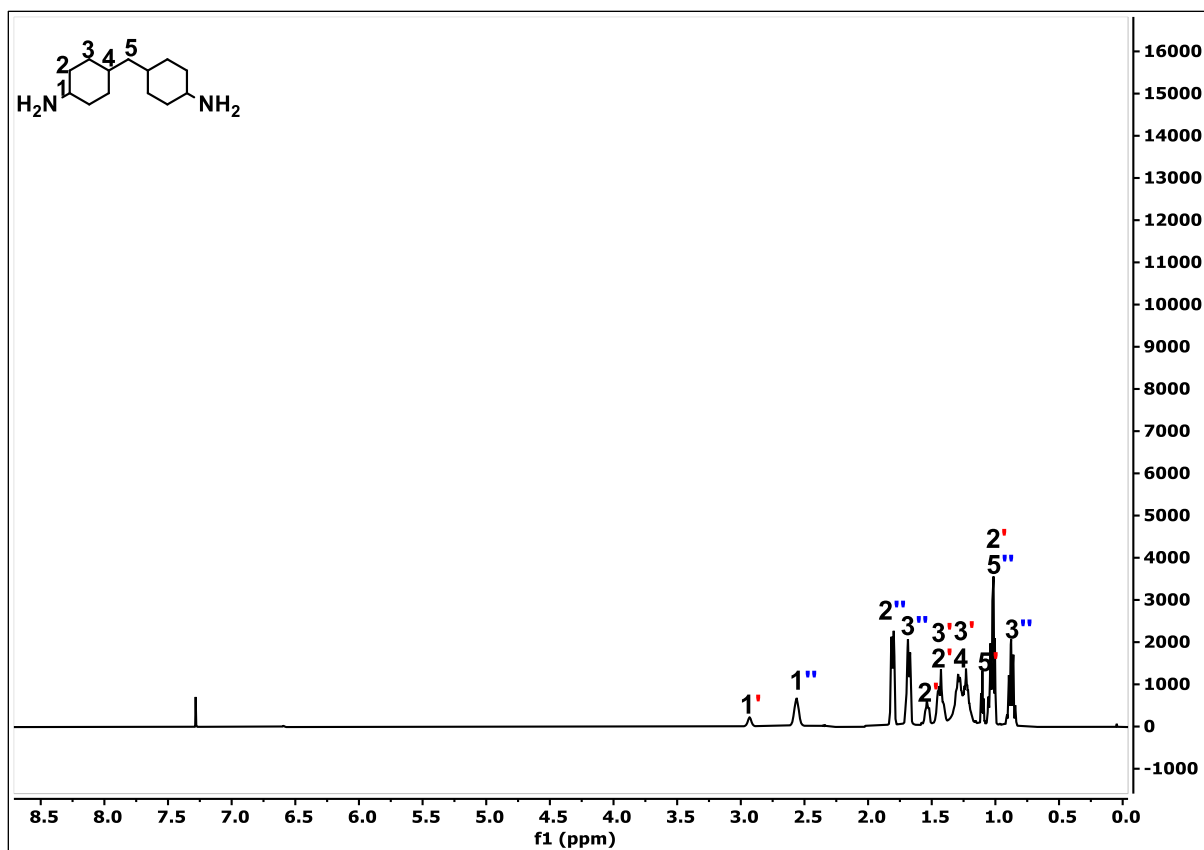


Figure S66. ^1H NMR spectrum of crude MBCA

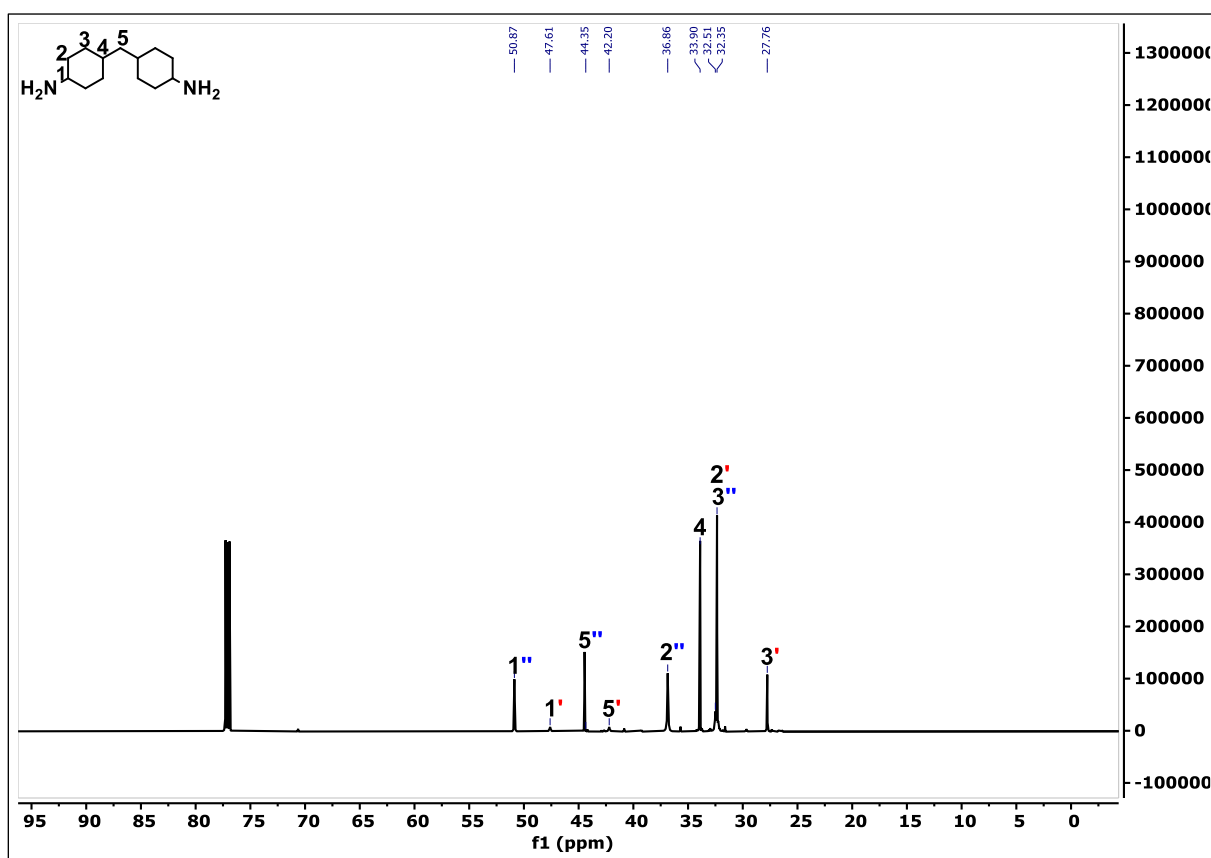


Figure S67. ^{13}C NMR spectrum of crude MBCA

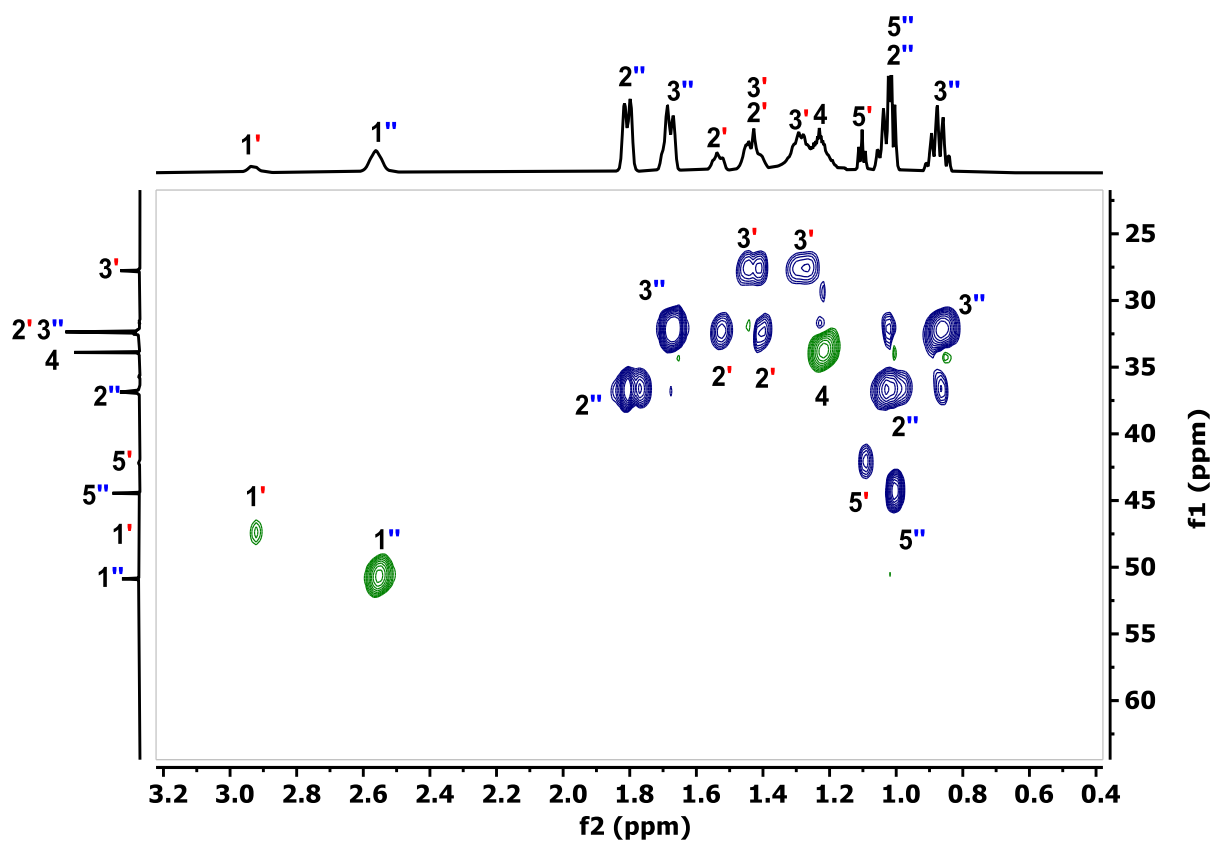


Figure S68. 2D HSQC spectrum of crude MBCA

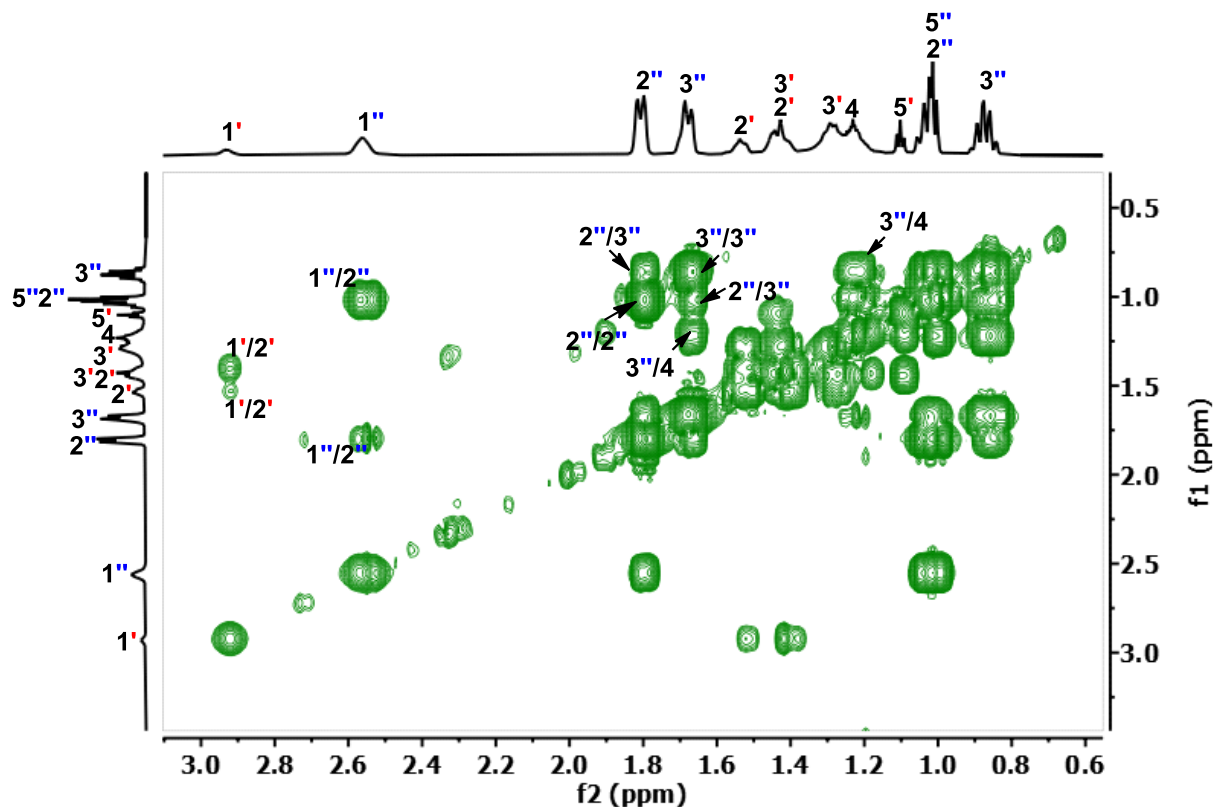


Figure S69. 2D COSY spectrum of crude MBCA

3.2 Recycling test for catalytic amination of MBC to MBCA over Raney nickel catalyst

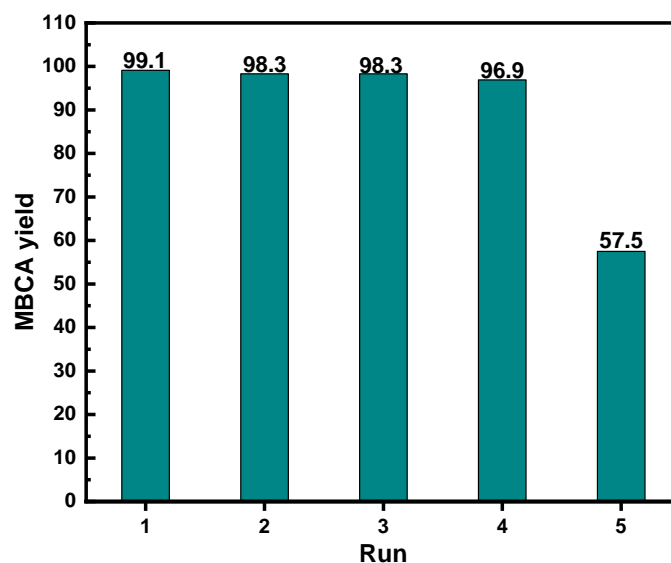


Figure S70. Recycling test for catalytic amination of **MBC** to **MBCA** over Raney nickel catalyst; Reaction conditions: 0.5 mmol **MBC**, 100 mg Raney nickel catalyst, 15 mL isopropanol, 7 bar NH_3 , 170 °C, 3h, 10 mg dodecane. Yield was determined by calibration curve using dodecane as internal standard. mass

The Ni leaching contents in the liquid solution (filtrate) was analyzed by Inductively coupled Plasma Mass Spectrometry (ICP-MS). As shown in **Table S4**, there is no obvious Ni leaching after sixth runs, indicating good stability of the employed catalytic systems.

Table S4. Ni leaching content was analyzed by ICP-MS

Catalytic system	Leached Ni from the catalyst/%	Ni concentration in filtrate/ppm	Ni amount in the filtrate/mg
Raney Ni (100 mg, 20 % water) isopropanol	0.2	306	0.16

4. Synthesis and characterizations of poly (S-MBCA), poly (PG-MBCA), poly (G-MBCA) and poly (E-MBCA)

4.1 DSC thermograms of S-MBCA, PG-MBCA, G-MBCA and E-MBCA

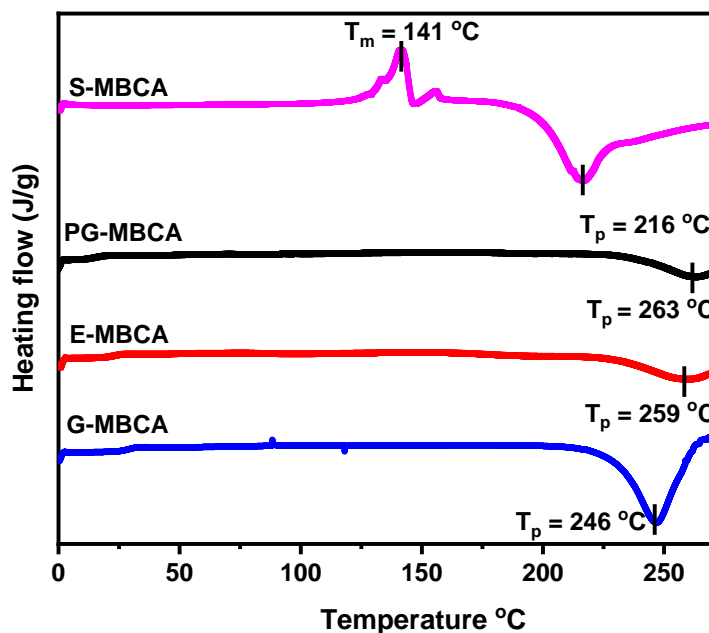


Figure S71. DSC thermograms of S-MBCA, PG-MBCA, G-MBCA and E-MBCA

4.2 TGA plots of poly (S-MBCA), poly (PG-MBCA), poly (G-MBCA) and poly(E-MBCA)

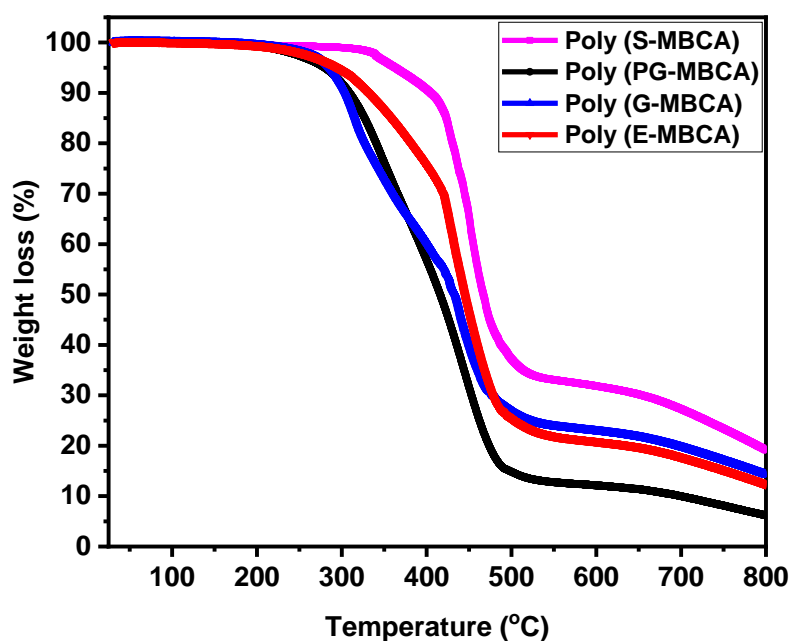


Figure S72. TGA plots of poly (S-MBCA), poly (PG-MBCA), poly (G-MBCA) and poly (E-MBCA)

4.3 DSC thermograms of poly (S-MBCA), poly (PG-MBCA), poly (G-MBCA) and poly (E-MBCA)

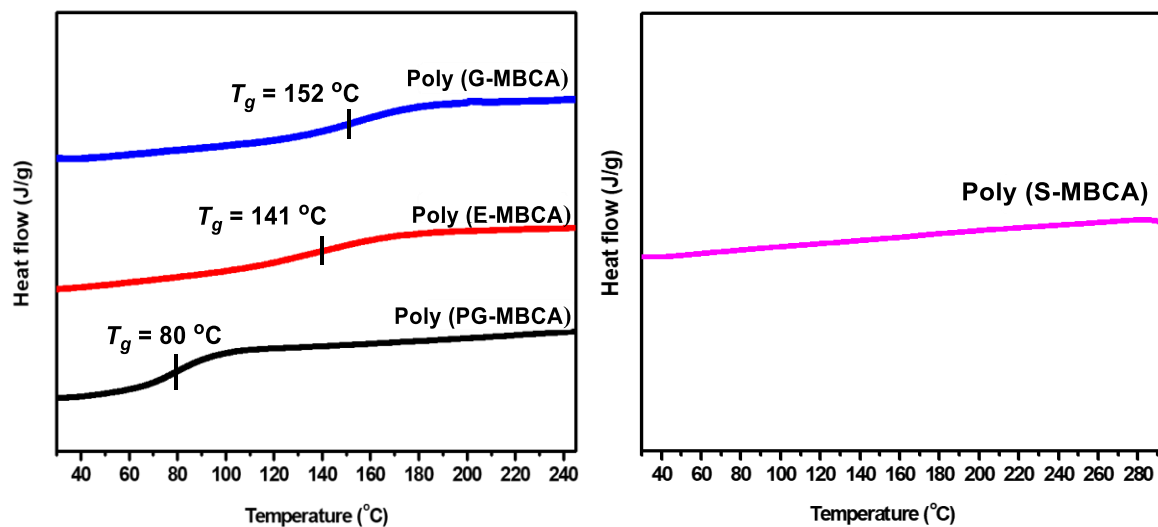


Figure S73. DSC thermograms of poly (S-MBCA), poly (G-MBCA), poly (PG-MBCA) and poly (E-MBCA)

4.4 FTIR spectra of S-MBCA, PG-MBCA, G-MBCA and E-MBCA before and after polymerization

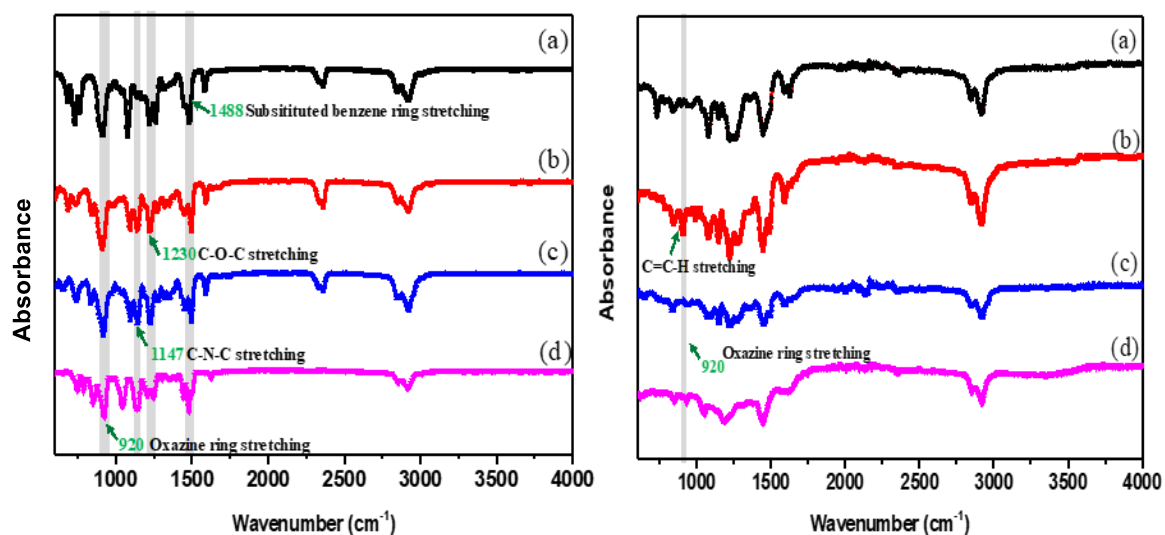


Figure S74. FTIR spectra of the S-MBCA, PG-MBCA, G-MBCA and E-MBCA before (left) and after (right) polymerization.

4.5 DMA curve of poly (S-MBCA)

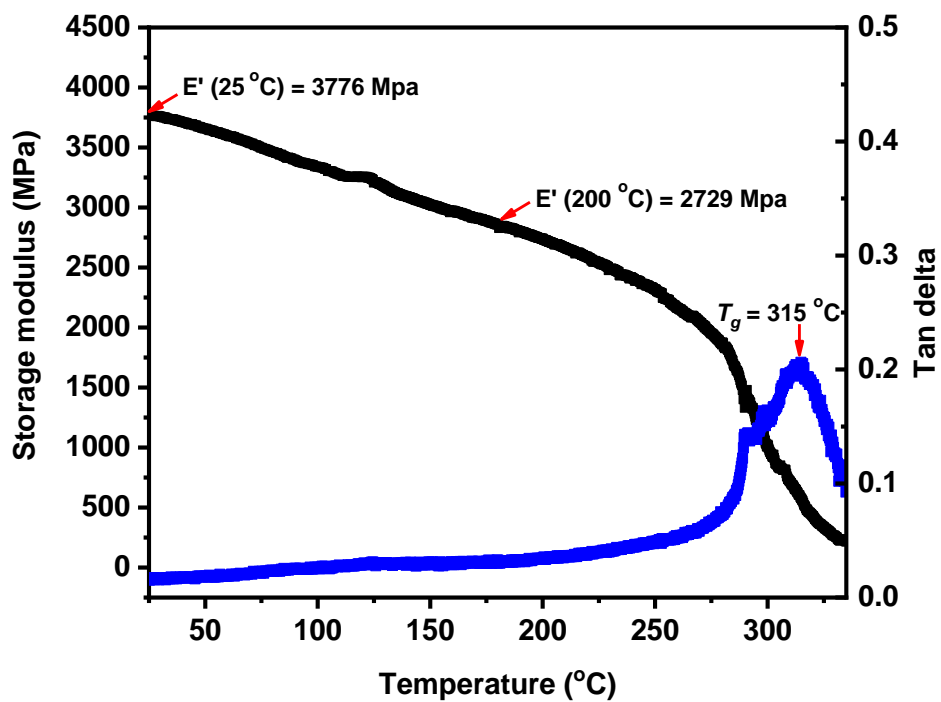


Figure S75. DMA curve of poly (S-MBCA)

5. Notes

Note S1: On using isopropanol as H-donor for conversion of BGH to MBC over other alcohols

The use of alcohols other than isopropanol, such as methanol or ethanol would be interesting as they can be relatively easily sourced from renewables. However, isopropanol, in combination with Raney Nickel is an excellent hydrogen donor, and it displays superior performance. In our previous work,⁷ we tested the effect of different alcohols (including methanol, ethanol), that could act as a hydrogen donor, for the demethoxylation and hydrogenation of 4-n-propanolguaiacol (**1G**) over Raney nickel catalyst. We confirmed that both ethanol and methanol lead to none, while butanol and 2-Me-butanol lead to poor conversion values. Previous work by Rinaldi and coworkers has also showed the same behavior and attributed the poorer performance in the case of methanol or ethanol, to the stronger adsorption of methyl- and ethyl- alcoholates to the surface of the catalyst Raney Ni catalyst.^{8,9}

Note S2: Considerations for the efficient catalytic activity of Raney Nickel in both key catalytic steps of our process (demethoxylation/hydrogenation of BGH and amination of MBC)

It is to be noted, that Raney Ni has turned out to be best performing for both key catalytic steps in our upgrading sequence. Raney Ni has previously shown great activity and selectivity in both the hydrodeoxygenation of guaiacol to cyclohexanol and reductive amination of biomass derived alcohols to amines. This is summarized excellently in this recent review paper.¹⁰ In summary, we attribute the high catalytic activity in both steps to the fact that Raney Nickel is a highly active transfer hydrogenation catalyst.

In case of the demethoxylation/hydrogenation step, the high transfer hydrogenation activity makes for a facile hydrogen abstraction from the H-donor isopropanol, as it has earlier been demonstrated in excellent works of Rinaldi.^{8,9} The other noble metal catalysts that were tested, possess higher affinity for aromatic ring reduction compared to Raney Nickel, while in this particular case, facile demethoxylation over aromatic ring hydrogenation is desired, since demethoxylation starting from the saturated ring is much slower. The latter was demonstrated in our earlier work regarding the demethoxylation/hydrogenation of propanol-guaiacol.

In case of the hydrogen borrowing amination step, we attribute the excellent selectivity to the ability of the catalyst to facilitate the two key steps in the hydrogen borrowing sequence: 1.) high activity for alcohol dehydrogenation 2.) facile hydrogen transfer to the imine and thereby rapid imine reduction. Furthermore, the high selectivity toward the primary amine **MBCA**, was achieved by increasing the pressure of NH₃ to 7 bar in our system, which facilitated imine formation and suppressed the further N-alkylation of **MBCA** with **MBC**. Higher secondary amine **8A**, selectivity was only observed with Ru/C (0.62 %).

Note S3: Sample calculations for estimating the amount of lignin/lignocellulose required for the production of MBC diol by the proposed pathways

In our system, phenol is being used as coupling partner which can be sustainably produced from

lignocellulose in relatively high yield. For example, Sels has described the production of phenol in 20% yield (based on lignin) by reductive catalytic fractionation of birch lignocellulose over Ni/SiO₂ catalyst.¹¹ Taking this as a state-of-the-art example, we have now calculated the amount of lignocellulose required for the production of phenol needed in this process. We have hereby considered several scenarios. In our case phenol is also the solvent which is recycled, so both the theoretical lignin amount of phenol consumed in the reaction as well as the total lignin/lignocellulose amount needed for the phenol required one time in the process are calculated.

Note S4: Sample calculation of materials required for the production of MBC diol, when phenol is obtained from birch lignocellulose and aldehydes are obtained from softwood lignosulfonate

Aldehydes: oxidative depolymerization of softwood lignosulfonate (1000 mg) (Syas paper-mill, Leningrad region, Russia)¹² delivers 0.79 mmol, 120 mg of **G-CHO** in a yield of 12 wt. %. Upon quantitative reduction, the amount of **G-OH** is: 0.79 mmol, 122 mg (subject to coupling).

Amount of 1 eq phenol required by the coupling reaction is: 0.79 mmol or **74 mg** and 10 equivalents are needed when the reaction is carried out in neat phenol, this is: **7.9 mmol, 743 mg** phenol.

The corresponding birch lignocellulose amount thus needed for the production of this amount of phenol is: For 74 mg phenol, the required amount of lignin is 74/0.20 mg = 370 mg, which is contained in 1897 mg of birch lignocellulose (at a lignin content: 19.5 wt. %, based on literature)¹¹.

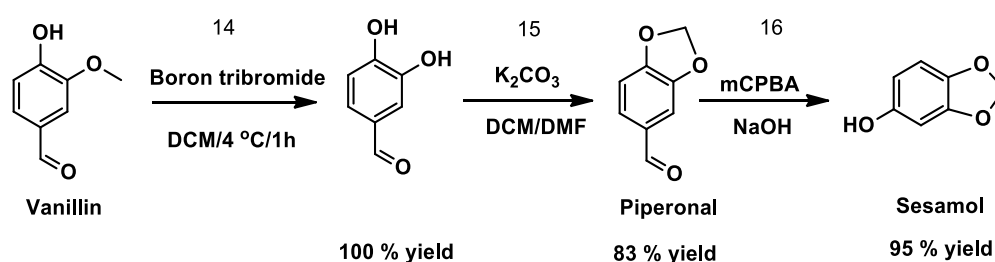
This means, following the results of this manuscript, this would give 0.72 mmol, 166 mg of **BSH** bisphenol in a yield of 90.8 mol %, which is further converted to 0.61 mmol, 129 mg of **MBC** in a yield of 84.8 mol %.

Summary: For 1 g total softwood lignosulfonate (for producing the aldehydes) 1.897 g lignocellulose (and 370 mg lignin) is needed (when considering producing 1 eq phenol for the reaction only) and 18.97 g lignocellulose (and 3.7 g lignin), when considering the whole process whereby phenol is recycled for a next step.

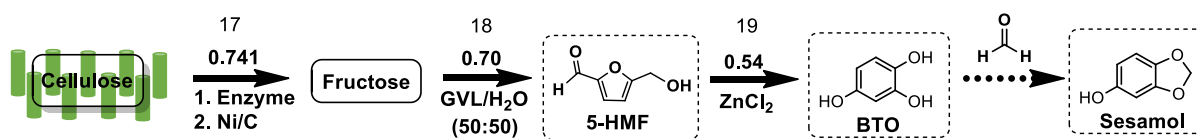
Note S5: Proposed reaction pathways for the production of sesamol

Sesamol can be obtained from natural sesame oil in relatively low, 0.3 wt. % yield (30.2 mg/100g) pure sesamol can be obtained from sesame powder by extraction and separation.¹³ In addition, based on existing literature (on individual steps), we have here proposed two possible reaction sequences to obtain sesamol from vanillin and cellulose derived **BTO**.

Starting from lignin derived vanillin

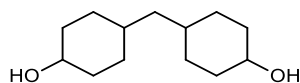


Starting from cellulose via BTO



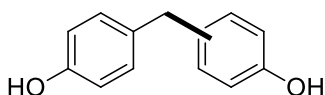
6. Spectral data of isolated compounds.

cis-cis, cis-trans, trans-trans-MBC



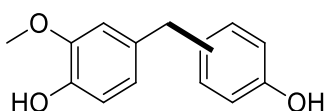
trans:trans: $^1\text{H NMR}$ (600 MHz, CDCl_3): $\delta = 3.54$ (tt, $J = 10.9, 4.3$ Hz, 2H), 2.01 – 1.89 (m, 4H), 1.78 – 1.67 (m, 4H), 1.46 (s, 2H), 1.32 – 1.18 (m, 6H), 1.04 (t, $J = 7.0$ Hz, 2H), 0.91 (tdd, $J = 13.7, 11.6, 3.3$ Hz, 4H). $^{13}\text{C NMR}$ (151 MHz, CDCl_3): $\delta = 71.2, 43.8, 35.6, 33.8, 31.5$. *cis:cis*: $^1\text{H NMR}$ (600 MHz, CDCl_3): $\delta = 3.95$ (tt, $J = 4.9, 3.0$ Hz, 2H), 1.69 (dt, $J = 13.7, 4.6$ Hz, 4H), 1.55 (ddt, $J = 14.2, 11.5, 3.5$ Hz, 4H), 1.48 (dq, $J = 12.9, 4.2$ Hz, 4H), 1.41 (dtt, $J = 13.5, 6.9, 3.2$ Hz, 4H), 1.36 – 1.28 (m, 4H), 1.17 (t, $J = 6.9$ Hz, 2H). $^{13}\text{C NMR}$ (151 MHz, CDCl_3): $\delta = 67.2, 33.0, 32.3, 27.3$. *cis:trans*: $^1\text{H NMR}$ (600 MHz, CDCl_3): $\delta = 3.95$ (tt, $J = 4.8, 2.9$ Hz, 1H), 3.54 (tt, $J = 10.9, 4.3$ Hz, 1H), 1.99 – 1.92 (m, 2H), 1.79 – 1.65 (m, 4H), 1.54 (ddt, $J = 14.3, 11.5, 3.4$ Hz, 2H), 1.50 – 1.44 (m, 5H), 1.39 (dtt, $J = 13.3, 6.7, 3.2$ Hz, 1H), 1.35 – 1.20 (m, 5H), 1.10 (t, $J = 7.0$ Hz, 2H), 0.91 (tdd, $J = 13.6, 11.5, 3.2$ Hz, 2H). $^{13}\text{C NMR}$ (151 MHz, CDCl_3): $\delta = 71.2, 67.2, 43.8, 35.6, 33.8, 33.6, 32.3, 31.5, 27.3$.

p, p' m, p'-BPP



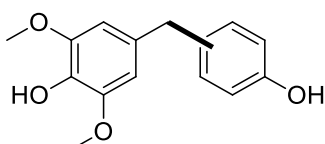
p, p'-BPP: $^1\text{H NMR}$ (600 MHz, MeOD): $\delta = 7.01 - 6.95$ (m, 4H), 6.72 – 6.65 (m, 4H), 3.77 (s, 2H). $^{13}\text{C NMR}$ (151 MHz, CDCl_3): $\delta = 159.0, 136.8, 133.2, 118.6, 43.6$. *m, p'-BPP*: $^1\text{H NMR}$ (600 MHz, MeOD): $\delta = 7.06 - 6.94$ (m, 2H), 6.79 – 6.66 (m, 2H), 3.84 (s, 1H). $^{13}\text{C NMR}$ (151 MHz, MeOD): $\delta = 154.9, 154.7, 132.2, 129.9, 129.4, 128.3, 126.6, 119.1, 114.5, 114.5, 34.3$.

p, p' m, p'-BGP



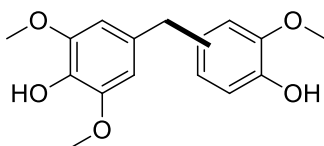
p, p'-BGP: $^1\text{H NMR}$ (600 MHz, CDCl_3): $\delta = 6.99-6.92$ (m, 2H), 6.76 (d, $J = 8.0$ Hz, 1H), 6.70–6.64 (m, 2H), 6.62–6.56 (m, 2H), 3.76 (d, $J = 7.0$ Hz, 5H). $^{13}\text{C NMR}$ (151 MHz, CDCl_3): $\delta = 153.8, 146.5, 143.9, 133.8, 133.4, 129.9, 121.5, 115.3, 114.2, 111.4, 55.9, 40.7$. *m, p'-BGP*: $^1\text{H NMR}$ (600 MHz, CDCl_3): $\delta = 7.08-7.02$ (m, 2H), 6.82 (td, $J = 7.4, 1.2$ Hz, 1H), 6.77 (d, $J = 7.9$ Hz, 1H), 6.72 (dd, $J = 8.0, 1.2$ Hz, 1H), 6.68–6.63 (m, 2H), 3.85 (s, 2H), 3.75 (s, 3H). $^{13}\text{C NMR}$ (151 MHz, CDCl_3): $\delta = 153.8, 146.8, 144.3, 131.5, 130.8, 127.9, 127.2, 121.3, 120.9, 115.8, 114.5, 111.2, 55.9, 36.2$.

p, p' m, p'-BSP



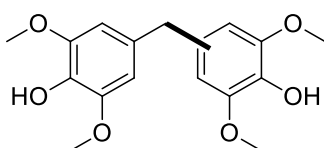
p, p'-BSP: $^1\text{H NMR}$ (600 MHz, MeOD): $\delta = 6.91-6.87$ (m, 2H), 6.62–6.55 (m, 2H), 6.33 (s, 2H), 3.67 (d, $J = 1.5$ Hz, 8H). $^{13}\text{C NMR}$ (151 MHz, MeOD): $\delta = 155.2, 147.8, 133.3, 132.8, 132.5, 129.3, 114.7, 105.7, 55.3, 40.5$.

***p, p'/m, p'*-BSG**



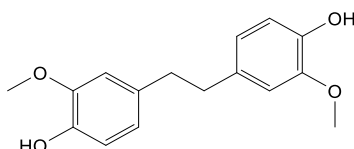
p, p'-**BSG**: $^1\text{H NMR}$ (600 MHz, CDCl_3): $\delta = 6.77$ (d, $J = 8.0$ Hz, 1H), 6.61 (dt, $J = 8.0, 1.4$ Hz, 1H), 6.58 (d, $J = 1.9$ Hz, 1H), 6.32 (s, 2H), 3.78–3.73 (m, 11H). $^{13}\text{C NMR}$ (151 MHz, CDCl_3): $\delta = 147.0, 146.5, 143.9, 133.1, 133.1, 132.5, 121.5, 114.3, 111.4, 105.6, 56.3, 55.9, 41.6$. *m, p'*-**BSG**: $^1\text{H NMR}$ (600 MHz, CDCl_3): $\delta = 6.74$ (d, $J = 8.0$ Hz, 1H), 6.64 (d, $J = 1.9$ Hz, 1H), 6.61 (dd, $J = 8.1, 1.9$ Hz, 1H), 6.50 (s, 2H), 3.79 (d, $J = 1.4$ Hz, 5H), 3.76 (s, 3H), 3.70 (s, 3H). $^{13}\text{C NMR}$ (151 MHz, CDCl_3): $\delta = 146.4, 146.3, 145.3, 143.8, 138.7, 133.3, 127.7, 121.5, 120.0, 114.1, 111.5, 106.3, 60.5, 56.2, 55.9, 35.2$.

***p, p'/m, p'*-BSS**



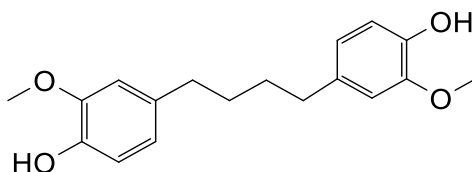
p, p'-**BSS**: $^1\text{H NMR}$ (600 MHz, CDCl_3): $\delta = 6.32$ (s, 4H), 5.33 (s, 2H), 3.77 (s, 14H). $^{13}\text{C NMR}$ (151 MHz, CDCl_3): $\delta = 147.0, 133.1, 132.2, 105.6, 56.3, 41.9$. *m, p'*-**BSS**: $^1\text{H NMR}$ (600 MHz, CDCl_3): $\delta = 6.58$ (d, $J = 2.2$ Hz, 2H), 6.43 (s, 2H), 3.87 (d, $J = 6.0$ Hz, 5H), 3.84 (s, 6H), 3.79 (s, 3H). $^{13}\text{C NMR}$ (151 MHz, CDCl_3): $\delta = 146.9, 146.4, 145.3, 138.6, 132.9, 132.4, 127.5, 119.9, 106.3, 105.6, 60.5, 56.3, 56.2, 35.7$.

β -1



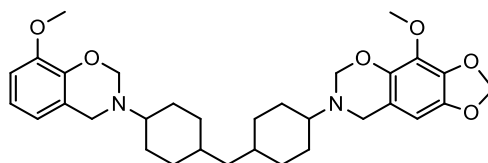
$^1\text{H NMR}$ (300 MHz, CDCl_3): $\delta = 6.84$ (d, $J = 8.0$ Hz, 1H), 6.68 (dd, $J = 8.0, 1.9$ Hz, 2H), 6.61 (d, $J = 1.9$ Hz, 2H), 5.49 (s, 2H), 3.84 (s, 6H), 2.82 (s, 4H). $^{13}\text{C NMR}$ (75 MHz, CDCl_3): $\delta = 146.2, 143.7, 133.8, 121.1, 114.2, 111.2, 55.9, 37.9$.

β - β



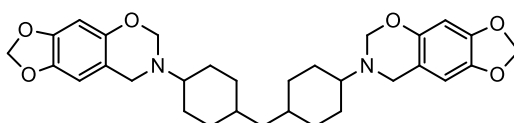
$^1\text{H NMR}$ (300 MHz, CDCl_3): $\delta = 6.82$ (d, $J = 8.5$ Hz, 2H), 6.67 (dd, $J = 5.9, 2.1$ Hz, 4H), 5.45 (s, 2H), 3.87 (s, 6H), 2.62–2.51 (m, 4H), 1.62 (p, $J = 3.6$ Hz, 4H). $^{13}\text{C NMR}$ (75 MHz, CDCl_3): $\delta = 146.3, 143.5, 134.6, 120.9, 114.1, 110.9, 55.8, 35.5, 31.3$.

G-MBCA



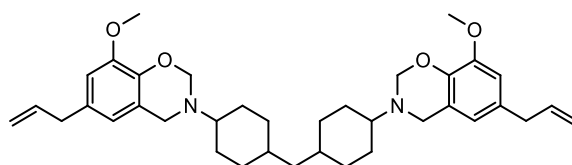
^1H NMR (600 MHz, CDCl_3): δ = 6.77 (t, J = 7.8 Hz, 2H), 6.70 (d, J = 8.1 Hz, 2H), 6.55 (d, J = 7.6 Hz, 2H), 5.05 (d, J = 3.9 Hz, 4H), 4.08–4.03 (m, 4H), 3.84 (s, 6H), 2.88–2.60 (m, 2H), 2.01–0.67 (m, 20H). ^{13}C NMR (151 MHz, CDCl_3): δ = 147.8, 147.6, 144.5, 144.4, 122.4, 122.3, 121.7, 119.6, 119.6, 119.2, 118.8, 109.3, 109.2, 80.9, 80.9, 80.6, 76.9, 59.4, 59.3, 55.8, 47.4, 47.0, 44.2, 34.1, 34.0, 32.5, 32.4, 31.5, 31.4, 28.3, 28.2, 27.5.

S-MBCA



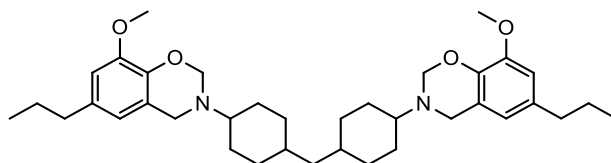
^1H NMR (600 MHz, CDCl_3): δ = 6.40 (d, J = 2.3 Hz, 2H), 6.31 (d, J = 2.4 Hz, 2H), 5.85 (d, J = 1.7 Hz, 4H), 4.89 (d, J = 3.3 Hz, 4H), 3.99–3.94 (m, 4H), 2.84–2.58 (m, 2H), 1.97–0.77 (m, 20H). ^{13}C NMR (151 MHz, CDCl_3): δ = 149.5, 149.5, 146.4, 146.4, 141.3, 141.2, 112.9, 112.9, 112.3, 106.3, 105.9, 100.7, 100.6, 98.6, 98.4, 80.4, 80.3, 80.0, 80.0, 59.2, 59.1, 47.8, 47.4, 44.3, 41.5, 34.2, 34.1, 32.5, 32.5, 31.9, 31.4, 31.4, 28.3, 28.3, 27.4. **HRMS** (APCI⁺, m/z) calculated for $(\text{M}+\text{H})^+$ 535.281053; found: 535.280263.

E-MBCA



^1H NMR (600 MHz, CDCl_3): δ = 6.53 (t, J = 2.3 Hz, 2H), 6.39 (t, J = 2.3 Hz, 2H), 5.94 (ddt, J = 16.8, 10.0, 6.8 Hz, 2H), 5.11–5.04 (m, 4H), 5.03 (d, J = 3.5 Hz, 4H), 4.06–4.01 (m, 4H), 3.84 (d, J = 1.8 Hz, 6H), 3.28 (d, J = 6.8 Hz, 4H), 2.68 (tt, J = 11.6, 3.7 Hz, 2H), 2.00–0.74 (m, 20H). ^{13}C NMR (151 MHz, CDCl_3): δ = 147.7, 147.5, 142.7, 142.6, 137.7, 131.4, 131.3, 122.1, 122.1, 121.4, 118.8, 118.4, 115.7, 115.7, 109.7, 109.6, 80.9, 80.9, 80.5, 59.3, 59.2, 55.8, 47.5, 47.1, 44.3, 39.9, 34.1, 34.0, 32.5, 32.4, 31.5, 31.4, 28.3, 28.3, 27.5. **HRMS** (APCI⁺, m/z) calculated for $(\text{M}+\text{H})^+$ 587.383523; found: 587.384335.

PG-MBCA



^1H NMR (600 MHz, CDCl_3): δ = 6.53 (t, J = 2.2 Hz, 2H), 6.38 (t, J = 2.3 Hz, 2H), 5.03 (d, J = 3.5 Hz, 4H), 4.07–4.01 (m, 4H), 3.84 (d, J = 1.8 Hz, 6H), 2.69 (ddp, J = 11.5, 7.4, 4.1, 3.6 Hz, 2H), 2.47 (t, J = 7.7 Hz, 4H), 1.98–0.77 (m, 30H). ^{13}C NMR (151 MHz, CDCl_3): δ = 147.5, 147.3, 142.3, 142.2, 134.2, 134.1, 121.8, 121.1, 118.6, 118.2, 109.6, 109.5, 80.7, 80.4, 59.3, 59.2, 55.8, 47.5, 47.1, 44.3, 37.9, 34.1, 34.0, 32.5, 32.4, 31.4, 31.4, 28.3, 28.3, 27.5, 24.7, 24.7, 13.9.

7. Supplemental references

1. Sun, Z.H., Vasconcelos, A.C., Bottari, G., Stuart, M.C.A., Bonura, G., Cannilla, C., Frusteri, F., and Barta, K. (2017). Efficient Catalytic Conversion of Ethanol to 1-Butanol via the Guerbet Reaction over Copper- and Nickel-Doped Porous. *ACS. Sustain. Chem. Eng.* 5, 1738-1746. <https://doi.org/10.1021/acssuschemeng.6b02494>.
2. Nicastro, K.H., Kloxin, C.J., and Epps III, T.H. (2018). Potential lignin-derived alternatives to bisphenol a in diamine-hardened epoxy resins. *ACS. Sustain. Chem. Eng.* 6, 14812-14819. <https://doi.org/10.1021/acssuschemeng.8b03340>.
3. Sun, Z.H., Bottari, G., Afanassenko, A., Stuart, M.C.A., Deuss, P.J., Fridrich, B., and Barta, K. (2018). Complete lignocellulose conversion with integrated catalyst recycling yielding valuable aromatics and fuels. *Nat. Catal.* 1, 82-92. <https://doi.org/10.1038/s41929-017-0007-z>.
4. Harvey, B.G., Sahagun, C.M., Guenther, A.J., Groshens, T.J., Cambrea, L.R., Reams, J.T., and Mabry, J.M. (2014). A High-Performance Renewable Thermosetting Resin Derived from Eugenol. *ChemSusChem* 7, 1964-1969. <https://doi.org/10.1002/cssc.201400019>.
5. Kotzebue, L.R.V., de Oliveira, J.R., da Silva, J.B., Mazzetto, S.E., Ishida, H., and Lomonaco, D. (2018). Development of fully biobased high-performance bis-benzoxazine under environmentally friendly conditions. *ACS Sustain. Chem. Eng.* 6, 5485-5494. <https://doi.org/10.1021/acssuschemeng.8b00340>.
6. Salum, M.L., Iguchi, D., Arza, C.R., Han, L., Ishida, H., and Froimowicz, P. (2018). Making benzoxazines greener: design, synthesis, and polymerization of a biobased benzoxazine fulfilling two principles of green chemistry. *ACS Sustain. Chem. Eng.* 6, 13096-13106. <https://doi.org/10.1021/acssuschemeng.8b02641>.
7. Wu, X.Y., Galkina, M.V., Sun, Z.H., Barta, K., Fully lignocellulose-based PET analogues for the circular economy. DOI: 10.26434/chemrxiv.14627745.v1.
8. Wang, X.Y., and Rinaldi, R. (2012). Exploiting H-transfer reactions with RANEY (R) Ni for upgrade of phenolic and aromatic biorefinery feeds under unusual, low-severity conditions. *Energ. Environ. Sci.* 5, 8244-8260. <https://doi.org/10.1039/C2EE21855K>.
9. Kennema, M., de Castro, I.B.D., Meemken, F., and Rinaldi, R. (2017). Liquid-Phase H-Transfer from 2-Propanol to Phenol on Raney Ni: Surface Processes and Inhibition. *ACS Catal.* 7, 2437-2445.
10. Sun, Z.H., Zhang, Z.H., Yuan, T.Q., Ren, X.H., and Rong, Z.M. (2021). Raney Ni as a Versatile Catalyst for Biomass Conversion. *ACS Catal.* 11, 10508-10536. <https://doi.org/10.1021/acscatal.1c02433>.
11. Liao, Y.H., Koelewijn, S.F., Van den Bossche, G., Van Aelst, J., Van den Bosch, S., Renders, T., Navare, K., Nicolai, T., Van Aelst, K., Maesen, M., et al. (2020). A sustainable wood biorefinery for low-carbon footprint chemicals production. *Science* 367, 1385-1390. <https://www.science.org/doi/10.1126/science.aau1567>.
12. Tarabanko, V.E., Fomova, N.A., Kuznetsov, B.N., Ivanchenko, N.M., and Kudryashev, A.V. (1995). On the Mechanism of Vanillin Formation in the Catalytic-Oxidation of Lignin with Oxygen. *React. Kinet. Catal. L.* 55, 161-170. <https://doi.org/10.1007/BF02075847>.

13. Zhou, S.Y., Zou, H.Y., Huang, G.L., and Chen, G.Y. (2021). Preparations and antioxidant activities of sesamol and its derivatives. *Bioorg. Med. Chem. Lett.* *31*, 127716 <https://doi.org/10.1016/j.bmcl.2020.127716>.
14. Sato, M., Murakami, K., Uno, M., Ikubo, H., Nakagawa, Y., Katayama, S., Akagi, K.-i., and Irie, K. (2013). Structure–activity relationship for (+)-taxifolin isolated from silymarin as an inhibitor of amyloid β aggregation. *Biosci. Biotechnol. Biochem.* *77*, 1100-1103. <https://doi.org/10.1271/bbb.120925>.
15. Dong, S.Y., Wang, T.T., Hu, C.D., Chen, X.D., Jin, Y., and Wang, Z.T. (2017). Design and Synthesis of 5-Substituted Benzo [d][1, 3] dioxole Derivatives as Potent Anticonvulsant Agents. *Arch. Pharm. Chem. Life Sci.* *350*, e1600274. <https://doi.org/10.1002/ardp.201600274>.
16. da Silva, E.T., Camara, C.A., Antunes, O.A.C., Barreiro, E.J., and Fraga, C.A.M. (2008). Improved solvent-free Dakin oxidation protocol. *Synthetic Commun.* *38*, 784-788. <https://doi.org/10.1080/00397910701820673>.
17. Sun, J.K., Li, H.L., Huang, H.Z., Wang, B., Xiao, L.P., and Song, G.Y. (2018). Integration of Enzymatic and Heterogeneous Catalysis for One-Pot Production of Fructose from Glucose. *Chemsuschem* *11*, 1157-1162. <https://doi.org/10.1002/cssc.201800015>.
18. Motagamwala, A.H., Won, W.Y., Sener, C., Alonso, D.M., Maravelias, C.T., and Dumesic, J.A. (2018). Toward biomass-derived renewable plastics: Production of 2,5-furandicarboxylic acid from fructose. *Sci. Adv.* *4*, eaap9722. <https://www.science.org/doi/10.1126/sciadv.aap9722>.
19. Kumalaputri, A.J., Randolph, C., Otten, E., Heeres, H.J., and Deuss, P.J. (2018). Lewis Acid Catalyzed Conversion of 5-Hydroxymethylfurfural to 1,2,4-Benzenetriol, an Overlooked Biobased Compound. *ACS Sustain. Chem. Eng.* *6*, 3419-3425. <https://doi.org/10.1021/acssuschemeng.7b03648>.